An investigation into the use of the yeast *Arxula adeninivorans* as the catalyst for a microbial fuel cell

---

A thesis submitted in partial fulfilment

of the requirements for the Degree of

Doctor of Philosophy

in Microbiology

School of Biological Sciences

University of Canterbury

New Zealand

By

Jonathan J H Y Williams

February 2017

Abstract

Microbial fuel cells (MFCs) are bioelectrochemical systems which convert chemical energy in organic matter into electrical energy. MFCs use a living microorganism or consortium thereof to metabolise an organic substrate, whereupon some of the electrons the organisms derive from this process are transferred to the anode of the MFC. These electrons will travel hrough an external circuit to a cathode, performing electrical work in the process.

Several yeasts have been investigated for their potential as microbial catalysts because of their robustness when subjected to physical and chemical stresses, coupled with their ability to metabolise a wide variety of organic substrates. One such yeast is *Arxula adeninivorans*, a dimorphic yeast which has been successfully used as the microbial catalyst of an MFC. It was noticed that *A. adeninivorans* was able to transfer electrons to the anode of the MFC in the absence of an artificial mediator by means of an unidentified, electrochemically active molecule secreted into the buffer solution.

In this thesis, high-performance liquid chromatography was used to fractionate extracellular buffer from suspensions of *A. adeninivorans* in order to isolate and collect the unidentified molecule. The molecule was then identified by mass spectrometry as being uric acid. This identification was supported by comparing UV spectra and cyclic voltammograms (CVs) to sodium urate. A transgenic strain of *A. adeninivorans* with an inducible urate oxidase gene was used to show that the molecule was a substrate for the enzyme urate oxidase, further confirming its identity.

CVs from a range of other yeasts also of the Saccharomycetaceae family were compared to those of *A. adeninivorans*, and it was observed that none of these other yeasts produced an electrochemical response indicating the presence of uric acid. A transgenic strain of *A. adeninivorans* with a disrupted xanthine dehydrogenase gene also failed to produce the electrochemical response corresponding to uric acid, indicating that the secreted uric acid is derived from the purine catabolism pathway.

To optimise production of uric acid by *A. adeninivorans*, linear sweep voltammetry (LSV) was used to measure the concentration of uric acid accumulated over 20 h in the extracellular buffer of *A. adeninivorans* cell suspensions subjected to a variety of culture conditions. More uric acid was accumulated in suspensions incubated under anaerobic conditions, but less was accumulated by cells derived from poorly-aerated growth cultures compared to well-aerated cultures. The presence of a carbon source in the suspension caused less uric acid to be accumulated. More uric acid was accumulated at 37 °C by suspensions of a mutant *A. adeninivorans* with a disrupted urate oxidase gene compared to the wild type, but while production increased for both strains at 45 °C (at the cost of greatly increased cell mortality), the wild type accumulated more at this temperature. A pH of 8 was

found to be optimal for uric acid production, but the yeast naturally reduces the pH of the buffer over time. In all cases, parameters resulting in increased uric acid production were accompanied by some drawback making it unsuitable for implementation in an MFC.

An MFC was constructed incorporating carbon cloth electrodes, a cation-exchange membrane in place of Nafion, and Dynawhite (3-5% NaOCl) as a chemical catholyte. The anolyte solution was an OD_{600} 2.5 suspension of *A. adeninivorans* in PBS. A peak power density of 25 mW m^{-1} with an external load of 3 kΩ was observed. With an external load of 100 Ω, power density diminished rapidly, in contrast to descriptions of such MFCs in the literature. Dynawhite and the cation-exchange membrane functioned acceptably in the short term, but extended use of the two in conjunction resulted in the degradation and failure of the membrane.

Acknowledgements

I'd like to thank my supervisor Kim Baronian for the assistance and support over the course of my research, especially for pushing me to get my work published and for the periodic reminders that the sky is not, in actual fact, falling, despite my repeated attempts to persuade myself that I'm sure I heard the trumpet sound for the end of days that time.

I'd also like to thank Craig Galilee for his consistent willingness to drop everything and help me out with whatever task I implored him to assist me with, whether I was missing reagents/equipment, or lacking a piece of microbiology-lab-wisdom, or had just caused a calamitous spill and needed to make it go away ASAP. My colleagues in other departments always moaned about their lab technicians, but I could only ever shrug and say "Well my lab's one is really good."

Thanks to Alan Woods for his assistance with fabricating the electrical components of my apparatus, even when the best description I could give of what I actually wanted done was vague and hand-wavy. Thanks also to Nick Etheridge and Rob McGregor for their efforts in helping me get bits and pieces fabricated.

Thanks to Meike Holzenkaempfer for her indefatigable enthusiasm and patient instruction in the use of the HPLC during the early stages of my research.

Thanks to Thomas Evans for putting up with the sudden incursion of my sprawl of equipment and the debris of my many half-finished or half-exploded experiments in his lab in 2016.

Thanks to Nicholas Glithero for his advice on MFC design and materials.

Thanks to Gotthard Kunze and his team at IPK for the supply of *Arxula adeninivorans* strains and customized transformants over the course of my research.

Thanks to all my friends and colleagues who put up with the endless streams of whining and complaining every time my experiments weren't going my way. Without your patience and sympathy I would have gone quite mad.

Thanks to my family, immediate and extended, for their unflagging support and unceasing prayers throughout the entire course of my studies.

Dedicated to the saints on whose intercession I relied during my research:

Saint Isidore of Seville

Bishop, Confessor and Doctor of the Church

Saint Thomas Aquinas

Priest, Religious and Doctor of the Church

Saint Albertus Magnus

Bishop, Religious and Doctor of the Church

and also

Sancta Maria, Mater Dei

Finally,

Non nobis, Domine, non nobis,

sed nomini tuo da gloriam!

Table of Contents

List of Figures

List of Tables

Published Work

The work described within this thesis has, at the time of writing, generated two papers for peer-reviewed publication.

The first, "Identification of uric acid as the redox molecule secreted by the yeast *Arxula adeninivorans*", authored by J. Williams, A. Trautwein-Schult, D. Jankowska, G. Kunze, M. A. Squire and K. Baronian, was published in *Applied Microbiology and Biotechnology*, volume 98, issue 5, pages 2223-2229 in 2014. The text of this paper was written primarily by J. Williams, and the work described in it conducted by J. Williams. The content of this paper substantially informs large portions of chapters 3 and 4 of this thesis.

The second, "Environmental and metabolic parameters affecting uric acid production by *Arxula adeninivorans*", authored by J. Williams, A. Trautwein-Schult, G. Kunze and K. Baronian, was accepted for publication in *Applied Microbiology and Biotechnology* on 12/02/2017. The text of this paper was written primarily by J. Williams, and the work described in it conducted by J. Williams, with the exception of work pertaining to the construction of the *A. adeninivorans* G1221 transformant. The content of this paper substantially informs large portions of chapter 5 of this thesis.

Chapter 1

Introduction

1.1 Background

Microbial fuel cells (MFCs) are bioelectrochemical systems that convert chemical energy from organic matter into electrical energy by exploiting the metabolism of living, whole-cell microorganisms as a catalyst. The microorganisms oxidise the organic material in the feedstock or substrate, and some of the electrons resulting from the process are transferred to the anode of the MFC, where they travel through an external circuit towards the cathode, doing electrical work in the process.

This principle is acknowledged as having significant potential for coupling energy recovery to the processing of heterogeneous waste streams. There is interest in developing MFC systems which use yeasts rather than bacteria due to their ease of cultivation, tolerance for a broad variety of environmental conditions and their ability to metabolise a wide variety of different substrates for energy.

One of the challenges involved in MFC design is the difficulty in mobilising electrons from metabolic processes within the cell and transferring those electrons to the anode. This is especially problematic in the case of eukaryotes, such as yeasts, which have the majority of the electrons generated by metabolic processes localised in the mitochondria. Artificial chemical mediators can be added to the MFC to act as shuttles, passing through the cell membrane in an oxidised form, to requisition electrons and become reduced, then leaving the cell and being oxidised at the anode. Artificial mediators do, however, present a range of problems including added cost, difficulty with implementation in continuous flow systems, and environmental toxicity. As a result there is significant interest in finding yeasts which are capable of transporting electrons to the anode of the MFC without assistance from artificial chemical mediators.

Arxula adeninivorans is a yeast which has demonstrated high thermal, pH, and salinity tolerance, as well as exhibiting the ability to metabolise a very diverse range of substrates as carbon and nitrogen sources. It has been successfully used as the catalyst in a laboratory-scale, artificially-mediated MFC, but it was noticed that it was also capable of transferring electrons to the anode by means of an unknown reduced species secreted into solution. This thesis is aimed at investigating this phenomenon

and determining if it can be enhanced and exploited to enable *A. adeninivorans* to serve as a self-mediating microbial catalyst for an MFC.

1.2 Objectives

- The objective of the first chapter is obtain and analyse samples of the unknown reduced species previously observed as being secreted by suspensions of *A. adeninivorans* into the extracellular buffer. High-performance liquid chromatography, UV-VIS spectroscopy, mass spectrometry and cyclic voltammetry will be used to discern its identity and hypothesise the pathways that may be responsible for its production.

- The objective of the second chapter is to determine if the secretion of the reduced species is a general property of Saccharomycetaceae yeasts, and to investigate the metabolic pathways which may be responsible for its production by conducting electrochemical studies of gene disruption mutants. Knowledge of the pathways responsible may assist in gaining an understanding of how production of the molecule of interest may be upregulated.

- The objective of the third chapter is to attempt to find a strategy for increasing the production of the reduced molecule. This will be done by using linear sweep voltammetry to quantify how the production of uric acid by *A. adeninivorans* responds to a variety of modifications to environmental and metabolic parameters such as aeration, pH, temperature and enzyme production. This will help to determine if there is some simple way to upregulate production of the reduced molecule which could implemented as part of the operating conditions of an *A. adeninivorans*-based, non-mediated MFC without significant drawbacks.

- The objective of the fourth chapter is to construct a laboratory-scale MFC using *A. adeninivorans* as the microbial catalyst, and characterise its behaviour. The first step will be to attempt to replicate the level of non-mediated electron transfer for *A. adeninivorans* described in the literature using a less expensive membrane material and less destructive chemical catholyte. If possible, the next objective will be to seek to implement any likely optimisation strategies developed over the course of the previous chapters, toward an end goal of a non-mediated *A. adeninivorans* MFC with an improved power density and/or economic viability.

Chapter 2

Background

2.1 Introduction: The microbial fuel cell (MFC)

In the present era, rising atmospheric CO_2 levels have led to a growing concern about releasing more sequestered carbon into the atmosphere. The current approach to addressing this issue is the development of new energy sources which do not release CO_2 in excess of that which is released as part of the normal carbon cycle. This has led to a rapid diversification and intensification of research and development of alternative energy sources over the past few decades. To date, no single solution has emerged providing the power and flexibility of fossil fuels such that it can entirely displace their use, so it is likely we will see the emergence of a series of alternative energy generation mechanisms, each specialised to exploit some particular niche. One such novel electricity producing technology is the microbial fuel cell (MFC).

The core attribute that distinguishes the MFC from other fuel cell types is that it incorporates at least one species of microorganism into the power generation process. Outside of this constraint, there is a vast amount of variation between different MFCs in regard to virtually every parameter, from physical layout, materials and structure of the MFC and its components, through to organism types, electron transport mechanisms, feedstocks and electrochemistry.

In principle, the most common manifestation of the MFC concept is that microbes will be used to oxidise some substrate. The electrons produced by this process are collected at the anode of the MFC, which serves as a local electron acceptor in the oxidation process. From there they can travel through an external electrical circuit toward the cathode, where they will be collected by the terminal electron acceptor. This movement of electrons can be harnessed as an electrical current.

This literature review will explore the history of MFCs, the range of structures and mechanisms by which they operate, their applications and the microorganisms they use as catalysts. The focus will then narrow to the context of the development of yeast-based MFCs, and discuss the yeast *Arxula adeninivorans* and its potential as a microbial catalyst for use in a self-mediating, yeast-based MFC.

2.2 Early history of the MFC concept

The first MFC to be constructed was probably the cell used in the investigation by Potter (1911). Potter's apparatus consisted of a porous cylinder suspended in a boiling tube, both filled with a nutrient medium and with a platinum electrode in each vessel. The fluid in one or the other chamber could be inoculated with *Saccharomyces cerevisiae* or *Escherichia coli* (at that time referred to as *Bacillus coli communis*). This arrangement is now typically referred to as a two-chambered MFC. While there was no load placed on the cell, a galvanometer was used to observe a voltage between what were termed the "fermenting" and "non-fermenting" chambers, with the current travelling from the fermenting chamber's electrode (functionally the anode) to the non-fermenting chamber's electrode (functionally the cathode). It was suggested that the observed electromotive force generated was the result of collecting electrons liberated into solution by the fermentative process. The experiments of Potter (1911) represent the first instances of both bacteria-based and yeast-based MFCs.

This work did not seem to generate a great deal of interest at the time, and the MFC concept was not immediately developed any further. The next MFC to appear was in the work of Cohen (1931), wherein several bacterial cultures (*Bacterium dysenteriae*, *Corynebacterium diphtheria*, *E. coli* (referred to by Cohen as *Bacterium coli*, although this nomenclature was obsolete even at the time), *Bacillus subtilis*, and *Proteus vulgaris*) were examined to investigate reduction potential of living bacterial cultures relative to a standard hydrogen electrode. As these potentials were found to be significant, it was concluded that theoretically a bacterial culture should be capable of doing electrical work. The investigations of this study explored several major factors in MFCs that would later go on to shape MFC research in the future. Firstly, Cohen comments that the current output from a bacterial culture is typically extremely low, despite the voltage. MFC research has predominantly aimed at finding ways to increasing this current. Second, admitting oxygen into the cell severely degrades the power that can be obtained due to its ability to act as a terminal electron acceptor for the electrons produced by the microorganisms. This is a persistent problem which has led to many MFCs favouring anaerobic modes of oxidation. Thirdly, Cohen (1931) is the first report of introducing secondary redox systems (in this case, either potassium ferricyanide or benzoquinone) to stabilise and enhance electron transfer between the cells and the electrode. While Cohen (1931) does not explore the details of the mechanism by which electron transfer is enhanced, this principle forms the basis of the mediated MFC concept that underlies many of the highest current producing MFCs studied today.

There was another period of relative silence in regard to MFC technology, until an exploratory study by Davis and Yarbrough Jr (1962), investigating the potential of MFCs as a method of degrading hydrocarbons for electrical energy by employing a non-specified strain of *Nocardia* as a bacterial microbial catalyst to oxidise hydrocarbons. These experiments, carried out by the oil industry, were

unfortunately unsuccessful, and the technology was shelved once more, but it does represent the first appearance of the concept of using an MFC to degrade atypical carbon sources or waste streams as a way of generating electricity.

Interest remained low over the following decades, but Pant et al. (2010) reports a 60-fold increase in MFC research over the decade spanning 1998-2008, and an ongoing exponential increase in citations and publications since 2004 (Venkata Mohan et al., 2014). It is likely this dramatic escalation in attention has a great deal to do with the concomitant escalation of awareness and politicisation of concerns about energy costs and environmental sustainability, particularly in regards to fossil fuels consumption and greenhouse gas emissions, which has driven a boom in funding for investigation into alternative energy sources. It would be unfair, however, to discount that novel materials technologies and genetic manipulation technologies have also emerged, opening up additional avenues of investigation.

2.3 Types of MFC: Physical arrangement

2.3.1 Poised Potential MFC

In a poised potential MFC, a potentiostat is use to fix the anode of the MFC at some specified potential, typically with the working electrode serving as the anode and the auxiliary electrode acting as the cathode (Fig. 2.1, A). In practice, the cathode and anode can be in a single compartment (Dumas et al., 2008; Milner et al., 2014; Niessen et al., 2004) in the mode of a single-chambered MFC, or separated by a salt bridge or proton/cation exchange membrane (Bond et al., 2002; Cho and Ellington, 2007; Chou et al., 2014). Functionally, one can interpret this type of arrangement as an analogue of a whole-cell biosensor; essentially it measures the current generated by the cells in a given environment in response to a fixed-potential anode.

A poised-potential mode of operation can also be used as a way of "jump-starting" other kinds of MFC employing microbial components that have long start-up times. The poised potential provides an environment which assists the microbial catalyst in acclimation to functioning in an MFC context and can also help drive forward natural substrate oxidation processes at an accelerated rate (Chou et al., 2013; Wang et al., 2009). Similarly, it can also be used to exert a selection pressure when attempting to develop new variant strains of microbial catalyst species (Yi et al., 2009) or enriching microbial consortia for power production (Finkelstein et al., 2006; Rabaey et al., 2004).

2.3.2 Double-chambered MFC

Double-chambered MFCs are typically defined by having separate compartments for the anode and the cathode, most commonly separated by a proton exchange membrane, a cation exchange membrane or a salt bridge (Fig 2.1, B). Depending on the design, either chamber may contain microorganisms or some fermentation product thereof. Electrons are received by the anode as a result of a redox half-reaction taking place into the anode compartment, travel through an external circuit and are supplied via the cathode to the redox half-reaction taking place in the cathode chamber. This movement of elections is balanced by the migration of protons/cations through the membrane/salt bridge to the cathode chamber. The potential difference between the redox potentials of each of the half reactions provides the driving force for the movement of electrons. They are one of the most heavily studied MFC formats, due to the natural compartmentalisation of the redox half-reactions.

2.3.3 Single-chambered MFC

A single-chambered MFC is simply an MFC which consists of a single chamber containing the microorganisms or some product thereof. The anode is typically positioned inside the chamber, while the cathode may or may not be inside the chamber, depending in the design of the MFC (Fig. 2.1, C). The most common arrangement where the cathode is not inside the chamber is in the case of an air cathode, which may or may not be attached to a proton/cation exchange membrane (Liu and Logan, 2004), although omitting the membrane can potentially introduce unintended oxidation reactions to the chamber.

2.3.4 Environmental MFCs

There are two primary forms of MFC which are designed to exploit their surrounding environment as a substrate: benthic MFCs and photosynthetic MFCs.

Benthic MFCs exploit bed sediments in aquatic/marine environments as a source of both substrate and microorganisms. The most common arrangement in a benthic MFC is to bury the anode in the anaerobic sediments in the bottom of a body of water, and harvest electrons from the microbial oxidation of organic substrates in the sediment. The cathode is suspended in the water column above the anode, using dissolved oxygen in the water as the terminal electron acceptor (Fig. 2.1, D). Such concepts have been implemented successfully in practice, particularly as power sources for scientific instruments studying ocean environments (Kim et al., 2014; Lee et al., 2015; Liu et al., 2015;

Schrader et al., 2016). They also have potential for use in remediating contaminated sediments (Li and Yu, 2015).

Photosynthetic MFCs differ chiefly and most commonly from other MFCs in that photosynthetic microorganisms supply the electrons to the anode rather than heterotrophic ones, and/or photosynthetic organisms are employed in supplying molecular oxygen to the cathode as a terminal electron acceptor. There are however a broad range of different MFCs that are grouped into this category, such as using phototrophs to produce molecular hydrogen to react at a catalytic anode, or photosynthetic/benthic hybrid MFCs exploiting synergistic relationships between sediment heterotrophs and aquatic phototrophs. The common variants are reviewed by Rosenbaum et al. (2010) and the related concepts which branch off from these in McCormick et al. (2015).

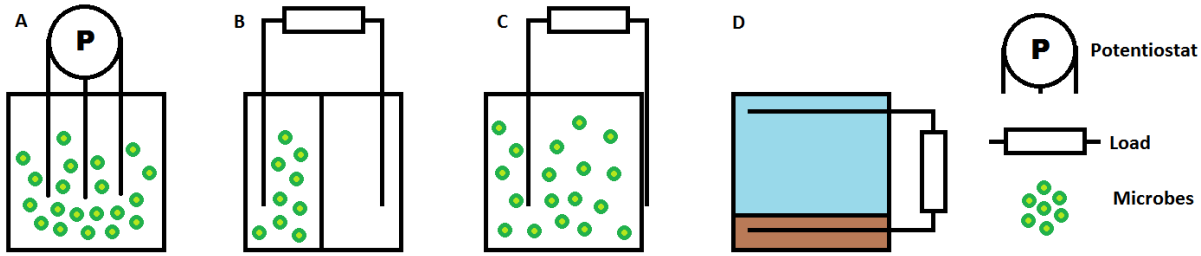

Figure 2.1: Schematic representation of four MFC arrangements: *A*: Poised potential MFC with a potentiostat setting the anode potential; *B*: Double-chambered MFC with a membrane separating the anode and cathode chambers; *C*: Single-chambered MFC with the cathode outside the chamber, exposed to air; *D*: Benthic MFC with the anode buried in sediment and the cathode suspended in the water above.

2.4 Types of MFC: Electron transfer mechanism

There are a many different mechanisms by which an MFC can harvest electrons from the microoragnisms it incorporates, but they can be broadly divided into two main categories: direct electron transfer and mediated electron transfer. These mechanisms are of critical importance, as the rate of extracellular electron transfer is a major limiting factor in the overall power output a particular MFC can attain (Xiao et al., 2013b).

2.4.1 Direct electron transfer

Direct electron transfer is most typically characterised by the transfer of an electron from the microorganism to an electrode without the involvement of any diffusional redox species. The two most common vehicles for this type of electron transfer are membrane-bound proteins and conductive nanowires (pili). This type of electron transfer requires direct physical contact with the electrode, and

as such, microoragnisms suited for being employed as microbial catalysts utilizing this form of electron transfer are limited chiefly to those which form biofilms adhering to the electrode surface.

Amongst the bacteria which have been observed to be able to efficiently transfer electrons directly to an anode as a terminal electron acceptor are *Geobacter*, *Rhodoferax* and *Shewanella* (Bond et al., 2002; Bond and Lovley, 2003; Kim et al., 1999; Kim et al., 2002; Liu et al., 2007). These microorganisms have been shown to possess membrane-bound electron transport proteins (e.g. C-type cytochromes) by which means they transfer electrons from the interior of the cell, through the outer membrane and to the anode surface (Myers and Myers, 1992). Because the transport system is bound directly to the cell surface, only the first layer of cells in a biofilm whose membranes are in direct contact with the anode surface are able to participate in this form of electron transfer.

The second mechanism entails the formation of conductive nanowires, known as pili, which connect surface-bound cytochromes such as those already mentioned, to the surface of the electrode. This allows bacteria which are further away from the anode, for example, cells in an anodic biofilm which are unable to make direct contact with the anode, to conduct electron flow to the anode. *Geobacter* and *Shewanella* have both been observed to have the ability to form such nanowires (Reguera et al., 2005).

2.4.2 Mediated electron transfer

Mediated electron transfer encompasses any form of electron transfer where some redox molecule (referred to as a “mediator”) acts as a shuttle to transport electrons from the cell metabolism to the electrode. Broadly speaking mediated systems may be divided into categories of artificially mediated, where solution species are added to an MFC to enhance electron transfer rates, and self-mediating systems, where one or more of the microoraganisms in the MFC produce their own electron shuttling solution species. While typically a single mediator is employed, double-mediator systems have also been investigated, employing a hydrophobic mediator paired with a hydrophilic one (Baronian et al., 2002; Haslett et al., 2011).

2.4.3 Artificial exogenous mediation

In the absence of direct electron transfer, the electrons involved in microbial metabolism are isolated within the cell, which is typically surrounded by an approximately 7 nm thick non-conductive membrane of lipopolysaccharides and a lipid bilayer with embedded proteins (some of which may participate in transplasma-membrane electron transport). In the case of yeasts, there is additional

chitinous cell wall layer surrounding the membrane, with a 5 nm periplasmic space sandwiched between them. As such, in order transfer electrons from the cell interior or periplasm-facing redox membrane proteins to the electrode, an oxidised species is introduced which is capable of moving across the cell wall and/or membrane to where it can be reduced by electrons from cell metabolism, before moving back across the cell membrane and wall into the anolyte solution. The reduced mediator can then be oxidised at the anode where the electrons are collected. While mediators are commonly added to the solution to facilitate transport of electrons to the anode from microbial catalysts which are not in direct contact with the electrode, they can also be immobilised onto the electrode surface (Ahmed and Kim, 2013; Wang et al., 2011b). The particulars of the mechanism vary with the redox species employed, and a broad range of different substances have been used. Some of these are shown in Table 2.1.

Table 2.1: Examples of artificial mediators

Mediator	**References**
Potassium ferricyanide	Gunawardena et al. (2008)
Neutral red	Babanova et al. (2011); Fathey et al. (2016); Park and Zeikus (2000)
Methylene blue	Babanova et al. (2011); Miroliaei et al. (2015); Mohan et al. (2008); Rahimnejad et al. (2011)
Methyl orange	Babanova et al. (2011); Hosseini and Ahadzadeh (2013)
Methyl red	Babanova et al. (2011); Hosseini and Ahadzadeh (2013)
Bromocresol green	Babanova et al. (2011)
2,3,5,6-tetramethyl-1,4-phenylenediamine	Haslett et al. (2011)
Thionine	Delaney et al. (1984); Rahimnejad et al. (2012); Subramanian and Sugandhraj (2015)
2-hydroxy-1,4-napthoquinone (HNQ)	Taskan et al. (2015)
2-amino-3-carboxy-1,4-napthoquinone (ACNQ)	Freguia et al. (2009); Yamazaki et al. (2002)
Fe(III) EDTA	Deng et al. (2009)
Riboflavin	Pandit et al. (2014)
Resorufin	Bennetto et al. (1983)
Menadione	Baronian et al. (2002)

While introducing an artificial mediator can sometimes be a quick way to realise a significant improvement in power density for an MFC, they often come with various limitations which can make practical, long-term or large-scale implementation difficult. One of these limitations is that many of these mediators, especially the synthetic dyes, are toxic to microorganisms and/or the environment. Toxicity to microorganisms may limit the efficiency obtainable by the MFC through impairing the vigour of the desired metabolic processes in the cells. In cases where a consortium of microbial catalysts is intended to be developed, toxicity will act as an additional selection pressure on the microbial population, potentially acting at cross-purposes to the desired properties of exoelectrogenicity. Toxicity to the environment implies additional processes and costs involved in remediating depleted feedstocks before disposal, either by rendering the mediator non-toxic or by salvaging it for recycling and re-use.

In addition, mediators can often be unstable for long-term use, or expensive for large-scale use. Naturally, these factors are tied together, as if the electron-shuttling capabilities of the mediator become depleted over time (either through degradation in batch systems or simply leaving the system with the depleted substrate in continuous-flow systems), it effectively becomes a feedstock, with the associated costs of continual replenishment. Furthermore, microbial reactors are being studied as a remediation mechanism for the disposal of ecotoxic dyes, including some of those commonly used as mediators (Murali et al., 2013; Yang et al., 2011). This suggests that these mediators will indeed potentially become inert after long term exposure to microbial metabolisms which have the capacity to endure their toxicity; in fact it is not unreasonable to suppose that in the aforementioned consortium selection process alluded to above, microorganisms capable of remediating certain mediators, possibly even as a nutrient source itself, may be selected for (Guo et al., 2014).

2.4.4 Self-mediation

Rather than requiring some additional component to be added to the MFC to serve as a shuttle to permit electron flow from cellular metabolism to the anode, some microorganisms naturally secrete molecules which can function as mediators, and are therefore self-mediating microbial catalysts. In some cases, the production of these electron-shuttling compounds appears to occur in response to being grown in conditions where there is no soluble electron acceptor present and the solid electron acceptor (anode) is some distance from the cell. Phenazine-1-carboxamide and pyocyanin, released by *Pseudomonas aeruginosa*, are two of the more well-studied examples of this phenomenon, being reversible electron shuttles also capable of augmenting electron transfer from other types of bacteria to the anode (Kannaiah Goud and Venkata Mohan, 2013; Rabaey et al., 2005), thereby synergising well with other microorganisms in a microbial consortium. In a similar way, *Propionibacterium freundenreichii* secretes the low molecular weight shuttle 2-amino-3-carboxy-1,4-napthoquinone

(ACNQ), which functions as a growth stimulator for several bacteria and can act as a mediator for NADH oxidation in other bacteria (Yamazaki et al., 2002). It can also be coupled into double-mediator systems with other secreted soluble compounds such as quinones (Freguia et al., 2009). Secreted quinone-containing compounds can also be involved in the reduction of ferric compounds as a source of electrons (Nevin and Lovley, 2000; Scott et al., 1998), such as that carried out by a number of microorganisms, thereby acting as electron shuttles. In general terms, however, such natural mediators tend to be secreted in very small quantities. This can impede their discovery and investigation, as well as their effectiveness when placed into practical contexts as an integral component in MFC-based electricity production.

2.4.5 Fermentation products

A third option, which does not quite fit neatly into the self-mediating category, is the use of fermentation products generated by the microbial component of the MFC, which supply electrons to the circuit by themselves reacting at the electrode. This is as opposed to the self-mediation mode described above, where the secreted molecules act primarily as reversible shuttles to conduct electrons from cell metabolism to anode. An example of such a system is a variant of biohydrogen production, utilising *Clostridium butyricum* and *Clostridium beijerinckii* as the microbial catalysts. While normally in biohydrogen production, the hydrogen is recovered as a desired product, it has been shown that the production can be coupled to *in situ* electricity generation, such that it falls into the category of MFCs (Niessen et al., 2004). In such an arrangement, however, the value of the electricity generated must outweigh the value of the fermentation product being depleted in generating the electricity, less the costs of collection and refining of the product in question. One advantage that *in situ* depletion of fermentation products can have however is in situations where the desired metabolic pathway for generating the product, such as hydrogen, suffers from feedback inhibition based on concentration (Levin et al., 2004). Constant depletion for electricity generation may be able to keep the production rate higher than it would be from conventional recovery processes. The vast majority of the literature focuses however on researching methods of efficient production and recovery of desirable fermentation products rather than using them for electricity generation *in situ*. While one can theoretically couple electricity and product generation using direct electron transfer or mediators, since the desired fermentation products are typically energy rich, such production pathways tend to compete with the flow of electrons to the anode by other means, e.g. in methane-producing MFCs, the vast majority of energy is sequestered in the methane, with only a small amount of electricity being generated (Choi and Ahn, 2014).

2.5 Applications of MFCs

2.5.1 Electricity generation

The conversion of the chemical energy of a substrate into electrical energy has been the central and primary aim of MFC development since Potter's original probative investigations near the beginning of the 20th century. So long as a substance can be metabolised by some microorganism, in theory it can be converted into electricity. Furthermore, the process is not constrained by the Carnot cycle, since electrons are apprehended directly from chemical processes without heat generation, meaning very high efficiencies are theoretically possible.

In terms of use as a standalone power supply, the benthic MFCs mentioned above are one of the most prominent examples. Research is being undertaken incorporating MFCs as on-board power supply units for autonomous robots, but there are significant challenges in terms of energy generation and efficiency that are as yet unsolved (Ieropoulos et al., 2012). This is true in general terms also; scaling up of MFCs from laboratory scale devices to practical sustainable bulk electricity generation, in no small part due to the high capital expenditure required for membrane and electrode materials, especially where noble metals are incorporated (Rozendal et al., 2008). Some examples of power densities from MFCs are shown in Table 2.2.

As a result of these upscaling limitations and bottlenecks, despite many decades of research, MFCs have not managed to rise to any truly significant position as commercial standalone electricity generators. One of the approaches to find a way around some of these issues has been an increasing interest in microscale MFCs. Miniaturised MFCs have certain fundamental design advantages, such as high surface area to volume ratios and short electrode distances. In addition, while the maximum power generation for microscale MFCs is limited, they are much more energy dense than conventional macroscale MFCs, and can be upscaled by being arranged in stacks or arrays to accomplish higher power densities (Aelterman et al., 2006). Investigation into miniature MFC stacks has resulted in the development of a number of promising new concepts, such as a disposable origami paper-based MFC battery running on wastewater (Fraiwan et al., 2016). A thorough review of developments in the field of miniaturised MFC technologies can be found in the review by Choi (2015).

Table 2.2: Examples of power densities in MFCs

Type	Inoculum	Power density	Reference
Single-chamber	Anaerobic activated sludge	6817 mW m^{-3}	You et al. (2006)
Single-chamber	Paper recycling plant wastewater	672 ± 27 mW m^{-2}	Huang and Logan (2008)
Single-chamber	Mixed bacterial culture enriched from domestic wastewater	2900 mW m^{-2}	Catal et al. (2009)
Single-chamber	Domestic wastewater	4200 mW m^{-3}	Sharma and Li (2010)
Single-chamber, air cathode	Anaerobic mixed consortium from brewery	669 mW m^{-2}	Wen et al. (2010)
Single-chamber, air cathode	Domestic wastewater	2110 ± 68 mW m^{-2}	Feng et al. (2011)
Single-chamber, air cathode	Anaerobic mixed consortium from operating MFC	101.2 W m^{-3}	Wen et al. (2011)
Two-chamber	Anaerobic activated sludge	2060 mW m^{-3}	You et al. (2006)
Two-chamber	Anaerobic sludge	1600 mW m^{-2}	Li et al. (2008)
Two-chamber	*Lactobacillus helveticus*, *Proteus mirabilis*, *Escerichia coli*	390 ± 21 W m^{-2}	(Kassongo and Togo, 2011a)
Two-chamber	*Lactobacillus* sp.	1800 ± 120 W m^{-2}	(Kassongo and Togo, 2011b)
Two-chamber	Cassava mill activated sludge wastewater	1771 mW m^{-2}	Kaewkannetra et al. (2011)

2.5.2 Waste treatment

While optimisation of electricity production via MFC technology has many challenges to overcome to achieve more broadly recognised credibility as a source of renewable energy, it has the distinct advantage of being a system uniquely capable of converting organic waste into a source of electricity. This means that MFCs can be used to couple waste treatment processes with electricity generation. For example, wastewater treatment processes such as activated sludge treatment could benefit from MFC technology, which potentially has substantially lower energy requirements than conventional methods (Watanabe, 2008). The power generated could defray costs further. Furthermore, various wastewater compositions which could make them unsuitable for conventional treatments, such as high volatile fatty acid content (Kaspar and Wuhrmann, 1978), could also potentially be addressed using MFC-based processing. Over the past decade, a spectacularly diverse range of industrial, agricultural and municipal wastewaters have been examined for their capacity to serve as organics-rich substrates for MFCs, and in almost all cases the potential exists for MFCs to function as a waste-treatment mechanism (Mathuriya and Yakhmi, 2016). This concept has been further expanded to the microbial oxidation of sediment organic matter, opening up the possibility of *in situ* microbial remediation of contaminated sediments coupled with electricity generation using MFCs (Hong et al., 2010). Such MFC-assisted biodegradation/bioremediation has been demonstrated in a number of studies, including for petroleum-contaminated sediment (Morris and Jin, 2012) and phenol-contaminated soil (Huang et al., 2011).

In addition to their capacity to oxidise organic wastes at the anode, MFCs have also been shown to have great potential for remediation of wastes containing metallic contaminants, causing them to be deposited at the anode or cathode, in some cases even rendering the metals recoverable for further economic benefit. Some examples of metals treated thus include silver (Choi and Cui, 2012), copper (Heijne et al., 2010), cobalt (Huang et al., 2013), chromium (Liu et al., 2011), and arsenic (Xue et al., 2013). Many other remediation processes incorporating MFCs for handling diverse types of waste are being developed, including nitrification/denitification (Virdis et al., 2010), phosphorous recovery (Ichihashi and Hirooka, 2012), selenite removal (Catal et al., 2009) and dye decolourisation (Murali et al., 2013; Solanki et al., 2013), as mentioned in the earlier discussion of artificial mediators. A comprehensive survey of remediation studies incorporating MFCs can be found in the review by Mathuriya and Yakhmi (2016).

2.5.3 Bioproduction

Another way in which electricity production using MFCs can be coupled to another process to add value is by incorporating the production of various fuels and chemicals into the reactions taking place in the cathode or anode chambers. While this is a broad and rapidly expanding field, one example of this is biomethane production. Studies have shown that methanogenic microorganisms can coexist alongside electrogenic ones in an MFC without problems, producing methane alongside electricity (Xiao et al., 2013a). This additional product has a high energy value and could be reclaimed for processing into fuels such as LNG (liquefied natural gas). Another example of coupling biofuel production to MFC technology is hydrogen production (Liu et al., 2005), although the MFC process is often coupled to a microbial electrolysis cell (MEC) system (Sun et al., 2010; Wang et al., 2011a) to improve efficiency by abstracting hydrogen production to a second stage using the energy generated by the MFC stage. Other chemicals that have been shown to be able to be produced using MFC technology include hydrogen peroxide (Fu et al., 2010) and acetic acid (Tanino et al., 2013).

2.6 Yeast MFCs: State of the art

Throughout the majority of MFC research, bacterial species have typically been the microbial catalyst of choice. This is likely because of the relatively well-understood electron transport mechanisms in popular bacterial microbial catalysts from the *Geobacter* and *Shewanella* genera, and these bacterial genera's natural adaptation to use external electron acceptors other than oxygen due to the anaerobic environments of the soils and sediments where they are generally found. Nonetheless, several yeasts have been examined in recent years as biocatalysts for microbial fuel cells, including *Saccharomyces cerevisiae* (Ganguli and Dunn, 2009; Gunawardena et al., 2008; Rahimnejad et al., 2011), *Hansenula anomala* (Amutha et al., 2010; Prasad et al., 2007), *Candida melibiosica* (Hubenova et al., 2014b; Hubenova and Mitov, 2010) and *Arxula adeninivorans* (Haslett et al., 2011).

Yeast as microbial catalysts present some additional challenges over their bacterial counterparts. Possibly the most obvious and significant of these is the fact that as eukaryotes, yeasts have a more complex and compartmentalised structure which localises the bulk of the electrons associated with the respiratory transport chains in the mitochondria, as opposed to the cell membrane, as in prokaryotes. This presents a significant impediment to direct electron transfer from cell to electrode in yeasts. Another confounding factor is that as fungi, yeasts have a chitinous outer cell wall. This wall is typically 100-200 nm thick, and adds a physical barrier between the cell membrane and the environment. While porous, the permeability properties of the wall can vary (Klis et al., 2002), potentially adding an additional impediment to ease of ion and electron transport out of the cell (Hubenova and Mitov, 2015). The chitin component of the cell wall also has charged groups which

can theoretically manifest electrostatic surface effects depending on the pH of the environment, adding yet another complication to transport of charged particles such as electrons and reduced molecules. Despite the challenges, yeasts are nonetheless easy to cultivate and robust against both physical and chemical stresses. Coupled with their diverse range of substrates, these attributes make them attractive as biocatalysts for MFCs, if the difficulties can be overcome.

The difficulties with yeast mediators can be broadly summarised as being kinetics issues with electron mobilisation which are qualitatively similar to those exhibited by their bacterial competitors, and as such, the artificial mediators mentioned earlier in the chapter can resolve these issues. The most commonly employed artificial mediator in studies of yeast-based MFCs is methylene blue, although other molecules, mostly dyes, have been examined also (Table 2.3).

Table 2.3: Some examples of artificially-mediated, yeast-based MFCs

Yeast species	Mediator	Power density	Reference
S. cerevisiae	Methylene blue	400 mW m^{-2}	Wilkinson et al. (2006)
S. cerevisiae	Neutral red	80 mW m^{-2}	Wilkinson et al. (2006)
S. cerevisiae	Methylene blue + Neutral red	500 mW m^{-2}	Wilkinson et al. (2006)
S. cerevisiae	Methylene blue + $K_3[Fe(CN)_6]$	147 mW m^{-3}	Gunawardena et al. (2008)
S. cerevisiae	Methylene blue	150 µW cm^{-2}	Ganguli and Dunn (2009)
S. cerevisiae	Methylene blue	4.4 mW m^{-2}	Rahimnejad et al. (2011)
S. cerevisiae	Thionine	60 mW m^{-2}	Rahimnejad et al. (2012)
S. cerevisiae	Riboflavin	40 mW m^{-2}	Arbianti et al. (2012)
S. cerevisiae	Methylene blue	65 mW m^{-2}	Walker and Walker Jr (2006)
S. cerevisiae	Neutral red	186 mW m^{-2}	Mokhtana et al. (2012)
S. cerevisiae	HNQ	850 W m^{-3}	Kaneshiro et al. (2014)
S. cerevisiae	Methylene blue	110 mW m^{-2}	Rossi et al. (2015)
C. melibiosica	Methylene blue	185 mW m^{-3}	Hubenova and Mitov (2010)
C. melibiosica	Methylene blue	640 mW m^{-2}	Babanova et al. (2011)
C. melibiosica	Neutral red	89 mW m^{-2}	Babanova et al. (2011)
C. melibiosica	Methyl red	113 mW m^{-2}	Babanova et al. (2011)
C. melibiosica	Methyl orange	137 mW m^{-2}	Babanova et al. (2011)
C. melibiosica	Bromocresol green	46 mW m^{-2}	Babanova et al. (2011)
A. adeninivorans	TMPD	1 W m^{-3}	Haslett et al. (2011)

Nonetheless, artificial mediators are, as described previously, problematic for practical implementation in scaled up MFC systems. Solving this problem is where yeasts tend to encounter more challenges than bacteria as biocatalysts. To the extent of current understanding of yeast biocatalysts, direct electron transport solutions such as surface cytochromes and conductive nanowires are generally unavailable. As a result, MFCs which employ yeast as a microbial catalyst without artificial mediators tend to have comparatively low power densities compared to their mediated counterparts (Table 2.4) As such, there is interest in developing electrodes that can overcome these limitations and identifying suitable yeast strains which are capable of naturally producing and secreting redox molecules which can serve as electron shuttles.

Table 2.4: Some examples of yeast-based MFCs which do not employ an artificial mediator or novel anode adornments

Yeast species	**Anode material**	**Power density**	**Reference**
S. cerevisiae	Graphite	26 mW m^{-2}	Raghavulu et al. (2011)
S. cerevisiae	Carbon paper	3 mW m^{-2}	Sayed et al. (2012)
S. cerevisiae	Nickel-coated iron-zinc alloy	4.8 mW m^{-2}	Khan and Naz (2014)
H.anomala	Graphite	0.69 W m^{-3}	Prasad et al. (2007)
C. melibiosica	Carbon felt	20 mW m^{-2}	Babanova et al. (2011)
C. melibiosica	Graphite	70 mW m^{-3}	Hubenova and Mitov (2010)
C. melibiosica	Carbon felt	27 mW m^{-2}	Hubenova et al. (2014b)
C. melibiosica	Carbon felt	45 mW m^{-2}	Hubenova et al. (2014a)
A. adeninivorans	Carbon mesh	70 mW m^{-2}	Haslett et al. (2011)

One approach that has been studied to address the electron transfer problem is modification of the MFC electrodes to interact more favourably with the biocatalyst to the extent that an artificial mediator is unneccessary. Carbon felt anodes adorned with nickel nanoislands have been shown to improve performance of MFCs utilising a *Candida melibiosica* biofilm as the biocatalyst, and it is believed that this improvement is derived from the presence of Ni inducing the expression of electrochemically active metalloprotein complexes on the cell surface, permitting improved direct

electron transfer (Hubenova et al., 2011) and obtaining a peak power density of 720 mW m^{-2} compared with 36 mW m^{-2} without modification. Another technique explored has been to genetically modify *Hansenula polymorpha* cells to overexpress flavocytochrome b_2 (FC b_2) and immobilise them on osmium-polymer-modified graphite electrodes. This close contact between the Os-polymer and cell wall is believed to facilitate penetration of the polymer through the cell wall permitting a direct electrical connection between the electrode and the periplasm-facing side of the FC b_2/L-lactate redox system, resulting in improved power density from the MFC (Shkil et al., 2011). It may not be necessary to form a direct electrical connection through the cell wall however, as Rawson et al. (2012) observed current from a *Saccharomyces cerevisiae* suspension when using an electrode with a covalently bound $Os(bpy)_2Cl$(4-aminomethyl pyridine)/carboxyphenyl film. This film effectively functioned as an immobilised mediator layer, with the Os(III) centres appearing to be reduced by electrons from the cell wall, then being re-oxidised by the electrode. The roughness of the mediator film was determined to be insufficient to facilitate penetration of the cell wall invoked by Shkil et al. (2011) as an explanation for increased power density. Regardless, neither of these approaches has been implemented in a functional standalone MFC unit, and given the relatively exotic nature of materials used, the practicality of upscale seems doubtful at this stage. Similarly, Prasad et al. (2007) reported high power densities from MFCs using cultures of *Hansenula anomala* adsorbed to graphite electrodes modified with polyaniline and platinum (2.9 W m^{-3}), however Pt catalysts present capital cost problems for upscale. The same study also reported high power densities using graphite felt (2.34 W m^{-3}), which may be more economical. In either case, direct electron transfer between the cell and electrode is apparent, and this is attributed to the presence of lactate dehydrogenase and ferricyanide reductase in the cell membrane. The authors do not, however, address the apparent permeability of the cell wall to electrons in this case. By way of comparison, Sayed et al. (2012) reports a non-mediated MFC utilising *Saccharomyces cerevisiae* and carbon paper electrodes, where it was concluded that the relatively low power density of 3 mW m^{-2} was attributable solely to cells in surface contact with the anode, a conclusion also reported by Kasem et al. (2013). However, Sayed et al. (2015) later concluded that yeast extract, included in the anolyte solution employed in Sayed et al. (2012), can operate in the capacity of a mediator with *Saccharomyce cerevisiae*-catalysed MFCs. Curiously, Sayed et al. (2015) reports a power density of 12.9 mW m^{-2} in the non-mediated case, improving to 32.6 mW m^{-2} with yeast extract present, but when the carbon paper electrode was sputtered with gold, the non-mediated performance decline to 2 mW m^{-2} whilst the mediated cell improved to 70 mW m^{-2}.

An alternative approach to anode modification is to directly modify the yeasts themselves to manifest novel direct electron transfer capabilities. One example of such a modification is the use of the yeast surface display system (Boder and Wittrup, 1997) to display proteins on the surface of yeast cells which may have the capability of carrying out direct electron transfer. Gal et al. (2016) uses this system to display two different hydrogenases, cellobiose dehydrogenase from *Corynascus*

thermophilus and pyranose dehydrogenase from *Agaricus meleagris*, on the surface of *S. cerevisiae*. *S. cerevisiae* cells with these surface displayed enzymes were used as microbial catalysts in the anode chamber of a mediatorless MFC, with a resulting power density for cellobiose dehydrogenase of 3.3 μW cm^{-2} (33 mW m^{-2}) using lactose as feedstock and for pyranose dehydrogenase, 3.9 μW cm^{-2} (39 mW m^{-2}) using D-xylose as feedstock.

In all of these cases, electron transfer is accomplished by direct cell-surface-to-electrode-surface contact, up to and including actual adsorption to the electrode surface. As mentioned previously, this constraint limits the microbial catalyst to a single layer of cells directly adhering to the electrode. While developing materials with greater surface area and higher affinity for promoting yeast biofilm formation is one way to increase the biomass of microbial catalyst able to be utilised by an MFC, power density can also be improved by identifying yeasts which can carry out indirect electron transfer.

Candida melibiosica cell suspensions and supernatant recovered from such suspensions by centrifugation have been studied using cyclic voltammetry, which revealed a metabolite with anodic and cathodic peaks at +225 mV and -45 mV (vs. Ag/AgCl) respectively (Hubenova et al., 2011), albeit with a substantial discrepancy in peak size. This is indicative of a molecule with quasi-reversible redox chemistry being secreted into the bulk solution. This exoelectrogenic property is the hallmark of a microorganism which may have the capacity to serve as a self-mediating MFC catalyst.

The other yeast which has been noted to secrete a solution species bearing electrons is the subject of this thesis, *Arxula adeninivorans*.

2.7 *Arxula adeninivorans* as a microbial catalyst

Arxula adeninivorans (also known as *Trichosporon adeninivorans*, sometimes also referred to a *Blastobotrys adeninivorans*) is an ascomycetous, arthroconidial, anamorphic, xerotolerant yeast. It was originally isolated from a soil sample, and was noted at that time to be able to utilise amines and purine compounds as a sole source of carbon and nitrogen and energy (Middelhoven et al., 1984). Upon further investigation, it was found that *A. adeninivorans* was capable of metabolising an uncommonly diverse range of carbon compounds, including many benzene compounds and phenylacetic acid derivatives (Middelhoven et al., 1991). It has also been shown that *A. adeninivorans* exhibits a high degree of temperature tolerance, growing at temperatures up to 48 °C, allowing it to be cultivated at a broad range of incubation temperatures. These increased temperatures do however trigger an environmentally-induced change in morphology from yeast to mycelial morphology at temperatures in excess of 42 °C (Wartmann et al., 1995). This shift in morphology triggers a change

in the levels of secreted proteins, with two-fold increases in glucoamylase and invertase in particular (Wartmann et al., 2000), however the details of the precise conditions and mechanisms involved in the change in morphology are not well-studied. *A. adeninivorans* has also been noted to be halotolerant (Yang et al., 2000) and pH tolerant, with maximal growth between pH 2.8 and 6.5, but potential growth between pH 2 and 10 (Stöckmann et al., 2014).

These attributes of broad substrate range and robustness to physiochemical stress are all favourable for use of *A. adeninivorans* as a microbial catalyst, particularly for an MFC which may be intended to utilise e.g. waste streams of variable or unknown composition as feedstocks. It was on this logic that Haslett et al. (2011) selected *A. adeninivorans* as the microbial catalyst in a yeast-based microbial fuel cell utilising potassium permanganate as the cathode electron acceptor. In this study, suspensions of *A. adeninivorans* were found to generate a much higher power density as a microbial catalyst for an MFC operating in a mediatorless mode compared to *S. cerevisiae* used in the same apparatus. *A. adeninivorans* was shown to produce short term surges in power density up to 70 mW m^{-2}, and a power output of approximately 28 mW m^{-2} after 30 minutes of continuous operation was reported. A study of the reduction of the hydrophilic mediator potassium ferricyanide showed that the electrons accessible from the cell membrane proteins in each of the two yeasts was approximately the same. Further investigation using cyclic voltammetry to examine cell creams of the two yeasts revealed the presence of an oxidation peak at +0.42 V (vs Ag/AgCl) in *A. adeninivorans* that was absent in *S. cerevisiae*. As this oxidation peak occurs at a more positive potential than the redox potential for ferricyanide (+0.28 V vs Ag/AgCl), the study of ferricyanide reduction would have excluded any contribution of this oxidation peak from detection. Plotting the faradic current of the oxidation peak against varying scan rates showed that peak current was proportional to the square root of the scan rate, which indicated that peak current magnitude is diffusion controlled and therefore indicative of a solution species. This was further confirmed by investigating freshly prepared cell creams of *A. adeninivorans*. Cyclic voltammetry did not reveal any oxidation peak in fresh cell creams, but grew progressively larger the long the cell cream was incubated. This suggests that the oxidation peak is the result of a secreted species that accumulates in the extracellular buffer over time.

In light of the discovery of this secreted exoelectrogenic molecule, *A. adeninivorans* was tentatively identified as a potential candidate microbial catalyst for a self-mediating MFC. This thesis is aimed at investigating the identity of this molecule, and its potential to be exploited as a naturally produced mediator for MFCs.

2.8 Electrochemical analytical techniques

The essential element of *A. adeninivorans*' potential value as a catalyst for a self-mediating MFC lies with the unknown reduced solution species and its associated redox behaviour. In order to investigate the behaviour of this molecule relative to an electrode, two main electrochemical techniques were employed: cyclic voltammetry (CV) and linear sweep voltammetry (LSV). Fundamentally, both of these techniques function by means of using a potentiostat to control the potential of a working electrode relative to a reference electrode, returning electrons to the solution being studied by means of an auxiliary electrode. This arrangement is called a three-electrode configuration. The potentiostat is used to vary the potential at the working electrode according to the user-specified wave excitation form such that the behaviour of the current generated as a function of the potential can be studied.

2.8.1 The three-electrode configuration

The three electrodes used in these techniques are typically designated the "working electrode", "reference electrode" and the "auxiliary electrode", sometimes referred to as a "counter electrode" (Fig. 2.1).

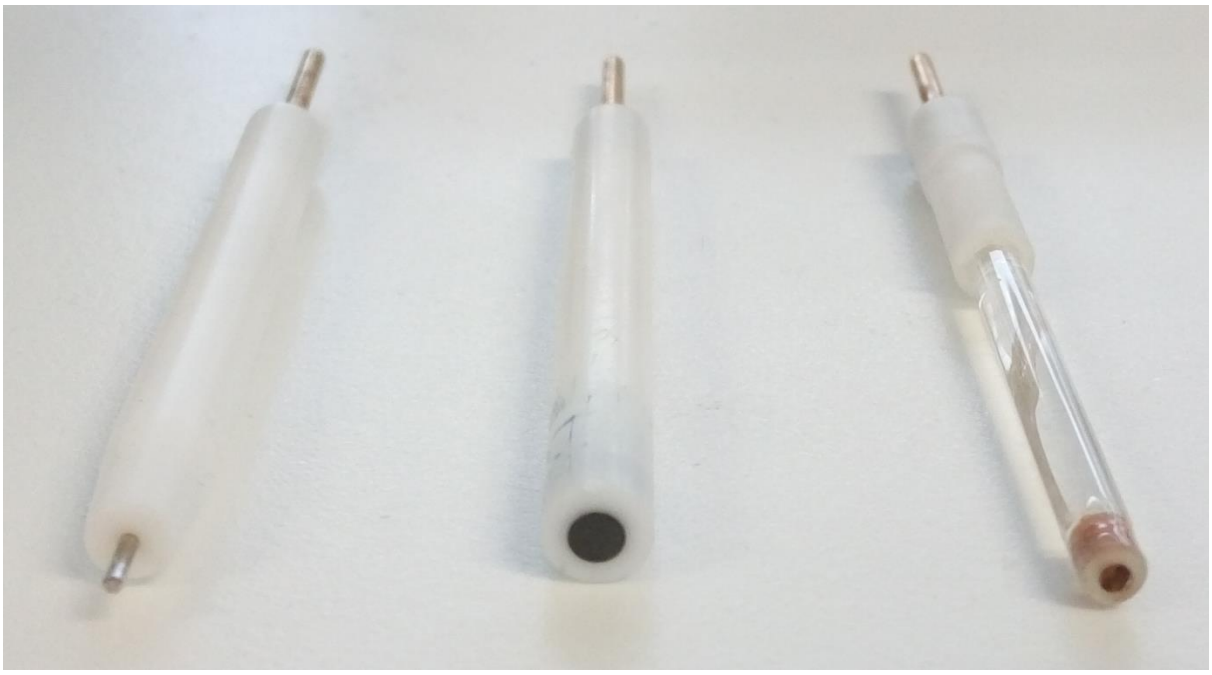

Figure 2.2: The three electrodes used in CV. *Left*: auxiliary electrode. *Centre*: working electrode. *Right*: reference electrode.

The auxiliary electrode is the simplest in design of the three, serving primarily as a simple conductor to complete the circuit by returning electrons to the solution at the rate that they are being transferred

to the working electrode. In the studies described in this thesis, the auxiliary electrode was made of platinum wire.

The reference electrode serves as a fixed potential relative to which the potentiostat will vary the potential at the working electrode. It is important that this electrode have a known, stable standard electrode potential, but that the electrode must have a sufficiently high internal resistance to prevent it from participating in the reactions being studied. In the studies described in this thesis, the reference electrode used is a Ag/AgCl reference electrode, comprising a silver wire in a 3M KCl solution, with a standard electrode potential of + 0.210 V.

The working electrode provides the anode surface on which the redox reaction being studied will take place. As such, its geometry has a profound effect on what the reaction looks like from the point of view of measuring the current generated. For the purposes of this thesis, working electrodes can be divided into two main categories: macro electrodes and micro electrodes. The macro electrode used in this thesis is a glassy carbon macrodisc of diameter 2 mm (area 3.1416 mm^2), while the micro electrode is a platinum microdisc of diameter 100 µm (area 0.007854 mm^2). The main effect of the differing areas on the reaction as observed is derived from the influence that the area has on the dominant mode of diffusion. In general terms, the smaller the electrode surface is, the higher the rate of mass transport to and from the surface of the electrode will be.

To put this in terms of the two types of electrodes described here, the mass transfer to and from the surface of the microdisc electrode is dominated by radial diffusion, which is relatively rapid, whereas the mass transfer to and from the surface of the macrodisc electrode tends to be dominated by planar diffusion, which is comparatively slower. In the latter case, there is a higher propensity for mass transport to become the rate-limiting factor, as the diffusion layer (the region of bulk solution affected by the reaction at the electrode) expands to the point that the solution local to the electrode surface is functionally depleted of the reduced molecule being examined. This makes this technique useful for examining the potential most favourable to the redox reaction taking place at the electrode. By contrast, the faster mass transfer rates taking place at the microdisc make it a better choice for examining the steady-state behaviour of the reduced molecule. In practical terms, as it applies to the design of the experiments carried out in this thesis, the macrodisc electrode is used for CV, while the microdisc is employed for LSV studies.

2.8.2 Cyclic voltammetry (CV)

Cyclic voltammetry derives its name from the wave excitation form employed to determine the pattern of variation in potential at the working electrode. In CV, the potential of the working electrode

is varied at a fixed scan rate from one potential to another, most commonly increasing from a more negative potential to a more positive one, then at the same rate, varied back to the starting potential. This forms one "cycle" of sweeping the voltage up, then back to the starting point, and may be repeated multiple times depending on the experiment. The scan rates used in CV tend to be relatively fast, to take advantage of the rate-limiting diffusion at the macro electrode.

In general terms, the form of a cyclic voltammogram for a solution containing a redox species will have a peak in current, i_p, at some potential E_{ox} on the forward sweep and, if the oxidation is reversible, a corresponding inverted peak at some potential E_{red}, where the formal redox potential $E°$ is the average of E_{ox} and E_{red}. The area between the peak and the extrapolated linear trend before the peak represents the amount of charge transferred. An example of a cyclic voltammogram is shown in Fig. 2.2.

As the potential moves from negative to positive, it rises past $E°$ for the redox couple, causing the concentration of the reduced species to rapidly decrease relative to the oxidised species, generating current from the electrons transferred to the working electrode as it does so. This is modelled using the Nernst equation (Eqn. 1.1).

$$E = E° + \frac{2.3RT}{nF}\log\frac{C_{ox}}{C_{red}} \qquad \text{(Equation 1.1)}$$

In this expression, E is the potential (in V), $E°$ is the formal redox potential of the redox couple in question (in V), R is the universal gas constant (8.314 J mol^{-}1 K^{-1}), T is the temperature (in K), n is the number of electrons transferred per molecule, F is the Faraday constant (9.648×10^4 C mol^{-1}), C_{ox} is the concentration of the oxidised species of the redox couple at the electrode, and C_{red} is the concentration of the reduced species of the redox couple at the electrode.

As the reduced form of the molecule is converted into the oxidised form, a concentration gradient relative to the bulk concentration of the solution forms at the electrode surface. Because of the rapid scan rate (in this thesis, a rate of 100 mV s^{-1} is used) quickly making the oxidation reaction more favourable, coupled with the planar diffusion characteristics of a macro electrode, the diffusion layer expands, making the concentration gradient becomes less steep over time as depletion of the reduced form outpaces diffusion from the bulk solution. Eventually the reduced form is effectively entirely depleted at the electrode surface, resulting in the peak in current described above, i_p, which can be predicted using the Randles-Sevick equation (Eqn. 1.2).

$$i_p = 0.4463\, nFAC\left(\frac{nF\upsilon D}{RT}\right)^{\frac{1}{2}} \qquad \text{(Equation 1.2)}$$

In this expression, n is the number of electrons transferred per molecule, F is the Faraday constant (9.648×10^4 C mol^{-1}), A is the electrode area (in cm^2), C is the concentration of the species in the bulk solution (in mol cm^{-3}), v is the scan rate (in V s^{-1}), D is the diffusion coefficient (in cm^2 s^{-1}), R is the universal gas constant (8.314 J mol^{-1} K^{-1}) and T is the temperature (in K).

Under these conditions, beyond the point where i_p occurs, the reaction, and therefore the current generated, becomes completely diffusion controlled, and can now be described by the Cottrell equation (Eqn. 1.3):

$$i = \frac{nFACD^{\frac{1}{2}}}{(\pi t)^{\frac{1}{2}}} \qquad \text{(Equation 1.3)}$$

In this expression, i is the current (in A) n is the number of electrons transferred per molecule, F is the Faraday constant (9.648×10^4 C mol^{-1}), A is the electrode area (in cm^2), C is the concentration of the species in the bulk solution (in mol cm^{-3}), D is the diffusion coefficient (in cm^2 s^{-1}) and t is time (in s).

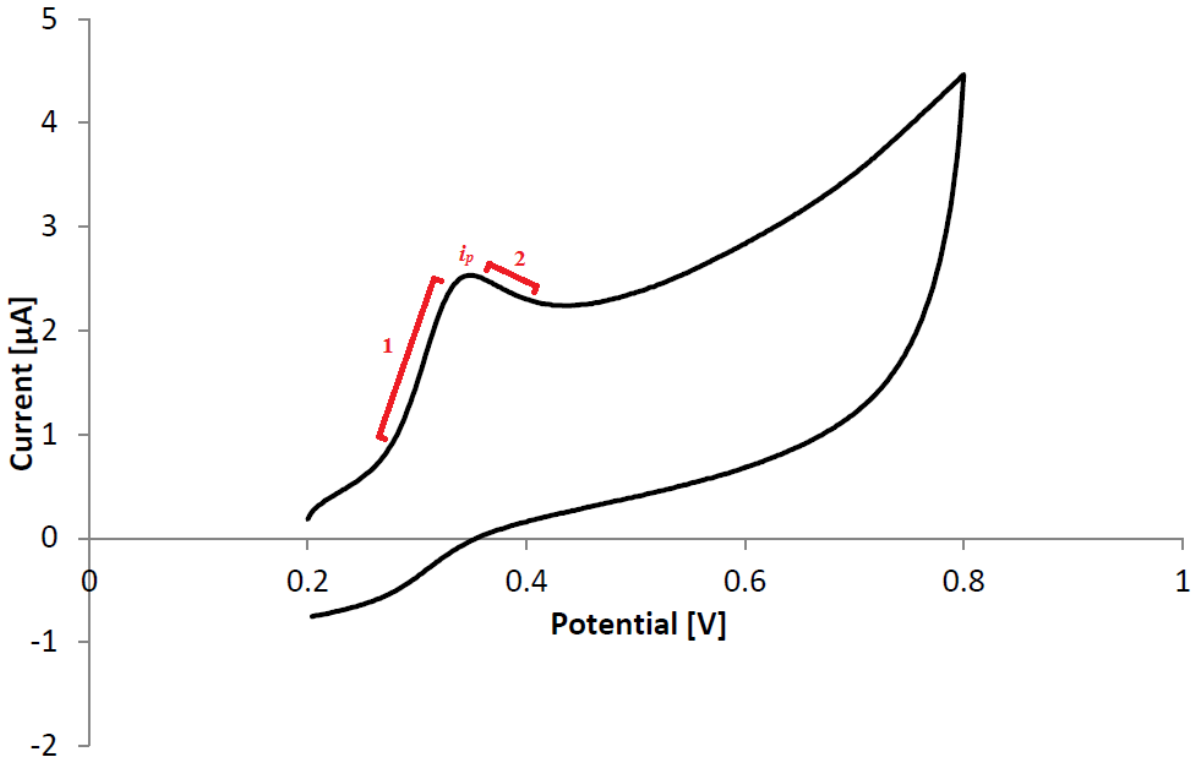

Figure 2.3: An example of a cyclic voltammogram for a quasi-irreversible oxidation. The peak at +0.35 V represents the oxidation of a redox molecule in the solution. Region 1 is modelled with Eqn. 1.1 and region 2 by Eqn. 1.3. Eqn. 1.2 can be used to predict peak current i_p.

2.8.3 Linear sweep voltammetry (LSV)

Linear sweep voltammetry also derives its name from the wave excitation form determining the variation in potential. In this case, the potential is simply swept from one potential to another at a fixed rate. LSV typically uses a slow scan rate, coupled with the radial diffusion characteristics of a micro-electrode to examine the current at steady state at a given potential; that is, it seeks to minimise the effects of diffusion rate on the rate of reaction at the working electrode. The typical LSV graph has a shape akin to that of a sigmoid curve (Fig. 2.3). In the case of the microdisc working electrode used in this thesis, it would be more properly defined as a pseudo-microdisc, as 100 µm is a somewhat large diameter for this purpose. To compensate for this and preserve as much of the steady-state character as possible, an extremely slow scan rate of 5 mV s^{-1} is used for LSV in this thesis.

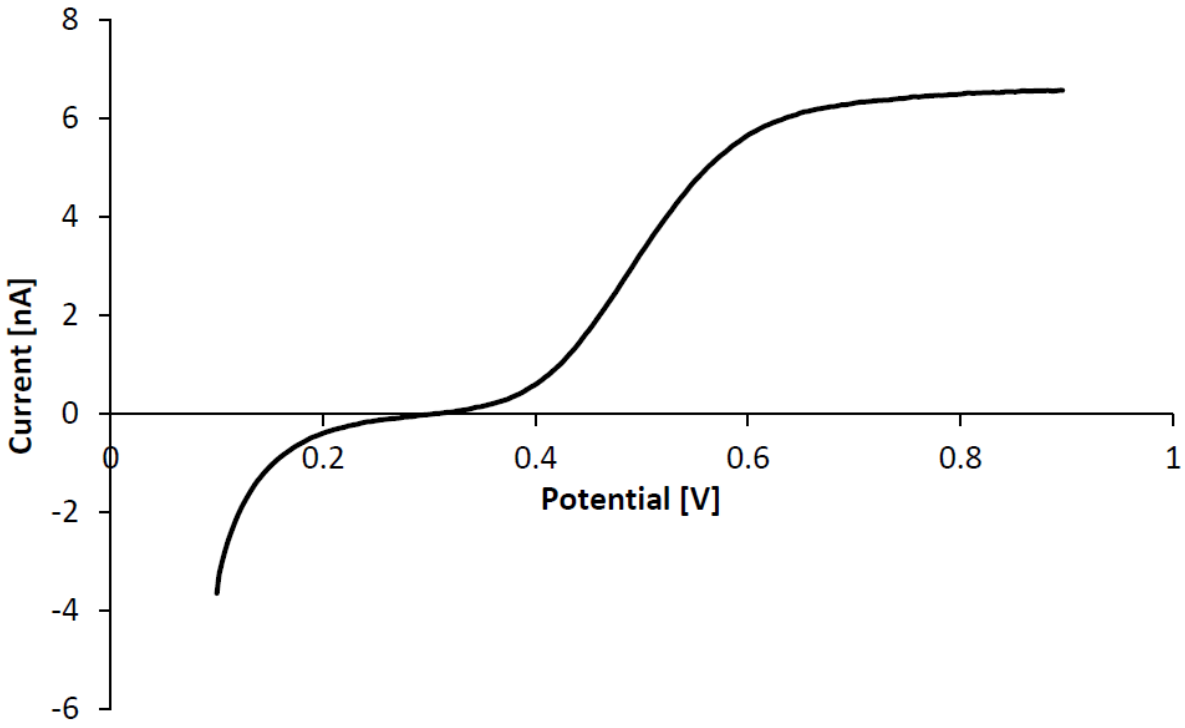

Figure 2.4: An example of a linear sweep voltammogram. The "step" in current between +0.25 V and +0.75 V represents the increasing current generated by oxidation of the redox molecule in the solution at steady-state as the potential becomes more positive.

2.9 References

Aelterman, P., Rabaey, K., Pham, H.T., Boon, N., and Verstraete, W. (2006). Continuous electricity generation at high voltages and currents using stacked microbial fuel cells. Environmental Science and Technology *40*, 3388-3394.

Ahmed, J., and Kim, S. (2013). Menadione-modified anodes for power enhancement in single chamber microbial fuel cells. Bulletin of the Korean Chemical Society *34*, 3649-3653.

Amutha, R., Josiah, J.J.M., Adriel Jebin, J., Jagannathan, P., and Berchmans, S. (2010). Chromium hexacyanoferrate as a cathode material in microbial fuel cells. Journal of Applied Electrochemistry *40*, 1985-1990.

Arbianti, R., Hermansyah, H., Utami, T.S., Zahara, N.C., Trisnawati, I., and Kristin, E. (2012). The usage of *Saccharomyces cerevisiae* in Microbial Fuel Cell System for Electricity Enegy Production. Journal of Chemistry and Chemical Engineering *6*, 814-819.

Babanova, S., Hubenova, Y., and Mitov, M. (2011). Influence of artificial mediators on yeast-based fuel cell performance. Journal of Bioscience and Bioengineering *112*, 379-387.

Baronian, K., Downard, A., Lowen, R., and Pasco, N. (2002). Detection of two distinct substrate-dependent catabolic responses in yeast cells using a mediated electrochemical method. Applied Microbiology and Biotechnology *60*, 108-113.

Bennetto, H.P., Stirling, J.L., Tanaka, K., and Vega, C.A. (1983). Anodic reactions in microbial fuel cells. Biotechnology and Bioengineering *25*, 559-568.

Boder, E.T., and Wittrup, K.D. (1997). Yeast surface display for screening combinatorial polypeptide libraries. Nature Biotechnology *15*, 553-557.

Bond, D.R., Holmes, D.E., Tender, L.M., and Lovley, D.R. (2002). Electrode-reducing microorganisms that harvest energy from marine sediments. Science *295*, 483-485.

Bond, D.R., and Lovley, D.R. (2003). Electricity production by *Geobacter sulfurreducens* attached to electrodes. Applied and Environmental Microbiology *69*, 1548-1555.

Catal, T., Bermek, H., and Liu, H. (2009). Removal of selenite from wastewater using microbial fuel cells. Biotechnology Letters *31*, 1211-1216.

Cho, E.J., and Ellington, A.D. (2007). Optimization of the biological component of a bioelectrochemical cell. Bioelectrochemistry *70*, 165-172.

Choi, C., and Cui, Y. (2012). Recovery of silver from wastewater coupled with power generation using a microbial fuel cell. Bioresource Technology *107*, 522-525.

Choi, J., and Ahn, Y. (2014). Increased power generation from primary sludge in microbial fuel cells coupled with prefermentation. Bioprocess and Biosystems Engineering *37*, 2549-2557.

Choi, S. (2015). Microscale microbial fuel cells: Advances and challenges. Biosensors and Bioelectronics *69*, 8-25.

Chou, T.Y., Whiteley, C.G., and Lee, D.J. (2014). Anodic potential on dual-chambered microbial fuel cell with sulphate reducing bacteria biofilm. International Journal of Hydrogen Energy *39*, 19225-19231.

Chou, T.Y., Whiteley, C.G., Lee, D.J., and Liao, Q. (2013). Control of dual-chambered microbial fuel cell by anodic potential: Implications with sulfate reducing bacteria. International Journal of Hydrogen Energy *38*, 15580-15589.

Cohen, B. (1931). The Bacterial Culture as a Microbial Half-cell. Journal of Bacteriology *21*, 18-19.
Davis, J.B., and Yarbrough Jr, H.F. (1962). Preliminary experiments on a microbial fuel cell. Science *137*, 615-616.

Delaney, G.M., Bennetto, H.P., Mason, J.R., Roller, S.D., Stirling, J.L., and Thurston, C.F. (1984). ELECTRON-TRANSFER COUPLING IN MICROBIAL FUEL CELLS. 2. PERFORMANCE OF FUEL CELLS CONTAINING SELECTED MICROORGANISM-MEDIATOR-SUBSTRATE COMBINATIONS. Journal of chemical technology and biotechnology Biotechnology *34 B*, 13-27.

Deng, L.F., Zhou, S.G., Zhang, J.T., Zhuang, L., Lu, N., and Zhang, L.X. (2009). Sustainable electricity generation in microbial fuel cells using Fe(III)-EDTA as cathodic electron shuttle. Huanjing Kexue/Environmental Science *30*, 2142-2147.

Dumas, C., Basseguy, R., and Bergel, A. (2008). Microbial electrocatalysis with Geobacter sulfurreducens biofilm on stainless steel cathodes. Electrochimica Acta *53*, 2494-2500.

Fathey, R., Gomaa, O.M., Ali, A.E.H., El Kareem, H.A., and Zaid, M.A. (2016). Neutral red as a mediator for the enhancement of electricity production using a domestic wastewater double chamber microbial fuel cell. Annals of Microbiology *66*, 695-702.

Feng, Y., Yang, Q., Wang, X., Liu, Y., Lee, H., and Ren, N. (2011). Treatment of biodiesel production wastes with simultaneous electricity generation using a single-chamber microbial fuel cell. Bioresource Technology *102*, 411-415.

Finkelstein, D.A., Tender, L.M., and Zeikus, J.G. (2006). Effect of electrode potential on electrode-reducing microbiota. Environmental Science and Technology *40*, 6990-6995.

Fraiwan, A., Kwan, L., and Choi, S. (2016). A disposable power source in resource-limited environments: A paper-based biobattery generating electricity from wastewater. Biosensors and Bioelectronics *85*, 190-197.

Freguia, S., Masuda, M., Tsujimura, S., and Kano, K. (2009). Lactococcus lactis catalyses electricity generation at microbial fuel cell anodes via excretion of a soluble quinone. Bioelectrochemistry *76*, 14-18.

Fu, L., You, S.-J., Yang, F.-l., Gao, M.-m., Fang, X.-h., and Zhang, G.-q. (2010). Synthesis of hydrogen peroxide in microbial fuel cell. Journal of Chemical Technology & Biotechnology *85*, 715-719.

Gal, I., Schlesinger, O., Amir, L., and Alfonta, L. (2016). Yeast surface display of dehydrogenases in microbial fuel-cells. Bioelectrochemistry *112*, 53-60.

Ganguli, R., and Dunn, B.S. (2009). Kinetics of Anode Reactions for a Yeast-Catalysed Microbial Fuel Cell. Fuel Cells *9*, 44-52.

Gunawardena, A., Fernando, S., and To, F. (2008). Performance of a yeast-mediated biological fuel cell. International Journal of Molecular Sciences *9*, 1893-1907.

Guo, W., Feng, J., Song, H., and Sun, J. (2014). Simultaneous bioelectricity generation and decolorization of methyl orange in a two-chambered microbial fuel cell and bacterial diversity. Environmental Science and Pollution Research *21*, 11531-11540.

Haslett, N.D., Rawson, F.J., Barrière, F., Kunze, G., Pasco, N., Gooneratne, R., and Baronian, K.H.R. (2011). Characterisation of yeast microbial fuel cell with the yeast *Arxula adeninivorans* as the biocatalyst. Biosensors and Bioelectronics *26*, 3742-3747.

Heijne, A.T., Liu, F., Weijden, R.V.D., Weijma, J., Buisman, C.J.N., and Hamelers, H.V.M. (2010). Copper recovery combined with electricity production in a microbial fuel cell. Environmental Science and Technology *44*, 4376-4381.

Hong, S.W., Kim, H.S., and Chung, T.H. (2010). Alteration of sediment organic matter in sediment microbial fuel cells. Environmental Pollution *158*, 185-191.

Hosseini, M.G., and Ahadzadeh, I. (2013). Electrochemical impedance study on methyl orange and methyl red as power enhancing electron mediators in glucose fed microbial fuel cell. Journal of the Taiwan Institute of Chemical Engineers *44*, 617-621.

Huang, D.Y., Zhou, S.G., Chen, Q., Zhao, B., Yuan, Y., and Zhuang, L. (2011). Enhanced anaerobic degradation of organic pollutants in a soil microbial fuel cell. Chemical Engineering Journal *172*, 647-653.

Huang, L., Li, T., Liu, C., Quan, X., Chen, L., Wang, A., and Chen, G. (2013). Synergetic interactions improve cobalt leaching from lithium cobalt oxide in microbial fuel cells. Bioresource Technology *128*, 539-546.

Huang, L., and Logan, B.E. (2008). Electricity generation and treatment of paper recycling wastewater using a microbial fuel cell. Applied Microbiology and Biotechnology *80*, 349-355.

Hubenova, Y., Georgiev, D., and Mitov, M. (2014a). Enhanced phytate dephosphorylation by using Candida melibiosica yeast-based biofuel cell. Biotechnology Letters *36*, 1993-1997.

Hubenova, Y., Georgiev, D., and Mitov, M. (2014b). Stable current outputs and phytate degradation by yeast-based biofuel cell. Yeast *31*, 343-348.

Hubenova, Y., and Mitov, M. (2010). Potential application of *Candida melibiosica* in biofuel cells. Bioelectrochemistry *78*, 57-61.

Hubenova, Y., and Mitov, M. (2015). Extracellular electron transfer in yeast-based biofuel cells: A review. Bioelectrochemistry *106*, 177-185.

Hubenova, Y.V., Rashkov, R.S., Buchvarov, V.D., Arnaudova, M.H., Babanova, S.M., and Mitov, M.Y. (2011). Improvement of yeast-biofuel cell output by electrode modifications. Industrial and Engineering Chemistry Research *50*, 557-564.

Ichihashi, O., and Hirooka, K. (2012). Removal and recovery of phosphorus as struvite from swine wastewater using microbial fuel cell. Bioresource Technology *114*, 303-307.

Ieropoulos, I.A., Greenman, J., Melhuish, C., and Horsfield, I. (2012). Microbial fuel cells for robotics: Energy autonomy through artificial symbiosis. ChemSusChem *5*, 1020-1026.

Kaewkannetra, P., Chiwes, W., and Chiu, T.Y. (2011). Treatment of cassava mill wastewater and production of electricity through microbial fuel cell technology. Fuel *90*, 2746-2750.

Kaneshiro, H., Takano, K., Takada, Y., Wakisaka, T., Tachibana, T., and Azuma, M. (2014). A milliliter-scale yeast-based fuel cell with high performance. Biochemical Engineering Journal *83*, 90-96.

Kannaiah Goud, R., and Venkata Mohan, S. (2013). Prolonged applied potential to anode facilitate selective enrichment of bio-electrochemically active Proteobacteria for mediating electron transfer: Microbial dynamics and bio-catalytic analysis. Bioresource Technology *137*, 160-170.

Kasem, E.T., Tsujiguchi, T., and Nakagawa, N. (2013). Effect of metal modification to carbon paper anodes on the performance of yeast-based microbial fuel cells part I: In the case without exogenous mediator. In Key Engineering Materials, pp. 76-81.

Kaspar, H.F., and Wuhrmann, K. (1978). Product inhibition in sludge digestion. Microbial Ecology *4*, 241-248.

Kassongo, J., and Togo, C.A. (2011a). The impact of electrode reuse on the biofilm community and performance of whey-fuelled H-type microbial fuel cell. African Journal of Microbiology Research *5*, 1090-1096.

Kassongo, J., and Togo, C.A. (2011b). Performance improvement of whey-driven microbial fuel cells by acclimation of indigenous anodophilic microbes. African Journal of Biotechnology *10*, 7846-7852.

Khan, A.M., and Naz, S. (2014). Biopower generation from kitchen wastewater using a bioreactor. Water Environment Research *86*, 3-12.

Kim, B.H., Kim, H.J., Hyun, M.S., and Park, D.H. (1999). Direct electrode reaction of Fe(III)-reducing bacterium, Shewanella putrefaciens. Journal of Microbiology and Biotechnology *9*, 127-131.

Kim, G., Wolfe, A., Bell, R., Bang, S., Lee, Y., Lee, I., Kim, Y., Hsu, L., Kagan, J., Arias-Thode, M., *et al.* (2014). Chip-on-mud: Ultra-low power ARM-based oceanic sensing system powered by small-scale benthic microbial fuel cells. Paper presented at: Proceedings - IEEE International Symposium on Circuits and Systems.

Kim, H.J., Park, H.S., Hyun, M.S., Chang, I.S., Kim, M., and Kim, B.H. (2002). A mediator-less microbial fuel cell using a metal reducing bacterium, *Shewanella putrefaciens*. Enzyme and Microbial Technology *30*, 145-152.

Klis, F.M., Mol, P., Hellingwerf, K., and Brul, S. (2002). Dynamics of cell wall structure in Saccharomyces cerevisiae. FEMS Microbiology Reviews *26*, 239-256.

Lee, I., Kim, G., Bang, S., Wolfe, A., Bell, R., Jeong, S., Kim, Y., Kagan, J., Arias-Thode, M., Chadwick, B., *et al.* (2015). System-On-Mud: Ultra-Low Power Oceanic Sensing Platform Powered by Small-Scale Benthic Microbial Fuel Cells. IEEE Transactions on Circuits and Systems I: Regular Papers *62*, 1126-1135.

Levin, D.B., Pitt, L., and Love, M. (2004). Biohydrogen production: Prospects and limitations to practical application. International Journal of Hydrogen Energy *29*, 173-185.

Li, W.W., and Yu, H.Q. (2015). Stimulating sediment bioremediation with benthic microbial fuel cells. Biotechnology Advances *33*, 1-12.

Li, Z., Zhang, X., and Lei, L. (2008). Electricity production during the treatment of real electroplating wastewater containing Cr6+ using microbial fuel cell. Process Biochemistry *43*, 1352-1358.

Liu, B., Weinstein, A., Kolln, M., Garrett, C., Wang, L., Bagtzoglou, A., Karra, U., Li, Y., and Li, B. (2015). Distributed multiple-anodes benthic microbial fuel cell as reliable power source for subsea sensors. Journal of Power Sources *286*, 210-216.

Liu, H., Grot, S., and Logan, B.E. (2005). Electrochemically assisted microbial production of hydrogen from acetate. Environmental Science and Technology *39*, 4317-4320.

Liu, H., and Logan, B.E. (2004). Electricity generation using an air-cathode single chamber microbial fuel cell in the presence and absence of a proton exchange membrane. Environmental Science and Technology *38*, 4040-4046.

Liu, L., Yuan, Y., Li, F.B., and Feng, C.H. (2011). In-situ Cr(VI) reduction with electrogenerated hydrogen peroxide driven by iron-reducing bacteria. Bioresource Technology *102*, 2468-2473.

Liu, Z.D., Du, Z.W., Lian, J., Zhu, X.Y., Li, S.H., and Li, H.R. (2007). Improving energy accumulation of microbial fuel cells by metabolism regulation using Rhodoferax ferrireducens as biocatalyst. Letters in Applied Microbiology *44*, 393-398.

Mathuriya, A.S., and Yakhmi, J.V. (2016). Microbial fuel cells - Applications for generation of electrical power and beyond. Critical Reviews in Microbiology *42*, 127-143.

McCormick, A.J., Bombelli, P., Bradley, R.W., Thorne, R., Wenzel, T., and Howe, C.J. (2015). Biophotovoltaics: Oxygenic photosynthetic organisms in the world of bioelectrochemical systems. Energy and Environmental Science *8*, 1092-1109.

Middelhoven, W.J., de Jong, I.M., and de Winter, M. (1991). *Arxula adeninivorans*, a yeast assimilating many nitrogenous and aromatic compounds. Antonie van Leeuwenhoek *59*, 129-137.

Middelhoven, W.J., Niet, M.C.H.T., and Rij, N.J.W.K.V. (1984). Trichosporon adeninovorans sp. nov., a yeast species utilizing adenine, xanthine, uric acid, putrescine and primary n-alkylamines as the sole source of carbon, nitrogen and energy. Antonie van Leeuwenhoek *50*, 369-378.

Milner, E., Scott, K., Head, I., Curtis, T., and Yu, E. (2014). Electrochemical investigation of aerobic biocathodes at different poised potentials: Evidence for mediated extracellular electron transfer. In Chemical Engineering Transactions, pp. 355-360.

Miroliaei, M.R., Samimi, A., Mohebbi-Kalhori, D., and Khorram, M. (2015). Kinetics investigation of diversity cultures of E. coli and Shewanella sp., and their combined effect with mediator on MFC performance. Journal of Industrial and Engineering Chemistry *25*, 42-50.

Mohan, Y., Manoj Muthu Kumar, S., and Das, D. (2008). Electricity generation using microbial fuel cells. International Journal of Hydrogen Energy *33*, 423-426.

Mokhtana, N., Daud, W.R.W., Rahimnejad, M., and Najafpouv, G.D. (2012). Bioelectricity generation in biological fuel cell with and without mediators. World Applied Sciences Journal *18*, 559-567.

Morris, J.M., and Jin, S. (2012). Enhanced biodegradation of hydrocarbon-contaminated sediments using microbial fuel cells. Journal of Hazardous Materials *213-214*, 474-477.

Murali, V., Ong, S.A., Ho, L.N., Wong, Y.S., and Hamidin, N. (2013). Comprehensive review and compilation of treatment for azo dyes using microbial fuel cells. Water Environment Research *85*, 270-277.

Myers, C.R., and Myers, J.M. (1992). Localization of cytochromes to the outer membrane of anaerobically grown *Shewanella putrefaciens* MR-1. Journal of Bacteriology *174*, 3429-3438.

Nevin, K.P., and Lovley, D.R. (2000). Potential for nonenzymatic reduction of Fe(III) via electron shuttling in subsurface sediments. Environmental Science and Technology *34*, 2472-2478.

Niessen, J., Schröder, U., and Scholz, F. (2004). Exploiting complex carbohydrates for microbial electricity generation - A bacterial fuel cell operating on starch. Electrochemistry Communications *6*, 955-958.

Pandit, S., Khilari, S., Roy, S., Pradhan, D., and Das, D. (2014). Improvement of power generation using Shewanella putrefaciens mediated bioanode in a single chambered microbial fuel cell: Effect of different anodic operating conditions. Bioresource Technology *166*, 451-457.

Pant, D., Van Bogaert, G., Diels, L., and Vanbroekhoven, K. (2010). A review of the substrates used in microbial fuel cells (MFCs) for sustainable energy production. Bioresource Technology *101*, 1533-1543.

Park, D.H., and Zeikus, J.G. (2000). Electricity generation in microbial fuel cells using neutral red as an electronophore. Applied and Environmental Microbiology *66*, 1292-1297.

Potter, M.C. (1911). Electrical Effects Accompanying the Decomposition of Organic Compounds. Proceedings of the Royal Society of London B: Biological Sciences *84*, 260-276.

Prasad, D., Arun, S., Murugesan, M., Padmanaban, S., Satyanarayanan, R.S., Berchmans, S., and Yegnaraman, V. (2007). Direct electron transfer with yeast cells and construction of a mediatorless microbial fuel cell. Biosensors and Bioelectronics *22*, 2604-2610.

Rabaey, K., Boon, N., Höfte, M., and Verstraete, W. (2005). Microbial phenazine production enhances electron transfer in biofuel cells. Environmental Science and Technology *39*, 3401-3408.

Rabaey, K., Boon, N., Siciliano, S.D., Verhaege, M., and Verstraete, W. (2004). Biofuel cells select for microbial consortia that self-mediate electron transfer. Applied and Environmental Microbiology *70*, 5373-5382.

Raghavulu, S.V., Goud, R.K., Sarma, P.N., and Mohan, S.V. (2011). Saccharomyces cerevisiae as anodic biocatalyst for power generation in biofuel cell: Influence of redox condition and substrate load. Bioresource Technology *102*, 2751-2757.

Rahimnejad, M., Najafpour, G.D., Ghoreyshi, A.A., Shakeri, M., and Zare, H. (2011). Methylene blue as electron promoters in microbial fuel cell. International Journal of Hydrogen Energy *36*, 13335-13341.

Rahimnejad, M., Najafpour, G.D., Ghoreyshi, A.A., Talebnia, F., Premier, G.C., Bakeri, G., Kim, J.R., and Oh, S.E. (2012). Thionine increases electricity generation from microbial fuel cell using Saccharomyces cerevisiae and exoelectrogenic mixed culture. Journal of Microbiology *50*, 575-580.

Rawson, F.J., Gross, A.J., Garrett, D.J., Downard, A.J., and Baronian, K.H.R. (2012). Mediated electrochemical detection of electron transfer from the outer surface of the cell wall of Saccharomyces cerevisiae. Electrochemistry Communications *15*, 85-87.

Reguera, G., McCarthy, K.D., Mehta, T., Nicoll, J.S., Tuominen, M.T., and Lovley, D.R. (2005). Extracellular electron transfer via microbial nanowires. Nature *435*, 1098-1101.

Rosenbaum, M., He, Z., and Angenent, L.T. (2010). Light energy to bioelectricity: Photosynthetic microbial fuel cells. Current Opinion in Biotechnology *21*, 259-264.

Rossi, R., Fedrigucci, A., and Setti, L. (2015). Characterization of electron mediated microbial fuel cell by Saccharomyces Cerevisiae. In Chemical Engineering Transactions, pp. 337-342.

Rozendal, R.A., Hamelers, H.V.M., Rabaey, K., Keller, J., and Buisman, C.J.N. (2008). Towards practical implementation of bioelectrochemical wastewater treatment. Trends in Biotechnology *26*, 450-459.

Sayed, E.T., Barakat, N.A.M., Abdelkareem, M.A., Fouad, H., and Nakagawa, N. (2015). Yeast extract as an effective and safe mediator for the baker's-yeast-based microbial fuel cell. Industrial and Engineering Chemistry Research *54*, 3116-3122.

Sayed, E.T., Tsujiguchi, T., and Nakagawa, N. (2012). Catalytic activity of baker's yeast in a mediatorless microbial fuel cell. Bioelectrochemistry *86*, 97-101.

Schrader, P.S., Reimers, C.E., Girguis, P., Delaney, J., Doolan, C., Wolf, M., and Green, D. (2016). Independent benthic microbial fuel cells powering sensors and acoustic communications with the MARS underwater observatory. Journal of Atmospheric and Oceanic Technology *33*, 607-617.

Scott, D.T., McKnight, D.M., Blunt-Harris, E.L., Kolesar, S.E., and Lovley, D.R. (1998). Quinone moieties act as electron acceptors in the reduction of humic substances by humics-reducing microorganisms. Environmental Science and Technology *32*, 2984-2989.

Sharma, Y., and Li, B. (2010). Optimizing energy harvest in wastewater treatment by combining anaerobic hydrogen producing biofermentor (HPB) and microbial fuel cell (MFC). International Journal of Hydrogen Energy *35*, 3789-3797.

Shkil, H., Schulte, A., Guschin, D.A., and Schuhmann, W. (2011). Electron transfer between genetically modified Hansenula polymorpha yeast cells and electrode surfaces via os-complex modified redox polymers. ChemPhysChem *12*, 806-813.

Solanki, K., Subramanian, S., and Basu, S. (2013). Microbial fuel cells for azo dye treatment with electricity generation: A review. Bioresource Technology *131*, 564-571.

Stöckmann, C., Palmen, T.G., Schroer, K., Kunze, G., Gellissen, G., and Büchs, J. (2014). Definition of culture conditions for *Arxula adeninivorans*, a rational basis for studying heterologous gene expression in this dimorphic yeast. Journal of Industrial Microbiology and Biotechnology *41*, 965-976.

Subramanian, K., and Sugandhraj, B. (2015). Bioelectricity from sugar factory effluent through a microbial fuel cell in presence of mediators. Asian Journal of Microbiology, Biotechnology and Environmental Sciences *17*, 615-621.

Sun, M., Mu, Z.X., Sheng, G.P., Shen, N., Tong, Z.H., Wang, H.L., and Yu, H.Q. (2010). Hydrogen production from propionate in a biocatalyzed system with in-situ utilization of the electricity generated from a microbial fuel cell. International Biodeterioration and Biodegradation *64*, 378-382.

Tanino, T., Nara, Y., Tsujiguchi, T., and Ohshima, T. (2013). Coproduction of acetic acid and electricity by application of microbial fuel cell technology to vinegar fermentation. Journal of Bioscience and Bioengineering *116*, 219-223.

Taskan, E., Ozkaya, B., and Hasar, H. (2015). Combination of a novel electrode material and artificial mediators to enhance power generation in an MFC. Water Science and Technology *71*, 320-328.

Venkata Mohan, S., Velvizhi, G., Annie Modestra, J., and Srikanth, S. (2014). Microbial fuel cell: Critical factors regulating bio-catalyzed electrochemical process and recent advancements. Renewable and Sustainable Energy Reviews *40*, 779-797.

Virdis, B., Rabaey, K., Rozendal, R.A., Yuan, Z., and Keller, J. (2010). Simultaneous nitrification, denitrification and carbon removal in microbial fuel cells. Water Research *44*, 2970-2980.

Walker, A.L., and Walker Jr, C.W. (2006). Biological fuel cell and an application as a reserve power source. Journal of Power Sources *160*, 123-129.

Wang, A., Sun, D., Cao, G., Wang, H., Ren, N., Wu, W.M., and Logan, B.E. (2011a). Integrated hydrogen production process from cellulose by combining dark fermentation, microbial fuel cells, and a microbial electrolysis cell. Bioresource Technology *102*, 4137-4143.

Wang, K., Liu, Y., and Chen, S. (2011b). Improved microbial electrocatalysis with neutral red immobilized electrode. Journal of Power Sources *196*, 164-168.

Wang, X., Feng, Y., Ren, N., Wang, H., Lee, H., Li, N., and Zhao, Q. (2009). Accelerated start-up of two-chambered microbial fuel cells: Effect of anodic positive poised potential. Electrochimica Acta *54*, 1109-1114.

Wartmann, T., Erdmann, J., Kunze, I., and Kunze, G. (2000). Morphology-related effects on gene expression and protein accumulation of the yeast *Arxula adeninivorans* LS3. Archives of Microbiology *173*, 253-261.

Wartmann, T., Krüger, A., Adler, K., Duc, B.M., Kunze, I., and Kunze, G. (1995). Temperature-dependent dimorphism of the yeast *Arxula adeninivorans* Ls3. Antonie van Leeuwenhoek *68*, 215-223.

Watanabe, K. (2008). Recent Developments in Microbial Fuel Cell Technologies for Sustainable Bioenergy. Journal of Bioscience and Bioengineering *106*, 528-536.

Wen, Q., Kong, F., Zheng, H., Cao, D., Ren, Y., and Yin, J. (2011). Electricity generation from synthetic penicillin wastewater in an air-cathode single chamber microbial fuel cell. Chemical Engineering Journal *168*, 572-576.

Wen, Q., Wu, Y., Zhao, L., and Sun, Q. (2010). Production of electricity from the treatment of continuous brewery wastewater using a microbial fuel cell. Fuel *89*, 1381-1385.

Wilkinson, S., Klar, J., and Applegarth, S. (2006). Optimizing biofuel cell performance using a targeted mixed mediator combination. Electroanalysis *18*, 2001-2007.

Xiao, B., Yang, F., and Liu, J. (2013a). Evaluation of electricity production from alkaline pretreated sludge using two-chamber microbial fuel cell. Journal of Hazardous Materials *254-255*, 57-63.

Xiao, Y., Wu, S., Zhang, F., Wu, Y.C., Yang, Z.H., and Zhao, F. (2013b). Promoting electrogenic ability of microbes with negative pressure. Journal of Power Sources *229*, 79-83.

Xue, A., Shen, Z.Z., Zhao, B., and Zhao, H.Z. (2013). Arsenite removal from aqueous solution by a microbial fuel cell-zerovalent iron hybrid process. Journal of Hazardous Materials *261*, 621-627.

Yamazaki, S.I., Kaneko, T., Taketomo, N., Kano, K., and Ikeda, T. (2002). Glucose metabolism of lactic acid bacteria changed by quinone-mediated extracellular electron transfer. Bioscience, Biotechnology and Biochemistry *66*, 2100-2106.

Yang, X.X., Wartmann, T., Stoltenburg, R., and Kunze, G. (2000). Halotolerance of the yeast *Arxula adeninivorans* LS3. Antonie van Leeuwenhoek, International Journal of General and Molecular Microbiology *77*, 303-311.

Yang, Y.Y., Du, L.N., Wang, G., Jia, X.M., and Zhao, Y.H. (2011). The decolorisation capacity and mechanism of *Shewanella oneidensis* MR-1 for Methyl Orange and Acid Yellow 199 under microaerophilic conditions. Water Science and Technology *63*, 956-963.

Yi, H., Nevin, K.P., Kim, B.C., Franks, A.E., Klimes, A., Tender, L.M., and Lovley, D.R. (2009). Selection of a variant of Geobacter sulfurreducens with enhanced capacity for current production in microbial fuel cells. Biosensors and Bioelectronics *24*, 3498-3503.

You, S.J., Zhao, Q.L., Jiang, J.Q., Zhang, J.N., and Zhao, S.Q. (2006). Sustainable approach for leachate treatment: Electricity generation in microbial fuel cell. Journal of Environmental Science and Health - Part A Toxic/Hazardous Substances and Environmental Engineering *41*, 2721-2734.

Chapter 3

Identification of the unknown redox molecule secreted by *Arxula adeninivorans*

3.1 Introduction

In the process of investigating the potential of *A. adeninivorans* for use as a biocatalyst in a microbial fuel cell (MFC), it was observed to transport electrons out of cells by means of exporting an electrochemically active reduced molecule (Haslett et al., 2011). The property of being able to provide easily accessible extracellular electrons in this way (exoelectrogenicity) adds an intriguing additional facet to *A. adeninivorans*' potential for use in a microbial fuel cell, in that it could potentially obviate the necessity of mediator molecules, which are often impractical to employ outside of batch systems.

Haslett et al. (2011) reported that cyclic voltammograms (CVs) of *A. adeninivorans* cell creams and samples of supernatant derived from them showed an apparently irreversible oxidation peak at +0.42 V and they determined that the peak was generated by a solution species that rapidly accumulated in extracellular buffer. They also reported that the peak potential was independent of pH in the pH 4-12 range but would shift in the positive direction as the pH decreased further. By contrast, such an oxidation peak appeared to be barely detectable in CVs of *Saccharomyces cerevisiae* cell creams after several days of incubation, where it was readily detectable in CVs of *A. adeninivorans* after a matter of hours.

In order to determine the identity of the unknown exoelectrogenic molecule, *A. adeninivorans* was cultured at temperatures observed to induce the culture to secrete a high concentration of the molecule into the supernatant. The supernatant was then isolated and the unknown molecule identified using a combination of high performance liquid chromatography (HPLC), UV spectroscopy, mass spectrometry (MS) and cyclic voltammetry (CV).

3.2 Materials and methods

3.2.1 Yeast strains, media, buffers and growth conditions

Six different strains of *A. adeninivorans* were used in this study. The wild-type strain, *A. adeninivorans* LS3 was isolated from wood hydrolysates from Siberia, Russia (Gienow et al., 1990)

and deposited as *A. adeninivorans* SBUG 724 in the strain collection of the Department of Biology of the University of Greifswald. *A. adeninivorans* 135 is a mutant strain derived from LS3, selected for expression of mycelial morphology at 30°C (Wartmann et al., 2000). *A. adeninivorans* G1212 (*aleu2 atrp1::ALEU2*) is a mutant strain developed as a selectable auxotrophic gene expression platform from *A. adeninivorans* G1211 (*aleu2*), replacing its leucine auxotrophy with tryptophan auxotrophy. *A. adeninivorans* G1212/YRC102 is a G1212 transformant containing an empty YRC102 vector, used as a control to exclude vector-only effects on the cell (Trautwein-Schult et al., 2013). *A. adeninivorans* G1212/YRC102-AYNI1-AUOR39 and G1212/YRC102-AYNI1-AUOR94 are G1212 transformants containing a YRC102 vector with an inserted *AYNI1* promoter-*AUOR* gene-*PHO5* terminator expression module which gives strong $NaNO_3$-inducible expression of the *AUOR* gene. All strains were obtained from the Leibniz Institute of Plant Genetics and Crop Plant Research (IPK), Gatersleben, Germany.

A. adeninivorans LS3, 135 and G1212 were grown under non-selective conditions for 20 hours at 37°C in a yeast extract peptone dextrose (YEPD) broth medium [yeast extract 10 g L^{-1} (Oxoid, LP0021, Oxoid Limited, Basingstoke, Hampshire RG24 8PW, UK), peptone 20 g L^{-1} (Oxoid, LP0044, Oxoid Limited, Basingstoke, Hampshire RG24 8PW, UK), dextrose 20 g L^{-1} (LabServ, AR, Thermo Fisher Scientific Australia Pty Ltd., Scoresby, Vic 3179, Australia) sterilised at 121°C], aerated by agitation in 250 mL indented flasks in a shaking incubator. Agar plates were prepared by addition of 15 g L^{-1} agar to the liquid media.

A. adeninivorans G1212/YRC102, G1212/YRC102-AYNI1-AUOR39 and G1212/YRC102-AYNI1-AUOR94 were grown under non-selective conditions for 20 hours at 37°C in a yeast nitrogen base (YNB) medium with ammonium, prepared as a 10-times concentrate [YNB (w/o ammounium sulphate or amino acids) 17 g L^{-1} (Difco, Franklin Lakes, NJ, USA), dextrose 200 g L^{-1}, ammonium sulphate 50 g L^{-1}] or YNB medium with nitrate, prepared as a 10-times concentrate [YNB (w/o ammounium sulphate or amino acids) 17 g L^{-1}, dextrose 200 g L^{-1}, sodium nitrate 36.55 g L^{-1}, sterilised by 0.45 µm filtration]. 10 mL of concentrate was added to 90 mL sterile deionised (DI) water. Cultures were aerated by agitation in a shaking incubator.

Cell cultures were grown in two stages. A pre-culture was prepared using a single colony from a YEPD agar plate culture to inoculate 100 mL of YEPD or YNB in a 250 mL indented culture flask and grown as described above. Experimental cell cultures were prepared using 1 mL of pre-culture as the inoculum and incubating under the same conditions.

Cell pellets were re-suspended in a variant of phosphate-buffered saline (PBS) adapted for use in electrochemistry (0.05 M K_2HPO_4/KH_2PO_4, 0.1 M KCl).

3.2.2 Electrochemistry

CV was performed using the ADInstruments PowerLab 2/20 with ML160 Potentiostat, using eDAQ EChem v2.5.4 data logging software (both eDAQ Pty Ltd., Denistone East, Australia). A three electrode configuration comprising a glassy carbon working electrode (2 mm diameter, Tianjin Aida Hengsheng Technology Co. Ltd., Nankai, Tianjin, China), platinum counter electrode and a Ag/AgCl reference electrode (3 M KCl) (G-Glass, Victoria, Australia) was used for voltammetry. The glassy carbon electrode was polished between each scan using aluminium oxide powder (0.3 μm, LECO, St Joseph, MI, USA) on a Lecloth (LECO, St Joseph, MI, USA). All CVs were performed in a Faraday cage and were scanned from +0.2 V to +0.8 V at 100 mV s^{-1} with three replicate CVs recorded for each sample. Measured potentials are vs. Ag/AgCl/3M KCl unless otherwise stated.

3.2.3 Accumulation of secreted electrochemically active molecule

Cells were harvested from the culture medium by centrifugation (Eppendorf Centrifuge 5810R) at an acceleration of 6797×g (8000 rpm on the aforementioned centrifuge) and a temperature of 4 °C for 10 minutes. The growth medium supernatant was then discarded, and the cells washed twice by re-suspending the cell pellet in 15 mL sterile DI water, centrifuging and discarding the supernatant. The wet weight of the pellet was determined and the cells re-suspended in PBS, 1:1 *w*/*v*. The airspace above the cell suspension was then flushed with N_2 gas to displace excess air, and the cells incubated anaerobically for 20 h at 37 °C or 47 °C with gentle agitation to keep the cells suspended. The cells were then centrifuged at 6797×g and 4 °C for 10 minutes, and the supernatant recovered and filtered through 0.45 μm pore filters. Supernatant samples that were not used immediately were sparged for 10 min with N_2 gas and stored in a sealed vessel under N_2 gas at 4 °C.

3.2.4 Preparation of supernatant samples for HPLC/MS

Cells were harvested, washed and weighed in the same manner as above. The cell pellet was then re-suspended in DI water, 1:1: *w*/*v*. The airspace above the cell suspension was then flushed with N_2 gas to displace excess air, and the cells incubated anaerobically for 72 h at 47 °C with gentle agitation to keep the cells suspended. The cells were then centrifuged at 6797×g and 4°C for 10 minutes, and the supernatant recovered and filtered twice through 0.45 μm pore filters.

3.2.5 HPLC isolation

100 µL of sample supernatant was separated on a 250 mm x 4.60 mm Phenomenex Jupiter C18 column (Torrance, CA, USA) at 20 °C ± 3 °C at a flowrate of 1.0 mL/min. An iterative series of separation protocols were tested in the process of identifying, isolating and collecting the desired electroactive molecule. The final separation protocol converged upon was 0 % acetonitrile/ 100 % water for 7 min, increasing linearly to 30 % acetonitrile/70 % water over 4 min, holding at this ratio for 2 min, increasing linearly to 100 % acetonitrile/0 % water over 2 min, holding at this ratio for 2 min, decreasing linearly to 0 % acetonitrile/100 % water over 2 min and re-equilibrating for 5 min. Absorbance peaks at 210 nm were detected using a Dionex UltiMate 3000 Diode Array Detector, and fractions corresponding to peaks were collected using a Dionex ASI-100 Autosampler (Sunnyvale, CA, USA).

3.2.6 MS analysis

High-resolution mass spectrometric data was collected on a maXis 3G UHR-Qq-TOF mass spectrometer (Bruker Daltonik GmbH, Bremen, Germany) coupled to a Dionex UltiMate 3000 LC system (Thermo Fisher Scientific Inc., Waltham, Ma, USA). 5 µL of sample was injected into a flow of 50:50 water (0.5 % formic acid)/acetonitrile at 0.2 mL/min. 5 µL of ESI-L Low Concentration Tuning Mix (Agilinet Technologies, Santa Clara, CA, USA) was injected after each sample to calibrate the system.

3.3 Results

3.3.1 Electrochemistry of the secreted electrochemically active molecule

CVs of supernatant derived from dense cell suspensions of *A. adeninivorans* LS3 (Fig. 3.1, a), 135 (Fig. 3.1, b) and G1212 (Fig. 3.1, c) were performed to investigate the oxidation peak described by Haslett et al. (2011). In all three strains, an oxidation peak was observed corresponding to the one previously reported, however in all cases, the anodic peak potential was slightly lower than the +0.42 V reported by Haslett et al. (2011) (table 3.1), falling in the range +0.388 V to +0.398 V for cell suspensions incubated at 37 °C and +0.369 V to +0.404 V for cell suspensions incubated at 47 °C.

In all three strains, a substantial increase in the area of the oxidation peaks was observed for cell suspensions incubated at 47 °C compared with those incubated at 37 °C (table 3.2), indicating a higher concentration of the electrochemically active molecule was present in the sample. This increase was somewhat less pronounced in the G1212 strain.

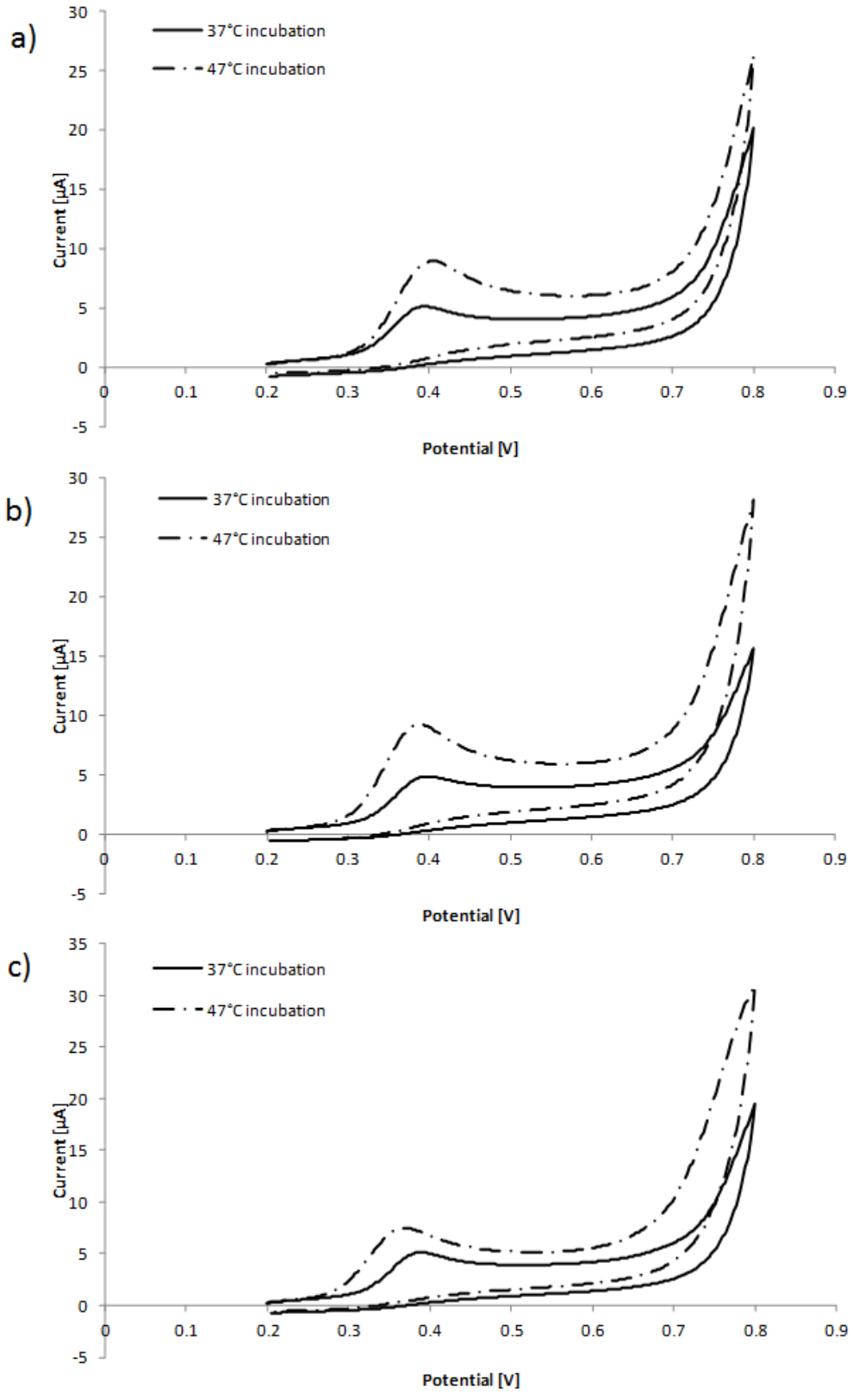

Figure 3.1: CVs for *A. adeninivorans* strains LS3 (a), 135 (b) and G1212 (c), showing the increased size of the oxidation peak between +0.35 V and +0.45 V in supernatants of dense cell suspensions incubated at 47°C compared with those incubated at 37°C.

Table 3.1: The peak anodic potentials of the unknown electrochemically active molecule under investigation. These figures are comparable to, but universally lower than, the value of +0.42 V reported by Haslett et al. (2011).

Strain	37 °C condition	47 °C condition
LS3	0.395 V	0.404 V
135	0.398 V	0.385 V
G1212	0.388 V	0.369 V

Table 3.2: The estimated area of the oxidation peaks of the unknown electrochemically active molecule under investigation. In LS3 and 135, the 47 °C condition yields more than a 2-fold increase in charge transferred. G1212 still shows an increase in charge transfer, but to a lesser extent.

Strain	37 °C condition	47 °C condition
LS3	3.79 µA.s	8.27 µA.s
135	3.71 µA.s	8.67 µA.s
G1212	3.74 µA.s	6.63 µA.s

Where Haslett et al. (2011) reported that the unknown electrochemically active solution species underwent an apparently irreversible oxidation process, close examination of the CVs of these supernatants reveals what may be a shallow reduction peak in the vicinity of +0.31 V (fig. 3.2). This suggests that either there is another electrochemically active molecule, one which undergoes reversible oxidation, with an oxidation peak subsumed by the primary one observed, or that the putative irreversibly oxidised electrochemically active molecule previously reported is in fact sparingly reversible.

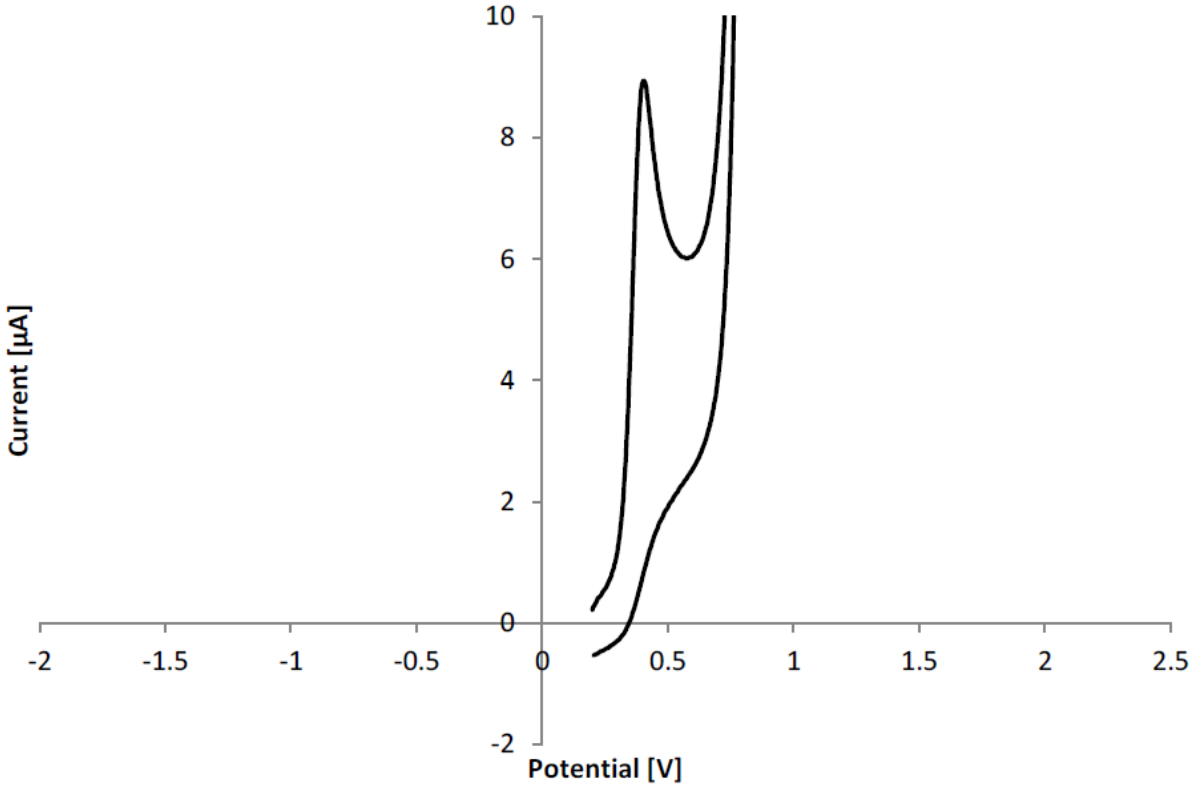

Figure 3.2: A CV of a supernatant from a dense cell suspension of *A. adeninivorans* LS3. With the CV trace compressed along the x-axis, a bulge in the reduction trace can be seen in the vicinity of +0.31 V. This is indicative of a reduction process taking place at the electrode.

3.3.2 Isolation and purification of the secreted electrochemically active molecule

Several HPLC protocols were used to attempt to isolate the electrochemically active molecule in a single elution peak. CV was used on collected fractions corresponding to peaks to determine if the desired molecule was present.

The initial purification attempts employed a simple concentration gradient of 10 % acetonitrile/90 % water increasing to 75 % acetonitrile/25 % water over 12 minutes. Early purification attempts used supernatants derived from cells that had been suspended in PBS, but this produced a broad over-range peak eluting at low acetonitrile concentrations, which was likely to conceal peak detail (Fig. 3.3). Electrochemical activity was detected in the fractions corresponding to these broad peaks, suggesting the electrochemically active molecule was likely to be polar. This protocol was repeated on a supernatant sample derived from cells which had been suspended in DI water. Eliminating the excess salts from the buffer clarified the early-eluting peaks somewhat (Fig. 3.4), but they remained broad, and electrochemical activity was still detected in the first peak.

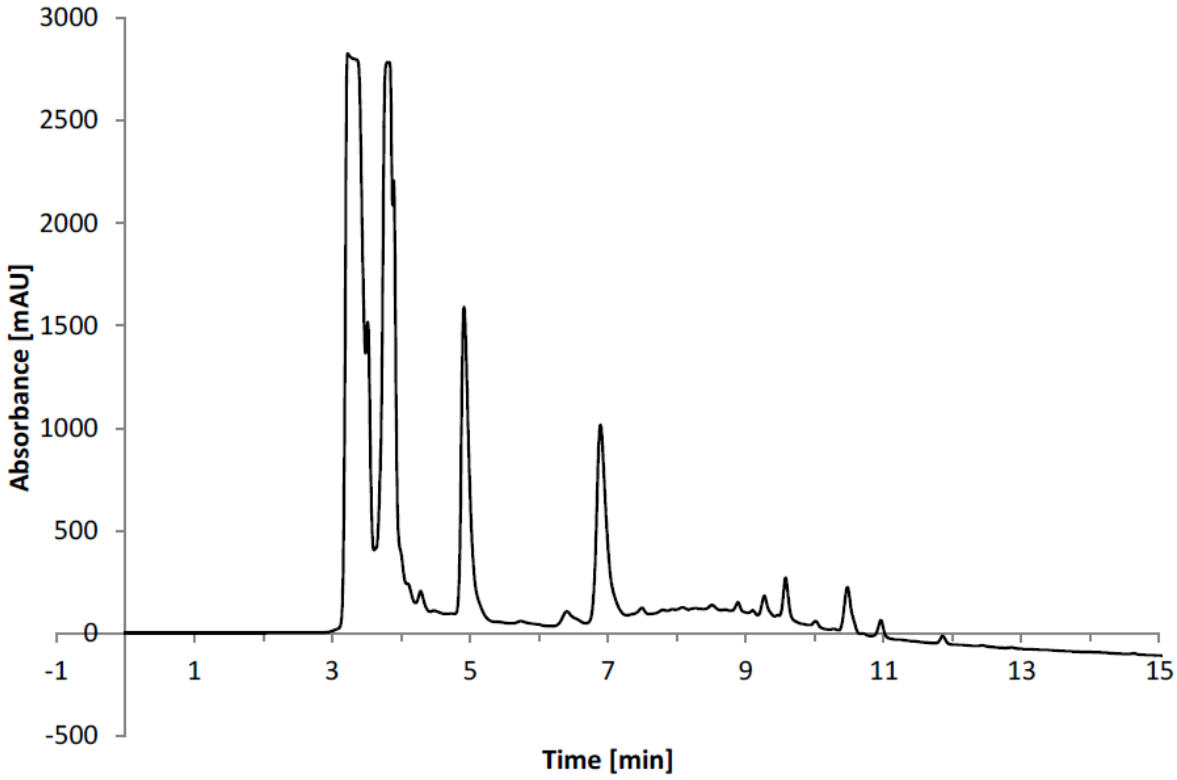

Figure 3.3: HPLC chromatogram from early purification attempts with PBS-based supernatant separated using a protocol of 10 % acetonitrile/90 % water increasing to 75 % acetonitrile/25 % water over 12 minutes. The very broad, over-range peaks in the fourth minute comprise all the very polar components of the supernatant eluting together, obscured by the salts in the PBS.

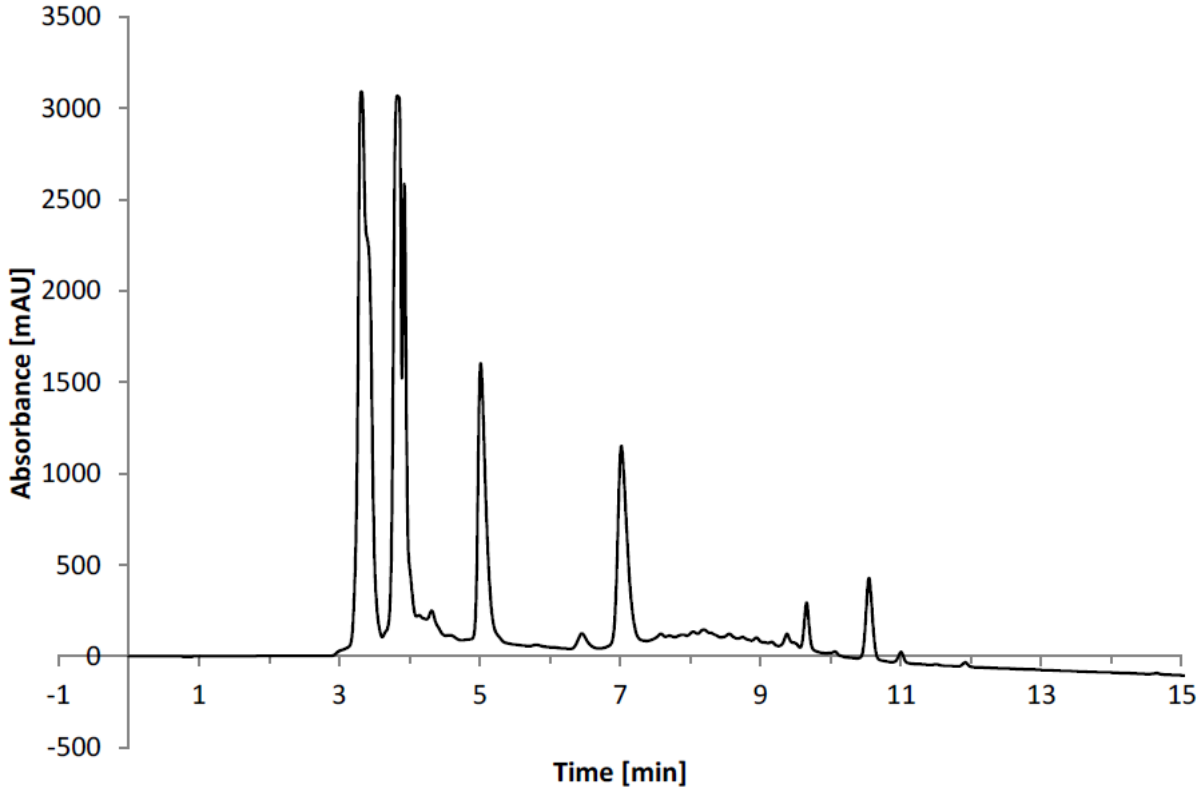

Figure 3.4: HPLC chromatogram of the same protocol as Fig. 3.3 applied to a supernatant sample with a DI water base rather than PBS. The early (polar) peaks in particular were more sharply defined with the excess salt excluded, however the shoulder on the first peak (where the electrochemical activity was detected) indicated that it was still a composited of multiple components.

An isocratic period using 0 % acetonitrile/100 % water was inserted at the beginning of the protocol to attempt to separate the early peaks. This approach allowed the most polar components of the supernatant sample to separate with much better resolution (Fig. 3.5). CVs of collected fractions were able to identify that the electrochemically active molecule was localised to a triplet of overlapping peaks eluting at 5.56 min, 5.77 min and 5.97 min.

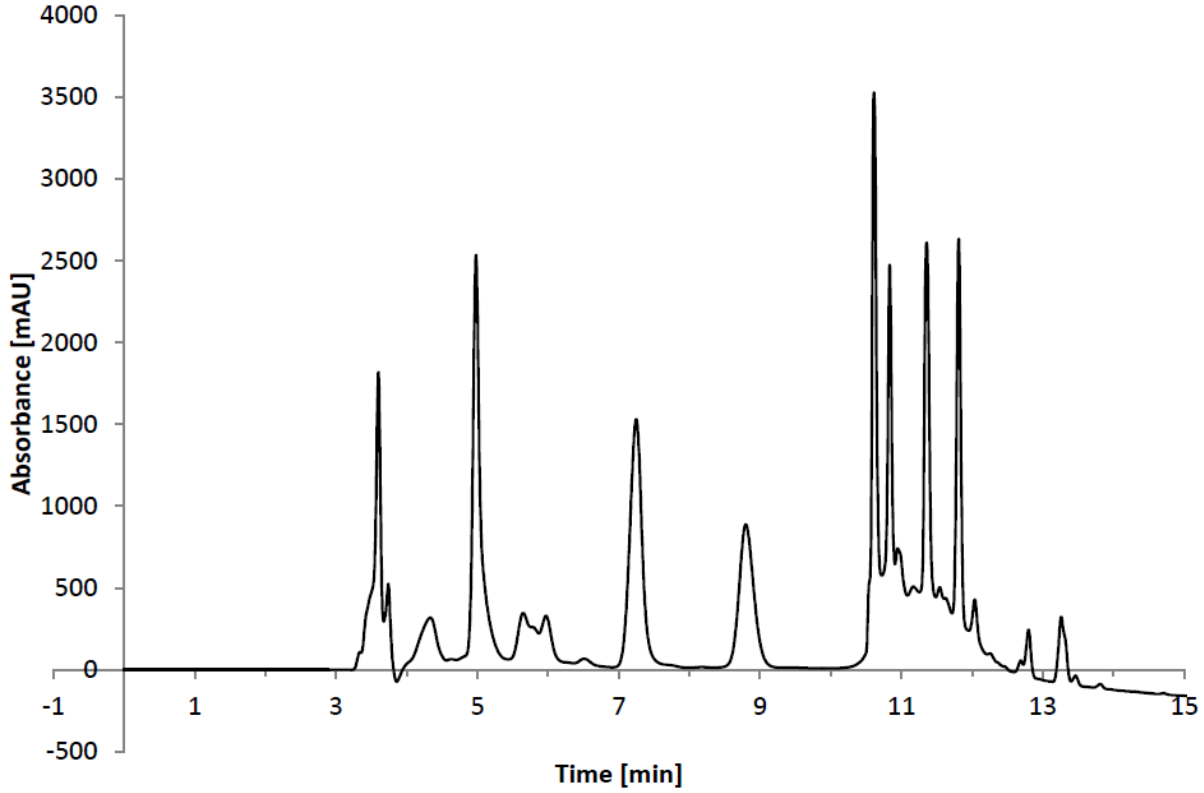

Figure 3.5: HPLC chromatogram of the same protocol as Fig. 3.4 with an initial 5 min period of 0 % acetonitrile/100 % water inserted at the beginning. The large early peaks are much more clearly separated. Electrochemical activity was detected in the triplet of overlapping peaks eluting at 5.65 min, 5.77 min and 5.97 min.

As the electrochemically active molecule was detected in a peak that elutes at a low acetonitrile concentration, it was presumed that it was relatively polar and interacted minimally with the C18 HPLC column. The protocol was amended, lengthening the initial isocratic 0 % acetronitrile/100 % water period to 7 minutes and using a short acetonitrile gradient, increasing 30 % acetonitrile/70 % water over 4 min. The peaks that eluted over the course of the first 9 minutes using the previous protocol displayed approximately the same retention times when applying the new protocol (Fig 3.6), affirming the assumption that the electrochemically active molecule did not interact to a significant degree with the C18 column. The electrochemically active molecule was once more observed in the same triplet of overlapping peaks, eluting in this case at 5.48 min, 5.70 min and 5.86 min.

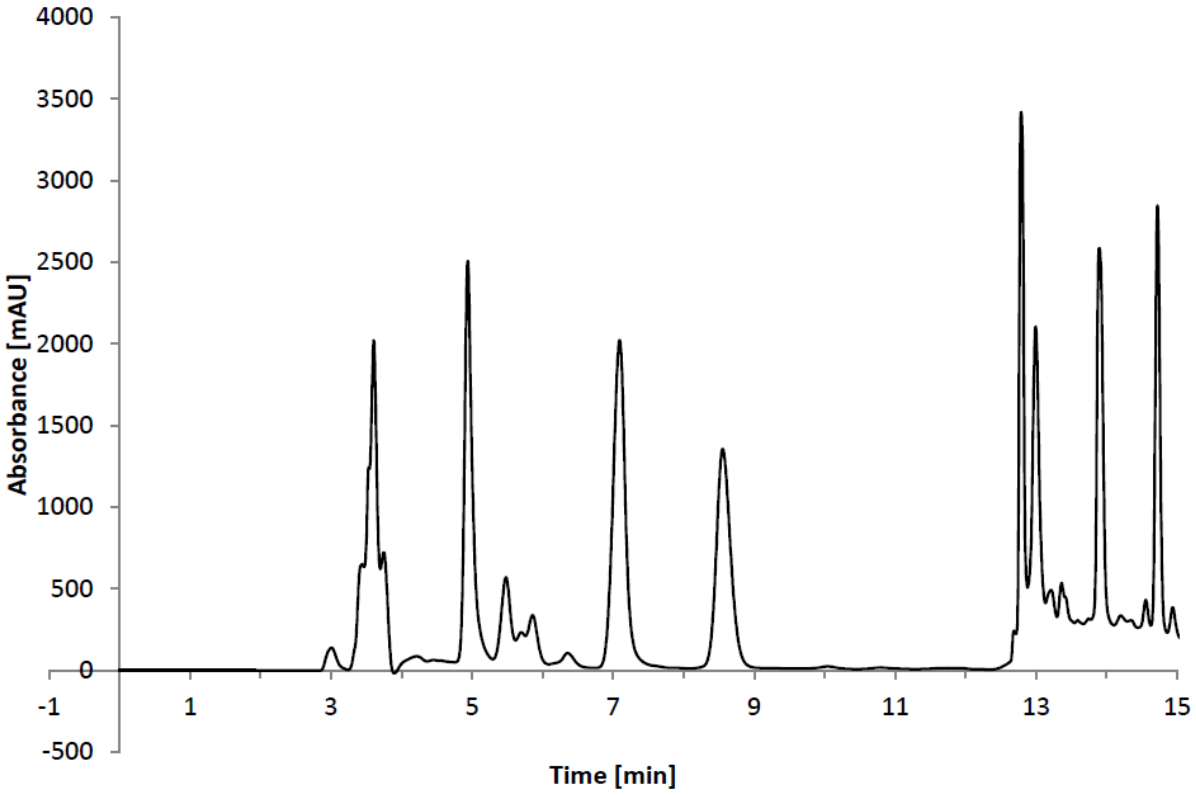

Figure 3.6: HPLC chromatogram of the protocol incorporating a 7 min 0 % acetonitrile/100 % water isocratic separation, followed by an acetonitrile gradient increasing to 30 % acetonitrile/70 % water over 4 min. The retention times are approximately the same for this protocol as those shown in Fig. 3.5.

In order to collect a sufficient volume of HPLC purified fractions to perform CV analyses and locate the target molecule, it was necessary to pool fractions corresponding to matching peaks collected across multiple purification runs. However, because of slight variations in elution times for the three overlapping peaks, the resolution of the peaks was degraded somewhat in the composite samples, resulting in electrochemical activity being observed to some extent in samples from all three peaks (e.g. Fig 3.7).

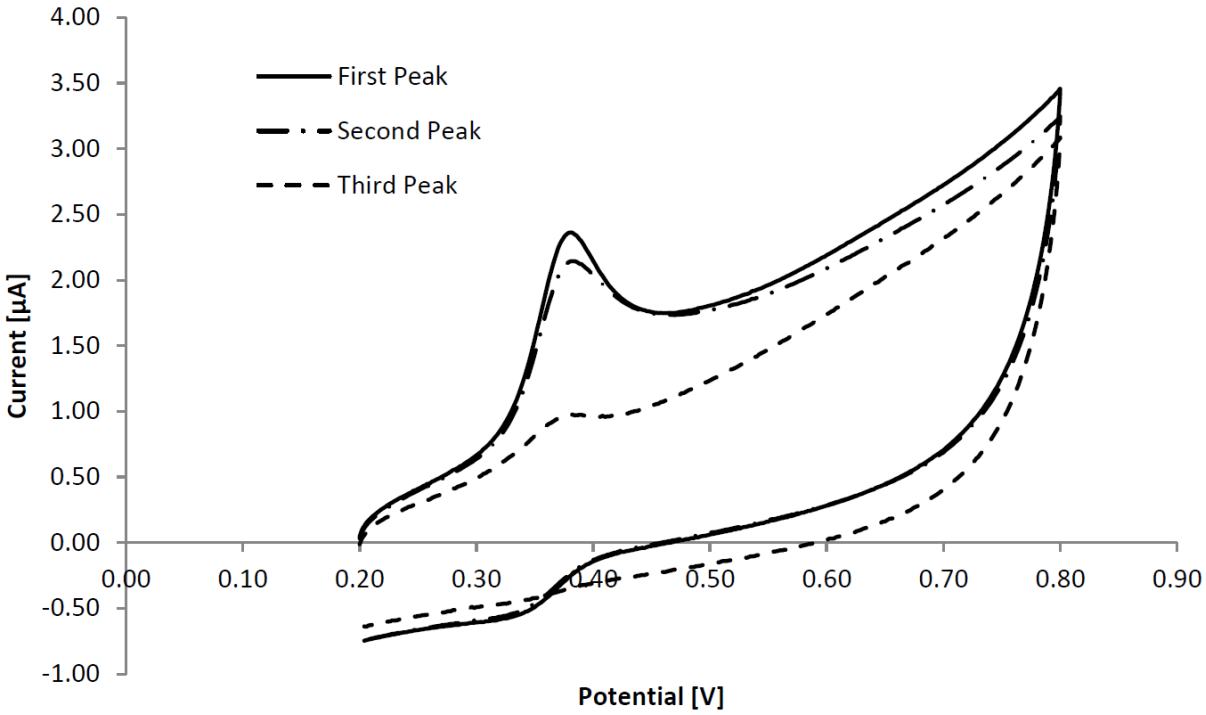

Figure 3.7: CVs for the pooled HPLC fractions corresponding to the three potential peaks containing the unknown electrochemically active molecule. All three peaks appeared to exhibit some electrochemical activity, though more electrochemical activity appeared to be localised in the earlier peaks.

It had been previously observed that the "shelf-life" of the unknown molecule in a supernatant sample was relatively low, leading to CVs showing a decrease in the size of the oxidation peak over time if the sample was not preserved by sparging and blanketing the sample with N_2 gas. It was presumed that this occurred as a result of the molecule being oxidised by dissolved oxygen present in the buffer. In order to determine which of the triplet of elution peaks corresponded to the reduced form of the unknown molecule, a sample of supernatant was shaken thoroughly to entrain air in the liquid, and left to sit without preservation for 72 hours before HPLC analysis.

When overlaid with chromatograms from preserved samples, it can be seen that there are in fact five peaks in the region of interest (Fig. 3.8). Peaks were matched by comparing their relative elution times and/or UV spectra. Peaks 3 and 5 showed a relatively consistent height between the fresh samples of supernatant and those which had been allowed to oxidise. Peaks 1 and 2 were both substantially smaller in the oxidised sample when compared with the fresh sample, with the second peak disappearing entirely. This suggested that these adjacent peaks were closely related molecules which were both readily oxidised. Peak 4, while almost imperceptible on chromatograms of fresh supernatant, showed a prominent peak larger than the other four in the region of interest. It was concluded that this peak likely corresponded to the oxidised form of the molecules in peaks 1 and 2, and that these peaks were most likely to contain the targeted molecule.

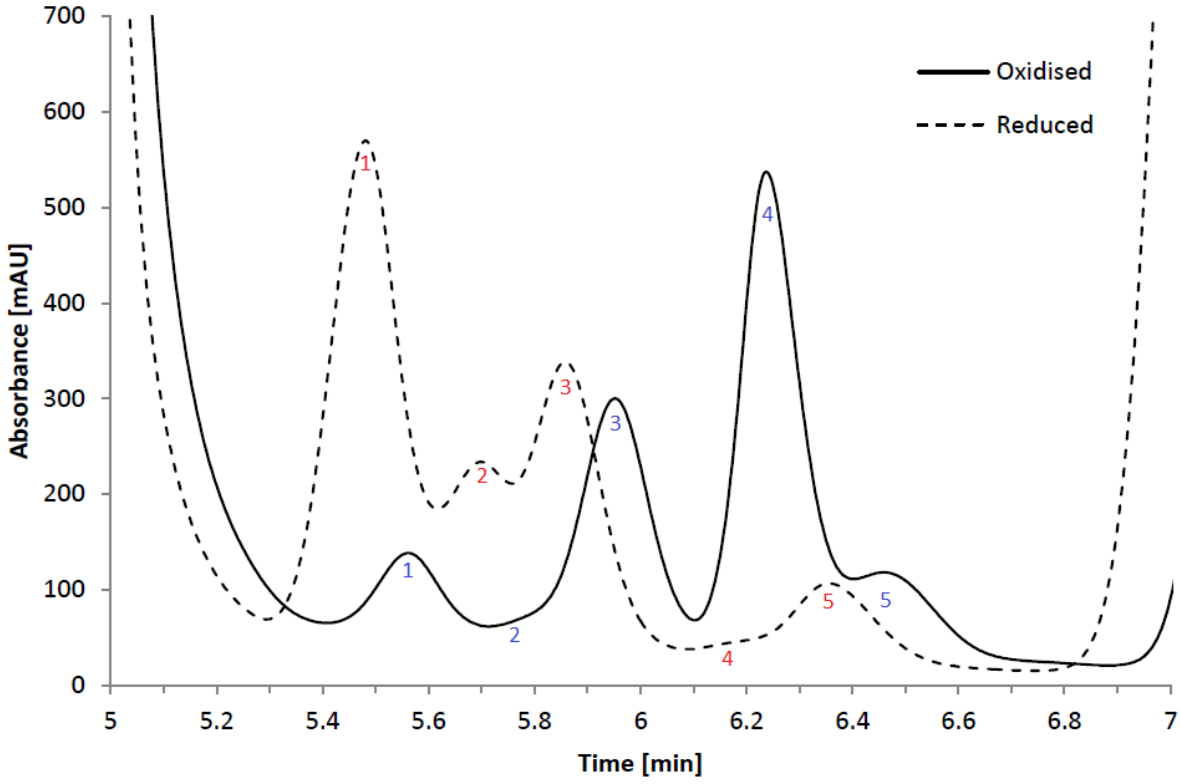

Figure 3.8: Superimposed HPLC chromatograms of minutes 6-7 of the purification protocol shown in Fig. 3.6 applied to a fresh supernatant sample and one which has been allowed to oxidise. Matching peaks share the same number. Oxidation dramatically reduced the heights of peaks 1 and 2, while the height of peak 4 greatly increased. Peaks 3 and 5 were largely unchanged. Differences in elution time appeared to be due to small natural variations in the elution process, with peaks eluting at the same times relative to one another.

3.3.3 Identification of the unknown electrochemically active molecule

A sample of peak 1 was collected over a series of purifications and analysed using mass spectrometry (Fig. 3.9). The strongest signal was observed at 169.0356 m/z, which is a high resolution fit for an empirical formula of $C_5H_5N_4O_3$. Based on the assumption that one of the hydrogen atoms is the source of the ionisation, the unknown molecule was tentatively identified as uric acid (M = 168.11 g/mol).

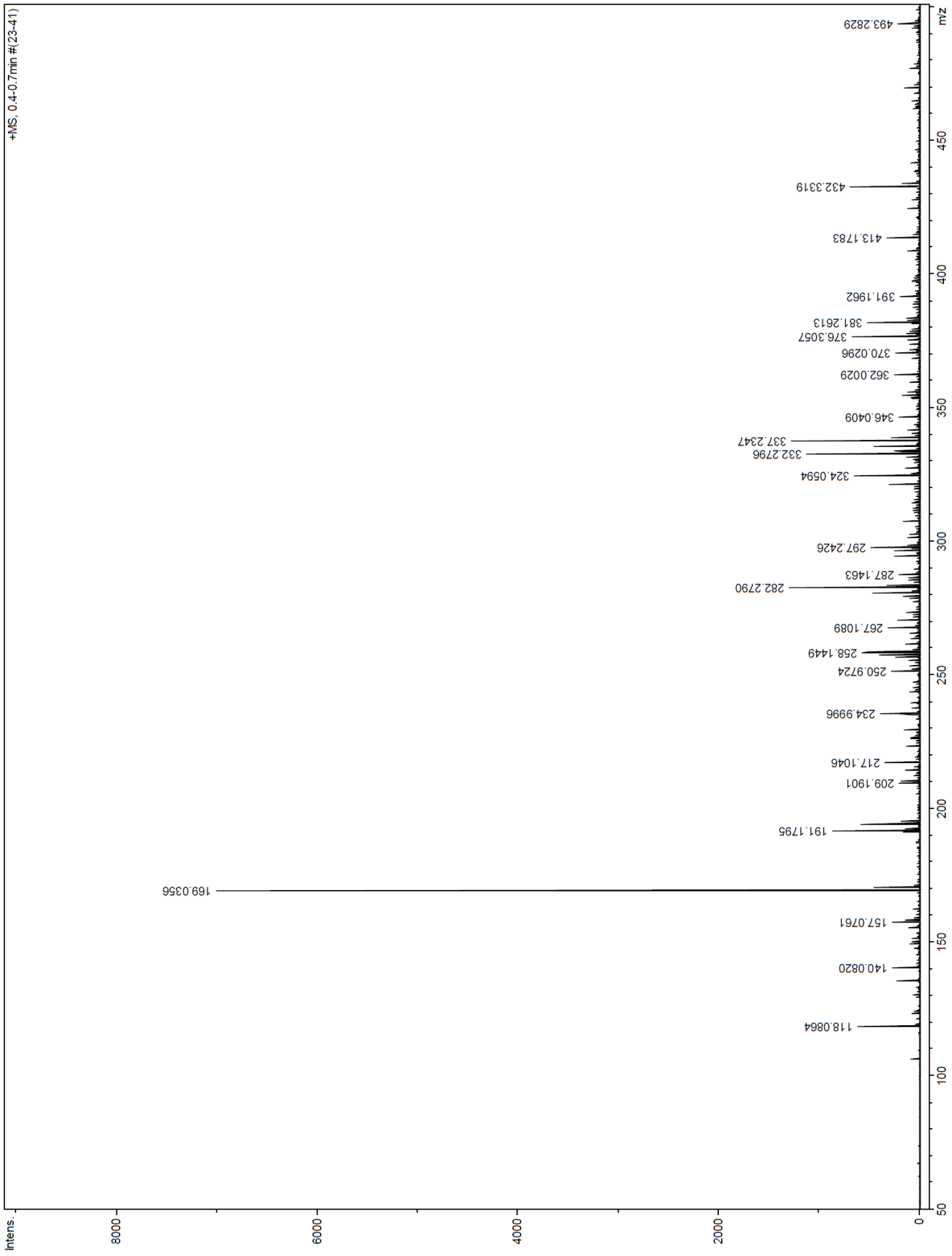

Figure 3.9: Mass spectrometry chart showing ion signal intensity vs. mass-charge ratio for a purified sample of peak 1 from Fig. 3.8, the peak believed to contain the reduced form of the unknown electrochemically active molecule. The highest intensity signal occurs at a m/z of 169.0356. This is a good fit for uric acid + one hydrogen atom used for ionization.

A 5 µL sample of sodium urate was injected onto the HPLC column and purified using the same protocol detailed for Fig. 3.6. The chromatogram showed a peak with an elution time comparable to that of the putative uric acid peak from the supernatant samples (Fig 3.8, peak 1) within the variation in elution times observed between supernatant samples (Fig. 3.10), with the sodium urate peak eluting 4.6 s later.

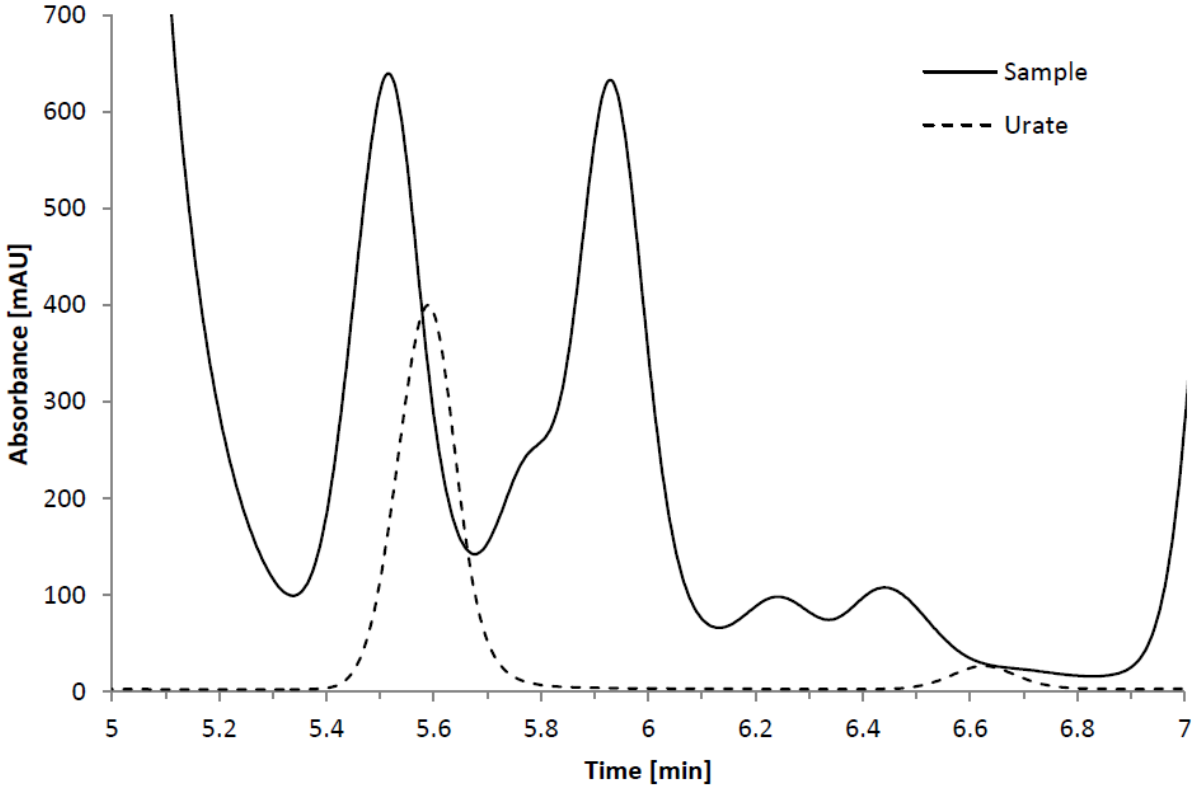

Figure 3.10: Superimposed HPLC chromatograms of minutes 6-7 of the purification of a supernatant sample and a sample of sodium urate. The elution times of the first peak from the supernatant sample and the first peak of the sodium urate sample correspond closely, separated by only 4.6 seconds.

The UV spectra of the putative uric acid peak from the supernatant sample and the first peak from the sodium urate sample were also compared, and found to correspond closely (Fig. 3.11). This suggests very strongly that the molecules represented by these peaks are either the same or closely structurally related.

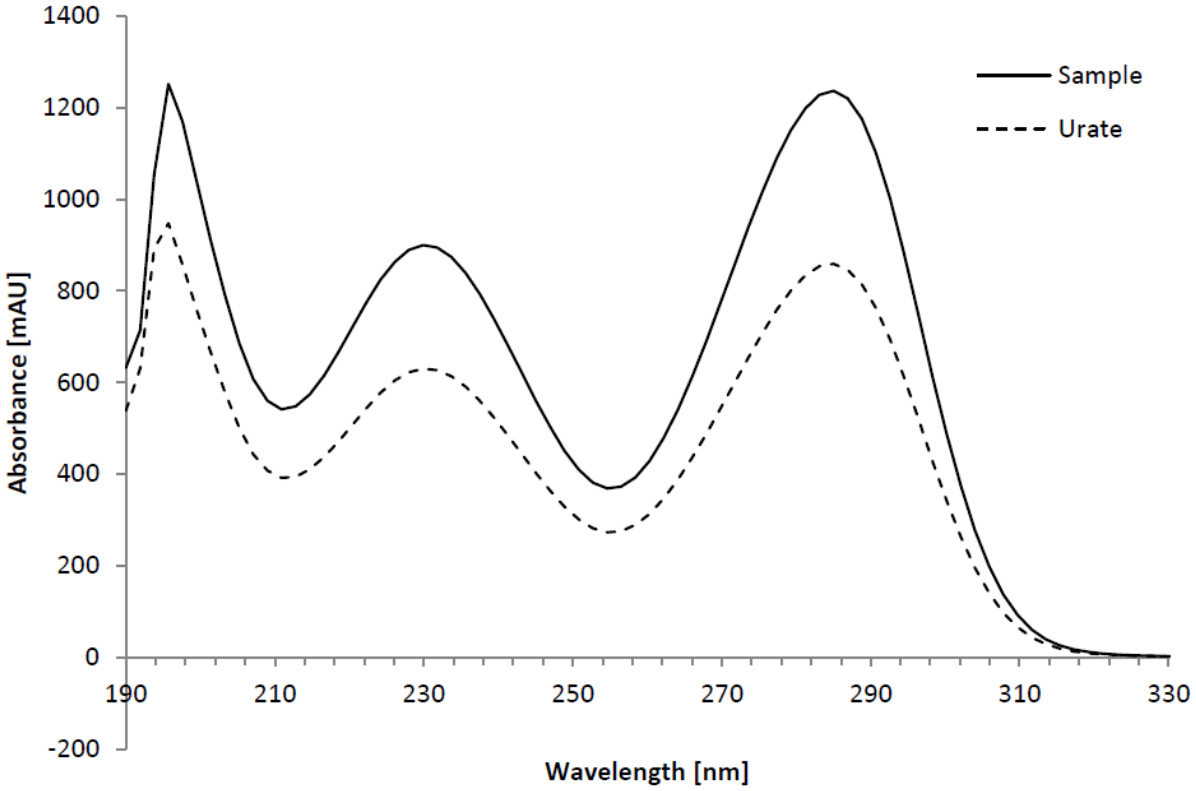

Figure 3.11: Superimposed UV spectra for the putative uric acid peak of a supernatant sample and the largest peak in a sodium urate sample purified by HPLC. The UV spectra are very similar (peak absorbances within 0.5 nm), implying that the peaks represent either the same or extremely similar molecules.

CV was performed on 1 mL PBS with 100 µL of 500 µM sodium urate added to it, on 1 mL of dilute supernatant from a dense suspension of LS3, and on 1 mL of dilute supernatant with 100 µL of 500 µM sodium urate added to it (Fig. 3.12). All three voltammograms showed a single oxidation peak in the region between +0.3 V and +0.4 V. The oxidation peak for the sample containing both supernatant and sodium urate solution was slightly larger than that of the supernatant alone with a single peak, implying that the redox properties of both solutions in this region are either the same or very similar.

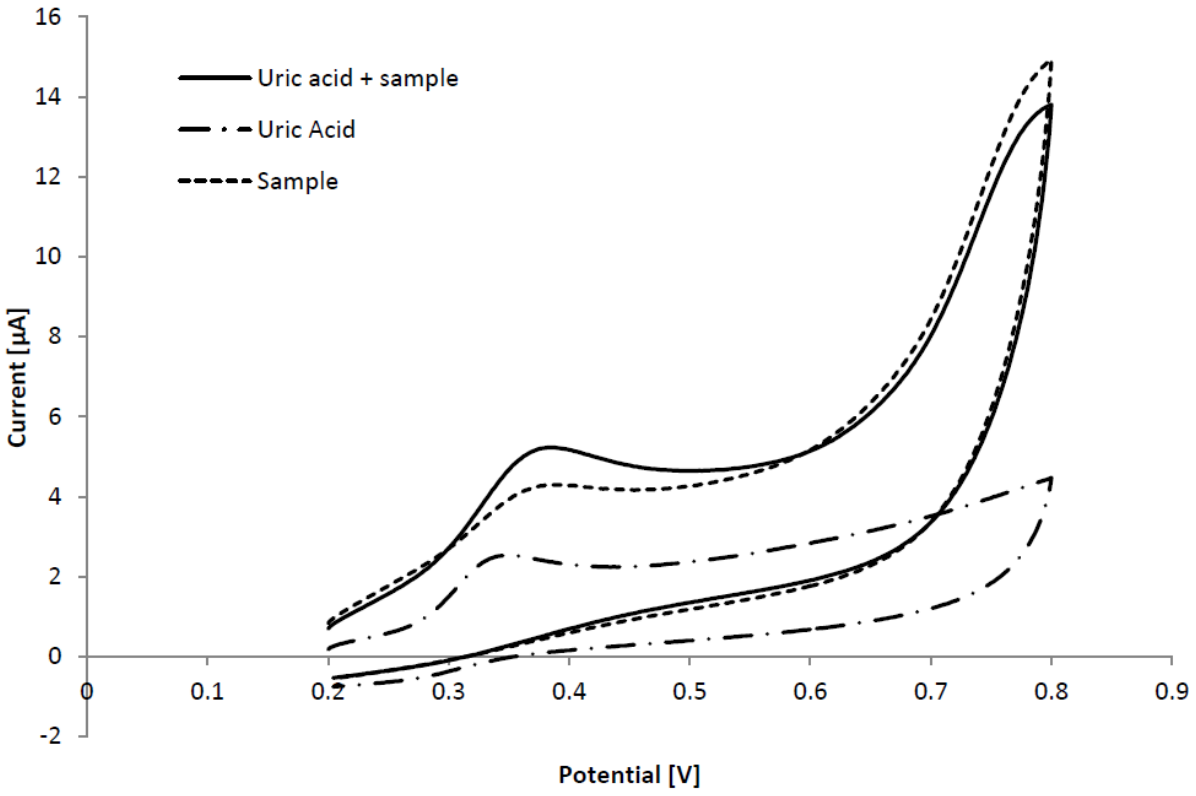

Figure 3.12: Superimposed CVs for uric acid solution, a sample of dilute supernatant from a dense cell suspension, and a combination of uric acid and supernatant. In all cases only a single oxidation peak is evident in the +0.3 V to +0.4 V region, and the combined uric acid + supernatant appear to display a cumulative peak area. This supports the hypothesis that the molecule responsible for the oxidation peak is the same in both solutions.

A pair of transgenic strains, *A. adeninivorans* G1212/YRC102-AYNI1-AUOR39 and G1212/YRC102-AYNI1-AUOR94 were developed at IPK. These strains have a gene for urate oxidase (*AUOR*) linked to a nitrate-induced promoter (*AYNI1*). CV was used to investigate the oxidation peak developed by these mutants in the presence (Fig 3.13) and absence (Fig. 3.14) of sodium nitrate.

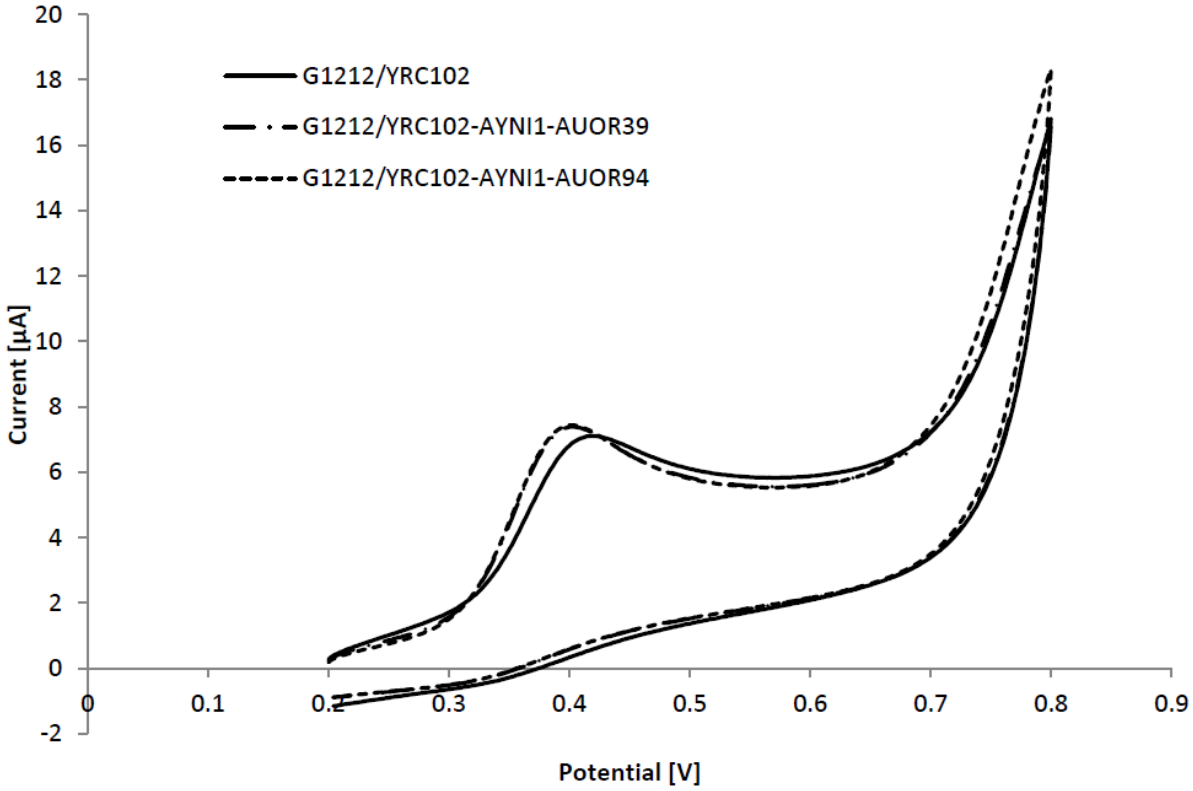

Figure 3.13: Superimposed CVs of supernatant samples from dense cell suspensions of *A. adeninivorans* mutants G1212/YRC102, G1212/YRC102-AYNI1-AUOR39 and G1212/YRC102-AYNI1-AUOR94 cultivated in YNB with ammonium sulphate as a nitrogen source. All three strains have an oxidation peak of similar size in the expected potential range.

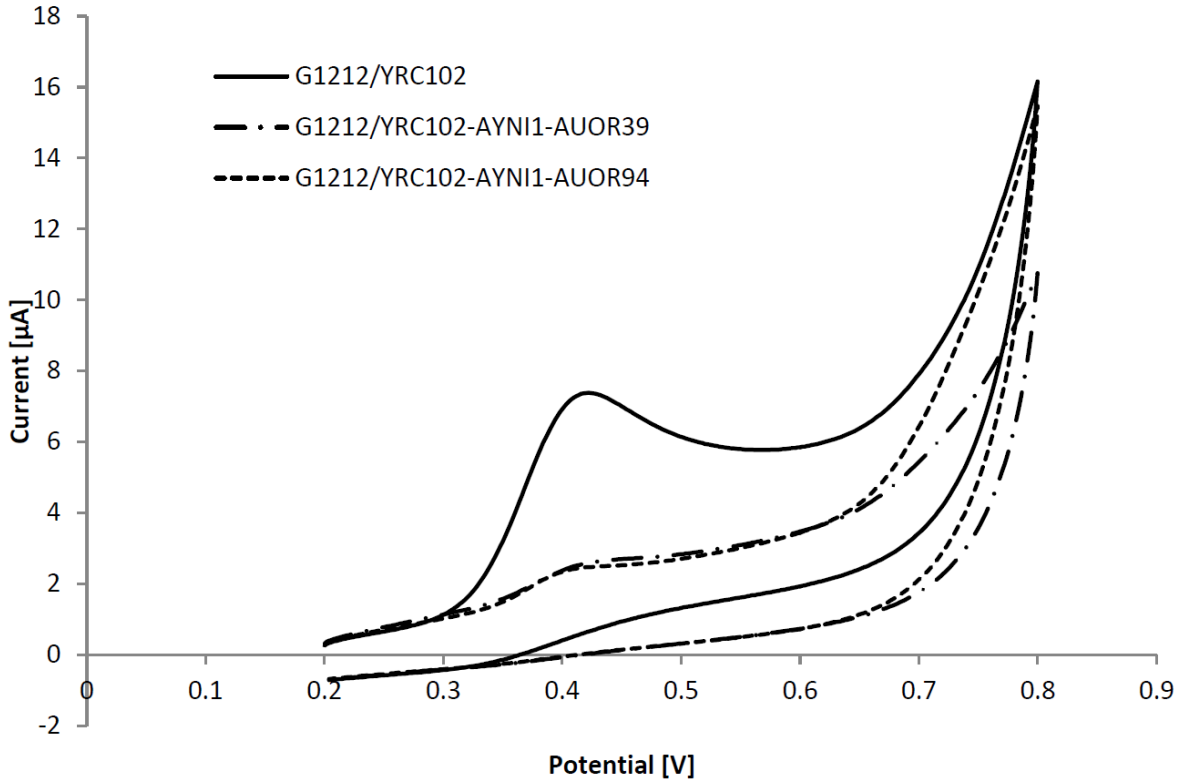

Figure 3.14: Superimposed CVs of supernatant samples from dense cell suspensions of *A. adeninivorans* mutants G1212/YRC102, G1212/YRC102-AYNI1-AUOR39 and G1212/YRC102-AYNI1-AUOR94 cultivated in YNB with sodium nitrate as a nitrogen source. G1212/YRC102 exhibited the same form of oxidation peak as it did with ammonium sulphate. The other two mutants show dramatically reduced oxidation peaks by comparison.

All three of these mutant strains exhibited oxidation peaks with recognisably similar shape and anodic peak potential to that of the wild type strain LS3 when cultured using ammonium sulphate as the nitrogen source. G1212/YRC102 continued to show a familiar peak when using sodium nitrate as a nitrogen source. By contrast, G1212/YRC102-AYNI1-AUOR39 and G1212/YRC102-AYNI1-AUOR94 only produced very shallow oxidation peaks in this condition, indicating that the molecule responsible for producing the oxidation peak typically observed in this region is a substrate for the enzyme urate oxidase.

3.4 Discussion

The experiments conducted in this study all point to the unknown electrochemically active molecule secreted by *A. adeninivorans* being uric acid. This conclusion provides a satisfactory explanation for the observations made throughout the investigation into the identity of the molecule.

The electrochemical properties of uric acid are well-documented, as it is a significant analyte for the development of voltammetric biosensors (Raj and Ohsaka, 2003; Ramesh and Sampath, 2004; Wang et al., 2002; Zhang and Lin, 2001). The oxidation peak corresponding to uric acid on the voltammograms recorded throughout these studies generally had a peak anodic potential falling between +0.35 V and +0.45 V, which is in agreement with the established oxidation potential in the literature for uric acid of +0.59 V vs. a normal hydrogen electrode (NHE) at neutral pH (Simic and Jovanovic, 1989), equivalent to +0.38 V with our reference electrode. There was some variation in the precise value, which is most likely attributable to surface effects local to the electrode, such as fouling or slight variations in pH or concentrations of other metabolites in the sample. Fouling is a factor which is believed to contribute to the broadness of the oxidation peak (Raj and Ohsaka, 2003). Early pilot experiments did not incorporate filtration, and the supernatant was simply decanted out of the centrifuge tube for measurement. These experiments typically exhibited broader oxidation peaks which tended to have slightly higher peak anodic potentials, which was attributed to fouling from cells and particulate matter in the sample. The working electrode surface was polished between every measurement to ameliorate the potential accumulation of electrode fouling.

The voltammetric observation of uric acid oxidation as irreversible, as per the work of Haslett et al. (2011) prior to the identification of the molecule, or quasi-irreversible, as suggested by the very shallow reduction peak shown in Fig. 3.2, is also consistent with the literature, however there is some evidence that to some extent the reversibility of uric acid can be influenced by the nature of the electrode. Safavi et al. (2006) reports a significant improvement in apparent reversibility of uric acid oxidation at a carbon ionic liquid electrode (CILE) compared with a conventional carbon paste electrode (CPE). A decrease in overpotential for the oxidation reaction at a CILE and a resistance to fouling were also reported.

Uric acid is a highly polar molecule, and when using HPLC to isolate and quantify it, a highly aqueous mobile phase is typically used, and short retention times are common (Zhou et al., 2013; Zuo et al., 2008). This coincides with the observations throughout the process of developing the HPLC protocol to purify the unknown molecule (uric acid), which tended to elute early and required an isocratic separation with water as the solvent to resolve a clear peak.

While the UV spectra for the uric acid peak from the supernatant and the analytical-grade sodium urate are a close match (Fig. 3.11), with peaks at 196 nm, 230 nm and 285 nm, these peaks differ

somewhat from those found in the literature. Zinellu et al. (2004) describes peaks at 197 nm, 233 nm and 292 nm, while Mei et al. (1996) depicts the latter two peaks as occurring at 238 nm and 292 nm. While the literature describes maxima occurring at slightly longer wavelengths that experimentally observed, the UV spectrum of uric acid does tend to shift slightly with pH, with maxima shifting toward longer wavelengths as it is deprotonated (Stimson Sr and Reuter Sr, 1943).

Given the identity of peak 1 (Fig. 3.8) as uric acid, it is possible that the other peaks nearby may have similar properties. Peak 2 overlapped too much with peaks 1 and 3 to obtain a clear UV spectrum, but peak 3 displayed a spectrum with maxima at 198 nm and 249 nm. This is close to the expected spectrum for hypoxanthine or possibly a similar purine derivative such as adenosine or inosine (Mei et al., 1996). MS of pooled fractions of peaks 2 and 3 did show a signal at 137.0459 m/z which strongly supports the presence of hypoxanthine ($M+H^+$) (Chen et al., 2015), although the highest intensity signal in both of these samples was at 157.0973 m/z, and the identity of this signal is not known. Since the UV absorption spectrum is a good match for a purine derivative, it follows that this signal is likely either a purine derivative itself or a molecule lacking a chromophoric system. Dimethyl sulfoxide contamination (as $2M+H^+$) is also a possibility, as it is a component in some commercial cryopreservatives, but it seems doubtful that a sufficient amount of this molecule would remain throughout the culturing and purification process to provide such a strong signal.

Uric acid is a relatively well-studied compound, largely due to its clinical significance. Abnormally high or low concentrations of uric acid in blood plasma (hyperuricemia and hypouricemia respectively) or urine (hyperuricosuria and hypouricosuria respectively) are markers for a number of medical conditions, hence the aforementioned interest in biosensor development to provide inexpensive and rapid clinical uric acid monitoring solutions. Furthermore, *A. adeninivorans* G1212/YRC102-AYNI1-AUOR39 and G1212/YRC102-AYNI1-AUOR94 were developed as part of research into the development of transgenic strains of *A. adeninivorans* capable of overexpressing the enzymes adenine deaminase (Jankowska et al., 2013a), xanthine oxidoreductase (Jankowska et al., 2013b) and urate oxidase with a view toward using the enzymes to reducing the purine content of food, as a method of enabling the consumption of foods which could otherwise potentially aggravate the conditions of sufferers of hyperuricemia.

Uric acid is also believed to be a marker for oxidative stress, and play a role as an antioxidant (Glantzounis et al., 2005), as it is a potent reducing agent. This function as a reducing agent is a product of the electrons it has available to donate, which are observed in CV as the charge transfer measured by the working electrode. Secreting a powerful reducing agent is an effective way of transferring electrons from inside the cell into the surrounding solution, which positions *A. adeninivorans* as a strong candidate for use as a microbial catalyst in a MFC. The necessity of preserving supernatant samples with N_2 in order to retain electrochemical activity does show however

that uric acid is very vulnerable to being oxidised by any dissolved oxygen which may be present, something which is a perennial problem in microbial fuel cells. Furthermore, as Haslett et al. (2011) shows, the amount of current attributable to non-mediated electron transfer by *A. adeninivorans*, which we can now presume can be attributed to secreted uric acid, is only a fraction of what can be accomplished by adding an artificial exogenous mediator. It will therefore be necessary to develop a strain and culture conditions which will elevate production of uric acid to higher levels in order to develop a high power density MFC based on self-mediating monoculture of *A. adeninivorans*.

3.5 References

Chen, J., Shi, Q., Wang, Y., Li, Z., and Wang, S. (2015). Dereplication of known nucleobase and nucleoside compounds in natural product extracts by capillary electrophoresis-high resolution mass spectrometry. Molecules *20*, 5423-5437.

Gienow, U., Kunze, G., Schauer, F., Bode, R., and Hofemeister, J. (1990). The yeast genus *Trichosporon* spec. LS3; molecular characterization of genomic complexity. Zentralblatt fur Mikrobiologie *145*, 3-12.

Glantzounis, G.K., Tsimoyiannis, E.C., Kappas, A.M., and Galaris, D.A. (2005). Uric acid and oxidative stress. Current Pharmaceutical Design *11*, 4145-4151.

Haslett, N.D., Rawson, F.J., Barrière, F., Kunze, G., Pasco, N., Gooneratne, R., and Baronian, K.H.R. (2011). Characterisation of yeast microbial fuel cell with the yeast *Arxula adeninivorans* as the biocatalyst. Biosensors and Bioelectronics *26*, 3742-3747.

Jankowska, D.A., Faulwasser, K., Trautwein-Schult, A., Cordes, A., Hoferichter, P., Klein, C., Bode, R., Baronian, K., and Kunze, G. (2013a). *Arxula adeninivorans* recombinant adenine deaminase and its application in the production of food with low purine content. Journal of Applied Microbiology *115*, 1134-1146.

Jankowska, D.A., Trautwein-Schult, A., Cordes, A., Hoferichter, P., Klein, C., Bode, R., Baronian, K., and Kunze, G. (2013b). *Arxula adeninivorans* xanthine oxidoreductase and its application in the production of food with low purine content. Journal of Applied Microbiology *115*, 796-807.

Mei, D.A., Gross, G.J., and Nithipatikom, K. (1996). Simultaneous determination of adenosine, inosine, hypoxanthine, xanthine, and uric acid in microdialysis samples using microbore column high-performance liquid chromatography with a diode array detector. Analytical Biochemistry *238*, 34-39.

Raj, C.R., and Ohsaka, T. (2003). Voltammetric detection of uric acid in the presence of ascorbic acid at a gold electrode modified with a self-assembled monolayer of heteroaromatic thiol. Journal of Electroanalytical Chemistry *540*, 69-77.

Ramesh, P., and Sampath, S. (2004). Selective determination of uric acid in presence of ascorbic acid and dopamine at neutral pH using exfoliated graphite electrodes. Electroanalysis *16*, 866-869.

Safavi, A., Maleki, N., Moradlou, O., and Tajabadi, F. (2006). Simultaneous determination of dopamine, ascorbic acid, and uric acid using carbon ionic liquid electrode. Analytical Biochemistry *359*, 224-229.

Simic, M.G., and Jovanovic, S.V. (1989). Antioxidation mechanisms of uric acid. Journal of the American Chemical Society *111*, 5778-5782.

Stimson Sr, M.M., and Reuter Sr, M.A. (1943). Ultraviolet absorption spectra of nitrogenous heterocycles. VII. The effect of hydroxy substitutions on the ultraviolet absorption of the series: Hypoxanthine, xanthine and uric acid. Journal of the American Chemical Society *65*, 153-155.

Trautwein-Schult, A., Jankowska, D., Cordes, A., Hoferichter, P., Klein, C., Matros, A., Mock, H.P., Baronian, K., Bode, R., and Kunze, G. (2013). Arxula adeninivorans Recombinant Urate Oxidase and Its Application in the Production of Food with Low Uric Acid Content. Journal of Molecular Microbiology and Biotechnology *23*, 418-430.

Wang, Z., Wang, Y., and Luo, G. (2002). A selective voltammetric method for uric acid detection at β-cyclodextrin modified electrode incorporating carbon nanotubes. Analyst *127*, 1353-1358.

Wartmann, T., Erdmann, J., Kunze, I., and Kunze, G. (2000). Morphology-related effects on gene expression and protein accumulation of the yeast *Arxula adeninivorans* LS3. Archives of Microbiology *173*, 253-261.

Zhang, L., and Lin, X. (2001). Covalent modification of glassy carbon electrode with glutamic acid for simultaneous determination of uric acid and ascorbic acid. Analyst *126*, 367-370.

Zhou, S., Zuo, R., Zhu, Z., Wu, D., Vasa, K., Deng, Y., and Zuo, Y. (2013). An eco-friendly hydrophilic interaction HPLC method for the determination of renal function biomarkers, creatinine and uric acid, in human fluids. Analytical Methods *5*, 1307-1311.

Zinellu, A., Carru, C., Sotgia, S., and Deiana, L. (2004). Optimization of ascorbic and uric acid separation in human plasma by free zone capillary electrophoresis ultraviolet detection. Analytical Biochemistry *330*, 298-305.

Zuo, Y., Wang, C., Zhou, J., Sachdeva, A., and Ruelos, V.C. (2008). Simultaneous Determination of Creatinine and Uric Acid in Human Urine by High-Performance Liquid Chromatography. Analytical Sciences *24*, 1589-1592.

Chapter 4

Exploration of the source and purpose of uric acid secretion by *Arxula adeninivorans*

4.1 Introduction

The yeast *Arxula adeninivorans* has been shown to secrete uric acid into its environment. This uric acid is observable using cyclic voltammetry as an oxidation peak with a peak anodic potential most typically observed between +0.35 V and +0.45 V at neutral pH. Being a strong reducing agent (electron donor), secreted uric acid has potential to be utilised as a vector for transporting electrons from cell metabolism to the anode of a microbial fuel cell without requiring the addition of an artificial mediator. However, the power density observed in studies of non-mediated MFCs using *A. adeninivorans* as the microbial catalyst is only a small fraction of that obtained when using an artificial mediator (Haslett et al., 2011), implying that the rate of uric acid secretion is relatively low. In order to address this, it is necessary to investigate the metabolic source and/or purpose of the uric acid produced by *A. adeninivorans.*

Uric acid ($C_5H_4N_4O_3$) is a bicyclic, heterocyclic, aromatic compound with a purine functional group. The most common biological source of uric acid is the purine catabolism pathway, which is responsible for the recycling of waste purine bases and disposal of excess nitrogen. Purine compounds such as adenosine, inosine, xanthosine and guanosine are converted through a series of enzymatic reactions to xanthine, which is then converted to uric acid by way of xanthine dehydrogenase. In many organisms, uric acid is then oxidised by urate oxidase to allantoin before excretion, although humans and other higher primates are an exception to this, lacking urate oxidase and excreting uric acid instead. Birds, reptiles and some desert-dwelling mammals also excrete uric acid, however they do so via a more complex and energetically costly metabolic pathway aimed at prioritising conservation of water.

The fact that *A. adeniniovrans* secretes sufficient uric acid so as to be readily detectable using electrochemical methods has not been previously reported outside of this work. Furthermore, there is no mention of elevated uricogenesis in yeasts in the literature at all. This study will electrochemically examine several common *Saccaromyces* and *Candida* species to determine whether or not secretion of high levels of uric acid is a general property shared by the Saccharomycetaceae family. In order to

determine if the purine degradation is the source of the uric acid, the uric acid production of an *A. adeninivorans* mutant with a gene knockout in the purine catabolic pathway will be studied.

4.2 Materials and methods

4.2.1 Yeast strains, media, buffers and growth conditions

Two different *A. adeninivorans* strains were used in this study. The control strain, *A.adeninivorans* G1212/YRC102 is described in section 3.2.1. *A. adeninivorans* G1224 [*aleu2::ALEU2 atrp1::ATRP1 axor*] is G1212 transformant with a gene disruption in the AXOR gene, preventing G1224 from producing xanthine dehydrogenase (Jankowska et al., 2013b). These strains were obtained from the Leibniz Institute of Plant Genetics and Crop Plant Research (IPK), Gatersleben, Germany.

Four other yeast strains were used in this study. A *Saccharomyces cerevisiae* diploid strain α/a F832×Y383 and a clinical isolate of *Candida albicans* were both obtained from the University of Canterbury School of Biological Sciences culture collection. *Candida parapsilosis*, CDC MCC499 and *Candida lambica*, ICMP 16880 were also used.

All yeast strains were grown under non-selective conditions for 20 hours at 37 °C in a YEPD broth medium [yeast extract 10 g L^{-1}, peptone 20 g L^{-1}, dextrose 20 g L^{-1}, sterilised at 121 °C], aerated by agitation in a shaking incubator. Agar plates were prepared by addition of 15 g L^{-1} agar to the liquid media.

Cell cultures were grown in two stages. A pre-culture was prepared using a single colony from a YEPD agar plate culture to inoculate 100 mL YEPD in a 250 mL indented culture flask and grown as described above. Experimental cell cultures were prepared using 1 mL of pre-culture as the inoculum and incubating under the same conditions.

Cell pellets were re-suspended in a variant of PBS adapted for use in electrochemistry (0.05M K_2HPO_4/KH_2PO_4, 0.1 M KCl).

4.2.2 Electrochemistry

CV was performed using the same apparatus described in section 3.2.2. CVs were performed in a Faraday cage and were scanned from +0.2 V to +0.8 V at 100 mV s^{-1} with three replicate CVs recorded for each sample. Measured potentials are vs. Ag/AgCl/3M KCl unless otherwise stated.

4.2.3 Uric acid accumulation

Cells were washed and re-suspended in PBS according to the methods described in section 3.2.3. The airspace above the cell suspension was then flushed with N_2 gas to displace excess air, and the cells incubated anaerobically for 20 h at 47 °C (for *A. adeninivorans*) or 37 °C (for other yeast species) with gentle agitation to keep the cells suspended. Supernatant was recovered from cell suspensions as described in section 3.2.3.

4.3 Results

4.3.1 Electrochemical activity in supernatants from other Saccharomycetaceae

CVs of supernatants derived from dense cells suspensions of *S. cerevisiae*, *C. albicans*, *C. lambica*, and *C. parapsilosis* were performed to determine if an oxidation peak corresponding to that commonly exhibited by *A. adeninivorans* could be observed in yeasts of the same family (Fig 4.1). None of the yeast species examined exhibited any oxidation peaks in the voltage range between +0.2 V and +0.6 V. This suggests that none of these species secretes uric acid into their environment to a readily measurable extent, if at all, in the way *A. adeninivorans* does.

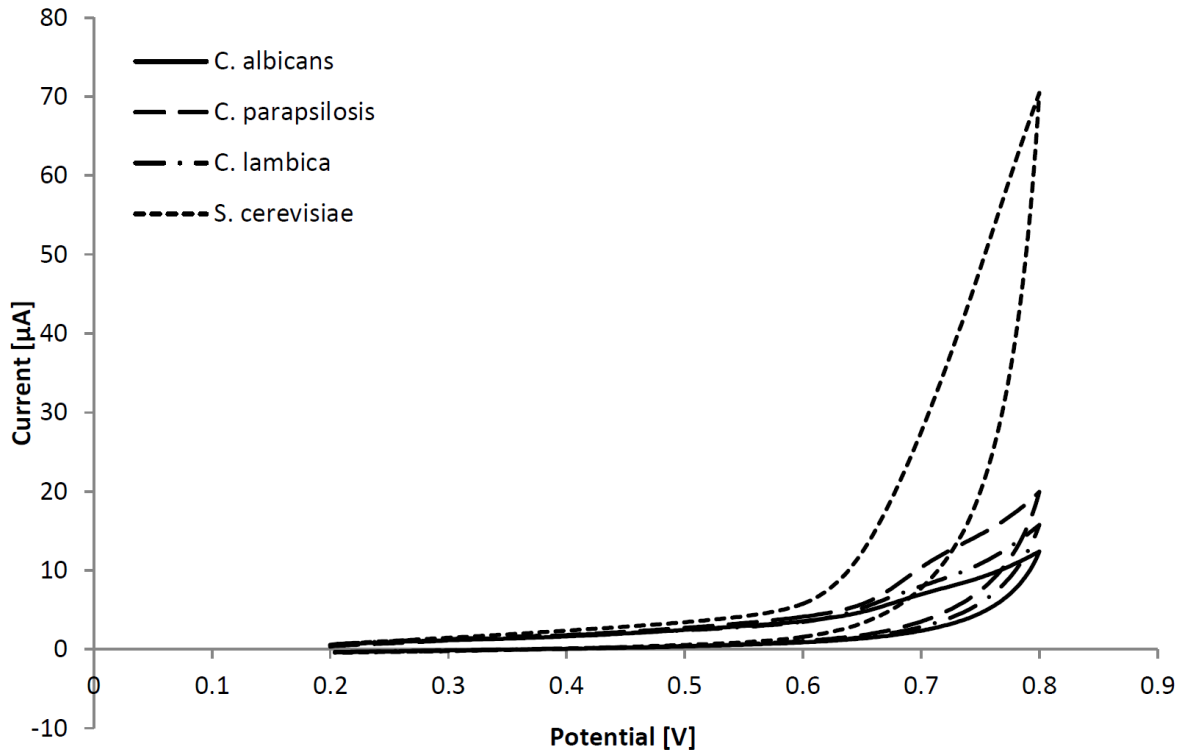

Figure 4.1: Superimposed CVs of supernatant samples from dense cell suspensions of *C. albicans*, *C. parapsilosis*, *C. lambica* and *S. cerevisiae* incubated at 37 °C. No oxidation peaks corresponding to uric acid are observed in any of these four yeast species.

4.3.2 Xanthine dehydrogenase knockout mutant

CVs of supernatants derived from dense cell suspensions of *A. adeninivorans* G1212/YRC102 and G1224 were performed to investigate the effect of truncating the purine degradation pathway in *A. adeninivorans* by introducing a disruption in the *AXOR* gene, such that the terminal products of this catabolic pathway are hypoxanthine or xanthine (Fig. 4.2). The supernatant derived from the control strain, G1212/YRC102, exhibits a peak corresponding to the oxidation of uric acid in the expected voltage region. By contrast, the voltammogram for the supernatant derived from G1224 displays no indication of any oxidation or reduction activity in a voltage range between +0.2 V and +0.6 V. This is consistent with what would be expected for a sample which contains no uric acid. An oxidation peak does appear to occur near the top of the scan range, at approximately + 0.78 V, but this potential is most likely too positive to be associated with uric acid.

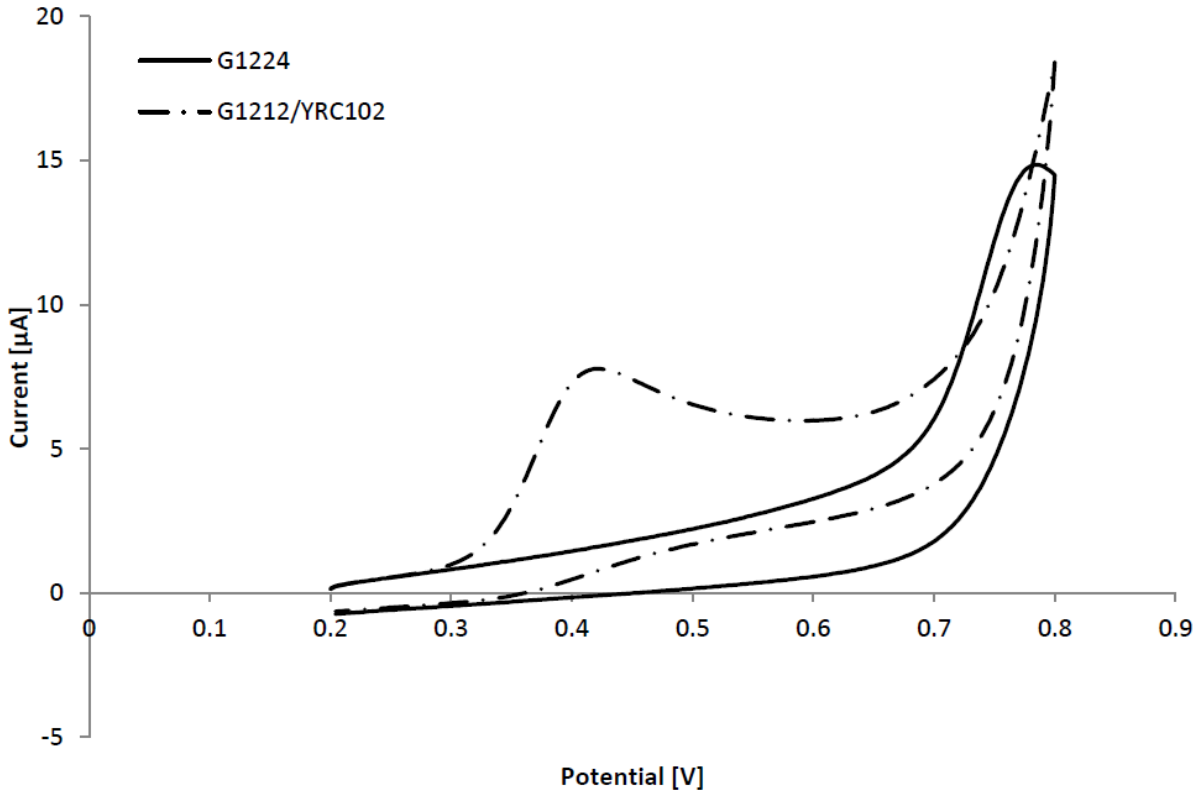

Figure 4.2: Superimposed CVs of supernatant samples from dense cell suspensions of *A. adeninivorans* mutants G1212/YRC102 and G1224, incubated at 47 °C. The oxidation peak corresponding to uric acid is present in the G1212/YRC102 supernatant but clearly absent in the G1224 supernatant.

4.4 Discussion

While this survey of several of Saccharomycetaceae-family yeasts is by no means supposed to be considered exhaustive, it does serve to illustrate that it is the trait of uric acid secretion, rather than its absence, that is the idiosyncratic property. This is consistent with the absence of any reports of uric acid secretion by electrochemical studies of yeasts in the literature. This further suggests it is some sort of metabolic novelty not present in similar yeasts which produces the observed extracellular uric acid.

The catabolic pathway for purine degradation for *A. adeninivorans*, in which uric acid is an intermediate step, is shown in Fig. 4.3. This pathway is similar to that found in some other yeasts, but differs from the pathway employed by higher eukaryotes (Jankowska et al., 2013a), which lack adenine deaminase, instead employing adenosine deaminase to convert adenosine to inosine.

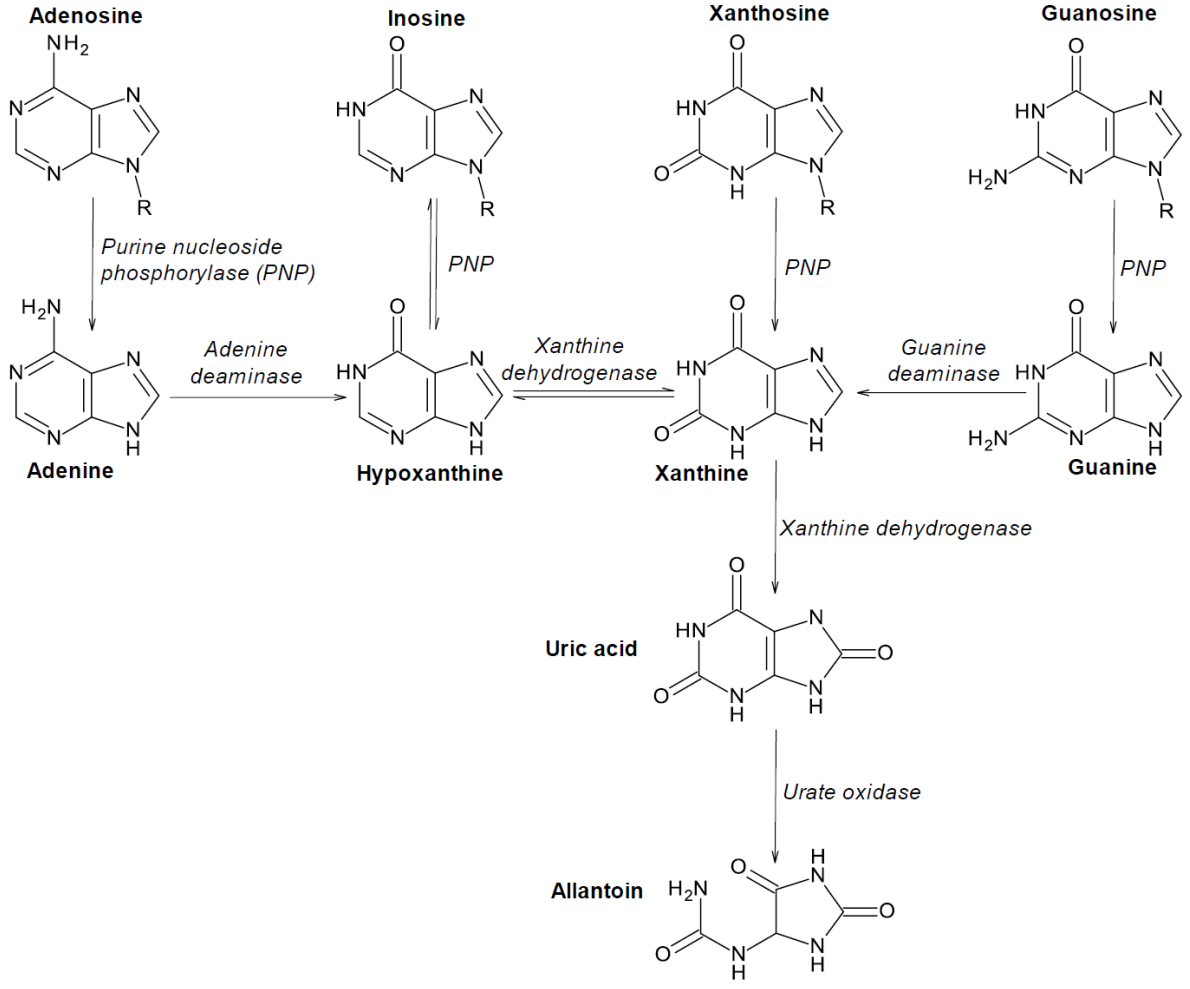

Figure 4.3: A schematic representation of the purine degradation pathway for *A. adeninivorans*. Purines that are not salvaged are degraded to uric acid and further to allantoin and allantoic acid via this pathway.

In the case of the mutant G1224, the mutant strain was incapable of producing the enzyme xanthine oxidoreductase. Xanthine oxidoreductase is a molybdenum-containing hydroxylase. It catalyses the oxidation of hypoxanthine to xanthine, and xanthine to uric acid. This can take place either using NAD^+ as an electron acceptor, via xanthine dehydrogenase activity (EC 1·17·1·4) or using O_2, via xanthine oxidase activity (EC 1·17·3·2). In a mutant that does not produce xanthine oxidoreductase, purine catabolism should terminate at xanthine and hypoxanthine, with no production of uric acid, allantoin or later breakdown products. As was shown in Fig 4.2, uric acid was not detected from G1224, implying that purine catabolism is indeed the source of either all or an overwhelming majority of the uric acid observed in *A. adeninivorans* cell suspensions.

Under normal conditions for most organisms, catabolism of purines through to uric acid (or on to further breakdown products, such as allantoin, allantoic acid, urea or ammonia, depending on the particular organism), followed by excretion is a mechanism for disposing of nucleic acids. Since nucleic acid turnover is a natural metabolic cycle continuously taking place in living cells (e.g. the synthesis and degradation of messenger-RNA), a substantial quantity of the purines freed during this cycle are normally salvaged for re-synthesis into nucleotides. Uric acid production from purine catabolism is therefore a function of excess metabolic purines. The secretion of substantial amounts of uric acid by *A. adeninivorans* is then logically derived from one of three sources. The first possibility is that the uric acid is a result of an excessive intake of purines from the environment (in this case, the growth medium), substantially surplus to the requirements of normal metabolism. This possibility can probably be eliminated; the YNB medium used to grow *A. adeninivorans* G1212/YRC102, G1212/YRC102-AYNI1-AUOR39 and G1212/YRC102-AYNI1-AUOR94 (as described in Chapter 3) did not contain purine or amino acid components, so all purines present must be synthesised *de novo* by the yeast. Despite this, high levels of uric acid were still observed via CV in the absence of nitrates.

The second possibility is that the purine salvage process is either not functioning or functioning to a reduced degree, resulting in an increased amount of purines being converted to uric acid and excreted as waste. An in-depth investigation into the purine salvage pathways of *A. adeninivorans* is beyond the scope of this thesis. It is worth noting however, that defective purine salvage has a well documented manifestation in human medicine in the form of Lesch-Nyhan syndrome (LNS) (Lesch and Nyhan, 1964). LNS is a heritable disorder caused by impaired function of the purine salvage pathway, resulting in overproduction of uric acid. This impairment is caused by mutation in the *HPRT1* gene causing deficiency of the enzyme hypoxanthine-guanine phosphoribosyltransferase (HGPRT) (Wilson and Kelley, 1983). HGPRT is a transferase which catalyses the conversion of hypoxanthine and guanine to inosine monophosphate (IMP) and guanosine monophosphate (GMP) respectively through a reaction with phosphoribosyl pyrophosphate (PRPP). Failure of HGPRT to fulfil its role results in the accumulation of an increased amount of uric acid from the inability to

recycle free hypoxanthine and guanine, leading to it being degraded to uric acid as waste. Furthermore, the excess PRPP not utilised by HGPRT up-regulates *de novo* production of purines, exacerbating uric acid production further (Rosenbloom et al., 1968). Partial deficiencies in HGPRT activity have also been observed, with milder increases in uric acid production resulting; this is named Kelley-Seegmiller syndrome (KSS) (Augoustides-Savvopoulou et al., 2002). *HPRT1* has a homolog observed in *S. cerevisiae* called *HPT1*. Mutations in this gene have been shown to result in decreased HGPRT activity, with the characteristic of purine excretion which is analogous to the hyperuricemia observed in sufferers of LNS or KSS (Woods et al., 1983).

The third possibility is that *A. adeninivorans* exhibits an undocumented metabolic trait of significantly elevated production (through biosynthesis or as a result of degradation of larger molecules with purine substituents) of one or more purines or purine derivatives, resulting in an increased surplus of free purine being disposed of as waste rather than being salvaged. Such a trait could be derived from, for example, a mutation resulting in a deregulation of *de novo* purine production pathways. An example of such a mutation has been observed in *S. cerevisiae* where a mutation in the *GUK1* gene resulted in the production of a low-activity guanosine monophosphate (GMP) kinase. This had the dual effects of derepressing adeninine production and causing an accumulation of GMP. This in turn caused feedback inhibition of HGPRT, phenocopying the characteristics of *HPT1* mutations, including purine excretion, although uric acid was not explicitly stated to have been observed amongst these secreted purines (Lecoq et al., 2000).

The literature does not appear to contain any descriptions of electrochemical analyses of mutant yeasts with the purine excretion phenotype, so it is not known whether such mutants replicate the electrochemical activity of *A. adeninivorans*. If future studies were to reveal similar electrochemical activity in samples derived from, for example, *S. cerevisiae* mutants with *HPT1* mutations, it opens the possibility that site-directed mutagenesis could be used to add the uric acid production trait to other microbial platforms for investigation as catalysts in a non-mediated MFC if *A. adeninivorans* proves unsuitable.

Regardless of the mechanism responsible for the uric acid overproduction, it seems unintuitive that an organism should maintain a mutant pathway whereby a strong reducing agent such as uric acid should be produced in abundance and then simply excreted into the environment. As a molecule bearing readily-liberated electrons, overproduction and export of uric acid is energetically costly; electrons that might otherwise be employed metabolically are being lost to the environment, and if *A. adeninivorans* uses any kind of active transport mechanism to export uric acid to the exterior of the cell, this would represent a further metabolic burden. The phenomenon seems further unusual when one considers that *A. adeninivorans* has been shown to be capable of assimilating uric acid as a sole carbon or nitrogen source (Middelhoven et al., 1984).

It is possible that a selection pressure may have given rise to and maintains this phenomenon, but the nature of this pressure is unclear. Masoud et al. (2012) reports that uric acid and metal-urate complexes exhibit some amount of biological activity and that such compounds could act as a basis for development of antimicrobial activity. The study does not, however, specify any effective concentrations for inhibition of microbial activity, and this property of urates does not appear to have been reported on further in the literature. In an early experiment in the course of the work described in this thesis, a cell suspension of *A. adeninivorans* LS3 became contaminated with one or more unknown strains of bacteria, causing the cell pellet to adopt a green-grey hue (as opposed to the normal cream colour). The supernatant from this suspension had a strong yellow colour and exhibited a dramatically larger than normal peak when examined using CV. Attempts to culture the contaminant yielded two main types of bacillus-shaped bacteria; one arranged in flat, dry colonies with a flaky surface, and the other producing copious quantities of translucent slime. When cultured and suspended, neither contaminant strain produced a supernatant displaying an oxidation peak corresponding to uric acid. Co-culturing these contaminants with *A. adeninivorans* did not reproduce the result originally observed, so the explanation for the enhanced uric acid production remains unknown.

Most of the studies of uric acid centre on its clinical significance; humans and other higher primates, having a defective urate oxidase gene that is not transcribed, tend to maintain a high concentration of around 200-400 μmol L^{-1} uric acid (ionised as urate with a single negative charge at biological pH) in blood plasma when compared with other mammals (Glantzounis et al., 2005). While the precise circumstances for the loss of urate oxidase activity in higher primates and why this mutation is maintained are not known, Ames et al. (1981) proposed that uric acid serves as a biologically significant antioxidant, serving as a powerful scavenger of peroxyl and hydroxyl radicals and singlet oxygen. Studies have shown that urate may contribute as much as 65.1% of human serum's antioxidant capacity (Maxwell et al., 1997). This indicates that the overproduction of uric acid could potentially serve a purpose in making *A. adeninivorans* more robust to oxidative stresses, and/or secretion of uric acid into the immediate environment could potentially provide some benefit to cells attempting to colonise an environment rich in (for example) free radicals or peroxides.

Another possibility is that uric acid is involved in some form of cell-cell interaction or signalling. Chen and Fink (2006) describe the use of secreted aromatic alcohols by *S. cerevisiae* as a key signal in a quorum sensing mechanism that induces the morphogenetic switch to the mycelial phase in nitrogen starvation conditions. While *A. adeninivorans* LS3 also exhibits a change in morphology from budding cells to mycelia in response to environmental conditions, in the case of LS3 this morphological shift is most obviously mediated by temperature, although the precise mechanism for the change is not fully elucidated, and seems to require a certain concentration of dissolved oxygen (which varies with the cultivation temperature) to be present (Wartmann et al., 2000). In the case of

anaerobic cultivation, only the budding cell phase appears to be maintained. In this regard, if uric acid is involved in the triggering or synchronisation of a change in morphology, it is worth noting that it is readily oxidised by dissolved oxygen. Given that the results described in section 3.3.1 appear to indicate that the observed uric acid concentration is highest in cell suspensions incubated at high temperature (favouring the mycelial phase) and low oxygen (favouring the budding yeast phase), if uric acid is indeed involved in regulation of cell morphology or signalling a change thereof, it is doubtful that it is used directly as a signalling molecule due to its low stability in aerobic conditions.

Secretion of purines has also been observed, independent of genetic defects, as a component in cell-cell interaction systems in the case of *S. cerevisiae*. Under conditions which induce sporulation (poor carbon source, nitrogen starvation), diploid *S. cerevisiae* cells heterozygous for the mating type locus (*MAT*a/*MAT*α) begin to secrete purines derived from degraded RNA into their environment, maintaining a pool of extracellular purines. Ascus formation is dependent on the uptake and re-utilisation of purines drawn exclusively from this extracellular reservoir, thereby synchronising the sporulation process between the cells taking up purines from the common pool (Jakubowski and Goldman, 1988). While this example may not have a direct analogue in *A. adeninivorans*, an anamorphic yeast without a known sexually reproducing stage, it does provide precedent for the use of excreted purines as an intercellular signalling mechanism in Saccharomycetaceae. Use of purines as chemical signals is extraordinarily widespread amongst living things in general (Burnstock and Verkhratsky, 2009), however extracellular purinergic signalling in fungi seems to be comparatively unexplored relative to other forms of life.

While there are few cases described in the literature, uric acid itself has been shown to be employed as a pheromone in nature. In the marine polychaete *Platynereis dumerilii*, the female releases a burst of uric acid in the water along with a cloud of eggs. Males respond to uric acid as a pheromone, releasing sperm when the uric acid concentration is sufficiently high as to indicate proximity to the egg cloud (Zeeck et al., 1998). While the metabolic pathways involved in the production and regulation of a reservoir of uric acid in the coelomic fluid does not appear to have been studied, if nothing else this case serves as a demonstration that uric acid can indeed serve the purposes of a signalling molecule.

An alternative hypothesis for the selection pressure maintaining excretion of uric acid is that *A. adeninivorans* might have some form of symbiotic relationship with another organism that utilises uric acid as a carbon and/or nitrogen source, in exchange for some benefit from the association. Amongst other yeasts there are several which are capable of using uric acid as a sole carbon source (Middelhoven et al., 1985). Furthermore a number of insects have been observed to have symbiotic relationships with uricolytic yeast or bacteria which recycle waste uric acid into forms that can be more easily metabolised by the host (e.g. Vera-Ponce De León et al. (2016)). It may be possible that

A. adeninivorans in its natural environment occurs as a member of a microbial community where the uric acid it excretes is catabolised into more easily utilised nitrogen compounds such as ammonia by other organisms.

There is a great deal which remains unknown about the role of uric acid plays in the metabolism of *A. adeninivorans* and why such an unusual characteristic has been retained by natural selection. It is theoretically possible that it is in fact no more than the result of a random mutation which is insufficiently deleterious to normal growth to be eliminated from the population, and no great purpose is served by its retention. For example, it has been reported that mutations to *HPT1* in *S. cerevisiae* are not significantly deleterious to vegetative growth, while producing the purine excretion phenotype (Guetsova et al., 1997; Lecoq et al., 2000). While this project was unable to determine a reason for the observed uric acid secretion, and a deep investigation into the regulation of purine metabolism in *A. adeninivorans* lies outside the scope of this thesis, nevertheless an understanding of the role of uric acid in this context would be beneficial to the goal of enhancing the performance of this yeast as a microbial catalyst for a non-mediated MFC.

4.5 References

Ames, B.N., Cathcart, R., Schwiers, E., and Hochstein, P. (1981). Uric acid provides an antioxidant defense in humans against oxidant- and radical-caused aging and cancer: A hypothesis. Proceedings of the National Academy of Sciences of the United States of America *78*, 6858-6862.

Augoustides-Savvopoulou, P., Papachristou, F., Fairbanks, L.D., Dimitrakopoulos, K., Marinaki, A.M., and Simmonds, H.A. (2002). Partial hypoxanthine-Guanine phosphoribosyltransferase deficiency as the unsuspected cause of renal disease spanning three generations: a cautionary tale. Pediatrics *109*.

Burnstock, G., and Verkhratsky, A. (2009). Evolutionary origins of the purinergic signalling system. Acta Physiologica *195*, 415-447.

Chen, H., and Fink, G.R. (2006). Feedback control of morphogenesis in fungi by aromatic alcohols. Genes and Development *20*, 1150-1161.

Glantzounis, G.K., Tsimoyiannis, E.C., Kappas, A.M., and Galaris, D.A. (2005). Uric acid and oxidative stress. Current Pharmaceutical Design *11*, 4145-4151.

Guetsova, M.L., Lecoq, K., and Daignan-Fornier, B. (1997). The isolation and characterization of Saccharomyces cerevisiae mutants that constitutively express purine biosynthetic genes. Genetics *147*, 383-397.

Haslett, N.D., Rawson, F.J., Barrière, F., Kunze, G., Pasco, N., Gooneratne, R., and Baronian, K.H.R. (2011). Characterisation of yeast microbial fuel cell with the yeast *Arxula adeninivorans* as the biocatalyst. Biosensors and Bioelectronics *26*, 3742-3747.

Jakubowski, H., and Goldman, E. (1988). Evidence for cooperation between cells during sporulation of the yeast Saccharomyces cerevisiae. Molecular and Cellular Biology *8*, 5166-5178.

Jankowska, D.A., Faulwasser, K., Trautwein-Schult, A., Cordes, A., Hoferichter, P., Klein, C., Bode, R., Baronian, K., and Kunze, G. (2013a). *Arxula adeninivorans* recombinant adenine deaminase and its application in the production of food with low purine content. Journal of Applied Microbiology *115*, 1134-1146.

Jankowska, D.A., Trautwein-Schult, A., Cordes, A., Hoferichter, P., Klein, C., Bode, R., Baronian, K., and Kunze, G. (2013b). *Arxula adeninivorans* xanthine oxidoreductase and its application in the production of food with low purine content. Journal of Applied Microbiology *115*, 796-807.

Lecoq, K., Konrad, M., and Daignan-Fornier, B. (2000). Yeast GMP kinase mutants constitutively express AMP biosynthesis genes by phenocopying a hypoxanthine-guanine phosphoribosyltransferase defect. Genetics *156*, 953-961.

Lesch, M., and Nyhan, W.L. (1964). A familial disorder of uric acid metabolism and central nervous system function. The American Journal of Medicine *36*, 561-570.

Masoud, M.S., Ali, A.E., Shaker, M.A., and Elasala, G.S. (2012). Synthesis, computational, spectroscopic, thermal and antimicrobial activity studies on some metal-urate complexes. Spectrochimica Acta - Part A: Molecular and Biomolecular Spectroscopy *90*, 93-108.

Maxwell, S.R.J., Thomason, H., Sandler, D., Leguen, C., Baxter, M.A., Thorpe, G.H.G., Jones, A.F., and Barnett, A.H. (1997). Antioxidant status in patients with uncomplicated insulin-dependent and non-insulin-dependent diabetes mellitus. European Journal of Clinical Investigation *27*, 484-490.

Middelhoven, W.J., de Kievit, H., and Biesbroek, A.L. (1985). Yeast species utilizing uric acid, adenine, n-alkylamines or diamines as sole source of carbon and energy. Antonie van Leeuwenhoek *51*, 289-301.

Middelhoven, W.J., Niet, M.C.H.T., and Rij, N.J.W.K.V. (1984). Trichosporon adeninovorans sp. nov., a yeast species utilizing adenine, xanthine, uric acid, putrescine and primary n-alkylamines as the sole source of carbon, nitrogen and energy. Antonie van Leeuwenhoek *50*, 369-378.

Rosenbloom, F.M., Henderson, J.F., Caldwell, I.C., Kelley, W.N., and Seegmiller, J.E. (1968). Biochemical bases of accelerated purine biosynthesis de novo in human fibroblasts lacking hypoxanthine-guanine phosphoribosyltransferase. Journal of Biological Chemistry *243*, 1166-1173.

Vera-Ponce De León, A., Sanchez-Flores, A., Rosenblueth, M., and Martínez-Romero, E. (2016). Fungal community associated with Dactylopius (Hemiptera: Coccoidea: Dactylopiidae) and its role in uric acid metabolism. Frontiers in Microbiology *7*.

Wartmann, T., Erdmann, J., Kunze, I., and Kunze, G. (2000). Morphology-related effects on gene expression and protein accumulation of the yeast *Arxula adeninivorans* LS3. Archives of Microbiology *173*, 253-261.

Wilson, J.M., and Kelley, W.N. (1983). Molecular basis of hypoxanthine-guanine phosphoribosyltransferase deficiency in a patient with the Lesch-Nyhan syndrome. Journal of Clinical Investigation *71*, 1331-1335.

Woods, R.A., Roberts, D.G., Friedman, T., Jolly, D., and Filpula, D. (1983). Hypoxanthine: Guanine phosphoribosyltransferase mutants in Saccharomyces cerevisiae. MGG Molecular & General Genetics *191*, 407-412.

Zeeck, E., Harder, T., and Beckmann, M. (1998). Uric acid: The sperm-release pheromone of the marine polychaete Platynereis dumerilii. Journal of Chemical Ecology *24*, 13-22.

Chapter 5

Environmental and metabolic parameters affecting the uric acid production of *Arxula adeninivorans*

5.1 Introduction

The yeast *Arxula adeninivorans* has been shown to exhibit the remarkable and apparently uncommon trait among yeasts of elevated uricogenesis via the purine catabolic pathway (Williams et al., 2014). This uric acid is excreted by the yeast into its immediate environment, which under batch conditions accumulates and is readily able to be measured using electrochemical methods, as demonstrated in previous chapters. This uric acid is believed to be the solution species responsible for the mediatorless electron transfer observed in the *A. adeninivorans*-catalysed MFC described by (Haslett et al. (2011)). The surge of current, corresponding to mediatorless electron transfer, yielded a very small current density of 70 mW m^{-2}, significantly less than the 1 W m^{-2} reported for an MFC using *A. adeninivorans* as a microbial catalyst in conjunction with 2,3,5,6-tetramethyl-1,4-phenylenediamine as a mediator. One of the measures that can be taken to improve the current density obtained in the MFC when relying solely on a non-mediated mode of operation is to optimize the conditions within the anode chamber for the production of uric acid by *A. adeninivorans.*

It was observed in Chapter 3 that in CV analyses of samples of supernatant derived from *A. adeninivcorans* suspensions, the charge transferred to the working electrode was markedly higher for suspensions which were incubated at 47 °C (Williams et al., 2014), near the upper limits of temperature where *A. adeninivorans* is able to grow (Wartmann et al., 1995). This suggests that improvements in the yield of uric acid might be obtained by subjecting *A. adeninivorans* to certain physiochemical conditions. In this study the effects of various conditions on the amount of uric acid accumulated by *A. adeninivorans* cultures is to be examined. Establishing these optimal conditions should improve the cells' performance as a potential microbial catalyst for a non-mediated MFC. Additionally, a mutant strain of LS3, termed G1221 is examined to determine the effects of elimination of urate oxidase on uric acid accumulation.

5.2 Materials and methods

5.2.1 Yeast strains, media and growth conditions

Four different strains of *A. adeninivorans* were used in this study. The wild-type strain, *A. adeninivorans* LS3, and the selectable auxotrophic gene expression platform mutant strain *A. adeninivorans* G1212 are described in section 3.2.1. The *AXOR* gene disruption mutant *A. adeninivorans* G1224 is described in section 4.2.1. *A. adeninivorans* G1221 [*aleu2 atrp1::ALEU2 auox::ATRP1*] is a mutant strain derived from G1212 with a deleted urate oxidase gene, preventing this strain from carrying out enzymatic oxidation of uric acid. These strains were obtained from the Leibniz Institute of Plant Genetics and Crop Plant Research (IPK), Gatersleben, Germany.

Escherichia coli XL1-Blue (*rec*A1 *end*A1 *gyr*A96 *thi*-1 *hsd*R17 *sup*E44 *rel*A1 *lac* [F' *pro*AB *lac*IqZΔM15 Tn10 Tet^r]) obtained from Stratagene (La Jolla, Calif., USA), served as the host strain for plasmid isolation. The strain was grown on LB medium supplemented with ampicillin (100 μg mL^{-1}) or kanamycin (50 μg mL^{-1}) for selection.

Yeast cultures involved in the construction of *A. adeninivorans* G1221 (Δ*auox*) were grown for 96 h at 30 °C under non-selective conditions in a yeast extract peptone dextrose (YEPD) medium [yeast extract 10 g L^{-1} (Oxoid, LP0044, Oxoid Limited, Basingstoke, Hampshire RG24 8PW, UK), peptone 20 g L^{-1} (Oxoid, LP0021, Oxoid Limited, Basingstoke, Hampshire RG24 8PW, UK), D-glucose 20 g L^{-1} (LabServ, AR, Thermo Fisher Scientific Australia Pty Ltd., Scoresby, Vic 3179, Australia)] or under selective conditions in a yeast minimal medium supplemented with 1% (w/v) glucose (YMM-glucose) containing different nitrogen sources at various concentrations (Tanaka, 1967). Agar plates were prepared by addition the of 15 g L^{-1} agar to the liquid media.

Yeast cultures involved in uric acid production studies were grown for 20 h at 37 °C in excess glucose conditions in YEPD medium or under glucose-free conditions in a yeast extract peptone glycerol (YEPG) medium [yeast extract 10 g L^{-1}, peptone 20 g L^{-1}, glycerol 20 g L^{-1} (Fisher Scientific, G/0650/15, Fisher Scientific UK Limited, Loughborough, Leicestershire LE11 5RG, UK)]. Agar plates were prepared by the addition of 15 g L^{-1} agar to the liquid media.

5.2.2 Construction of A. adeninivorans G1221 (Δauox)

Construction of *A. adeninivorans* G1221 was carried out at IPK by Anke Trautwein-Schult specifically for the purposes of the work described in this thesis.

5.2.2.1 Isolation of the AUOX gene and construction of the gene-disruption mutant A. adeninivorans G1221 (Δ*auox*)

The potential *A. adeninivorans* urate oxidase (*AUOX*) gene was identified using the fully sequenced and annotated genome data for *A. adeninivorans* LS3 (GenBank/EMBL data libraries, HF558665).

The ORF was amplified by PCR with chromosomal DNA of *A. adeninivorans* LS3 as template, using primers that incorporated flanking *Eco*RI and *Not*I restriction sites. The amplified *Eco*RI-*AUOX*- *Not*I gene fragment, which corresponds to the complete ORF, was disrupted by the insertion of the *ATRP1* gene into the *AOUX* gene. *ATRP1* acts as an auxotrophic marker.

5.2.2.2 Construction of Δauox mutants by gene disruption

To generate an *AUOX* gene replacement vector, the complete 2925 bp *AUOX* gene fragment including promoter and terminator structure was amplified by PCR using the primers AUOX-1 (5´-CCGAGGTGACTACCGCCATGA-3´ - nucleotide positions -1000 - -979) and AUOX-2 (5´-CCCAGAAAGATACTCCCGCAT-3´ - nucleotide positions 2925 - 2905) and inserted into the *E. coli* vector pCR4 (Invitrogen, Waltham, Massachusets, USA). Subsequently, 1000 bp of the 5´- and 1007 bp of the 3´-regions were amplified by whole vector PCR using two anti-parallelly orientated primers flanked by *Kpn*2I restriction sites on their 5´-ends (AUOX-3: 5´-**TCCGGA**GGTTTGTTCTTTTGTTTAAAACTATG-3´, nucleotide positions -1 - -26, *Kpn*2I restriction site in bold type and underlined; AUOX-4: 5´-**TCCGGA**GTAATTTAGCTACAGTTTATTATTTTAT-3´, nucleotide positions 922-949, *Kpn*2I restriction site in bold type and underlined). After self-ligation of the newly derived vector now containing the deleted *auox* gene fragment, the *Kpn*2I-flanked *ATRP1m* selection marker (Steinborn et al., 2007) was inserted into the *Kpn*2I site located between the 5´- and the 3´-*auox* gene fragments. In a last PCR step, the 1000 bp 5´-*auox* region – *ATRP1m* gene - 1004 bp 3´-*auox* region enclosing DNA fragment was amplified using the primers AUOX-1 and AUOX-2. The resulting amplification product was transformed into *A. adeninivorans* strain G1212 (Steinborn et al., 2007).

A. adeninivorans transformants were generated according to Rösel and Kunze (1998). Stable yeast transformants were obtained by passaging the cells on selective (YMM-glucose) and non-selective (YEPD) media (Klabunde et al., 2003).

5.2.3 Electrochemistry

CV was performed using an ADInstruments PowerLab 2/20 with ML160 Potentiostat, controlled by eDAQ EChem v2.5.4 data logging software. A three electrode configuration comprising a glassy carbon working electrode, platinum counter electrode and a Ag/AgCl reference electrode (3 M KCl) was used for voltammetry. The glassy carbon electrode was polished between each scan using aluminium oxide powder (0.3 μm, LECO) on a Lecloth. All CVs were performed in a Faraday cage and were scanned from 0 to +1.5 V at 100 mVs^{-1} with three replicate CVs recorded for each sample.

Linear sweep voltammetry (LSV) was performed using a similar three electrode configuration, with a Pt micro-disc working electrode (100 μM diameter, Tianjin Aida Hengsheng Technology Co. Ltd., Nankai, Tianjin, China). All LSVs were performed in a Faraday cage and were scanned +0.1 to +0.9 V at a scan rate of 5 mVs^{-1} with three replicate LSVs recorded for each sample. These values were converted to an equivalent uric acid concentration using a standard concentration curve generated from LSVs by plotting known concentrations of sodium urate solution against ΔI between +0.25 V and +0.75 V. The linear relationship between ΔI [nA] and urate concentration [μM] was determined to be

$$Concentration = \frac{\Delta I - 0.4595}{0.0125}$$

with an R^2 value for the linear fit of 0.9987.

5.2.4 Accumulation of uric acid in aerobic conditions

A. adeninivorans LS3 was cultivated aerobically in indented culture flasks containing 100 mL YEPD broth. The cells in each flask were centrifuged (10,000× g 8 min, 4 °C), discarding the supernatant, and washed twice with sterile deionised water. Each cell pellet was then re-suspended in 15 mL phosphate buffered saline (PBS, 0.05 M K_2HPO_4/KH_2PO_4, 0.1 M KCl) at pH 7 and transferred to a culture flask. OD_{600} for each sample was determined by measuring absorbance at 600 nm on an Amersham Biosciences Novaspec III visible spectrophotometer. The flasks were capped either with a loose metal cap (aerobic condition) or the airspace in the flask was flushed with N_2 gas and the flask sealed with a fermentation lock containing deionised water (anaerobic condition). Suspensions for each condition were prepared in triplicate. Flasks were then incubated in a shaking incubator for 20 hours at 45 °C and 120 rpm. The cell suspensions were then centrifuged and the supernatants recovered for analysis by LSV.

5.2.5 Accumulation of uric acid from high-aeration and low-aeration growth flasks

A. adeninivorans LS3 was cultivated aerobically in each of two varieties of culture flasks; a standard non-indented Erlenmeyer flask, or a flask modified to have deep indentations in the sides (Fig. 5.1). Flasks contained 100 mL of YEPD broth. Cells were harvested and washed as described above. Each cell pellet was then re-suspended in 15 mL PBS and the OD_{600} of each cell suspension determined as described above. Samples were prepared for incubation by pipetting 1.2 mL volumes of cell suspension into micro-centrifuge tubes, and incubated horizontally in a shaking incubator (150 rpm) for 20 hours at 45 °C. Samples for each aeration condition were prepared in triplicate. The samples were then centrifuged (10,000 g 8 minutes, 4 °C) and the supernatant recovered by pipette for LSV.

Figure 5.1: Culture flask types used in these experiments. LEFT: non-indented Erlenmeyer flask; CENTRE: commercial indented culture flask (Kimble Chase, Rockwood, TN, USA); RIGHT: deeply-indented flask (standard flasks modified by the Department of Chemistry, University of Canterbury).

5.2.6 Accumulation of uric acid under starvation, with-glucose, and with-glycerol conditions

A. adeninivorans LS3 was cultivated aerobically in indented culture flasks containing 100 mL YEPG broth, and the cells harvested and washed as described above. Each cell pellet was then re-suspended in 15 mL of either PBS, PBS containing 20 g L^{-1} dextrose, or PBS containing 20 g L^{-1} glycerol and transferred to a culture flask. OD_{600} for each sample was determined as described above. The flasks then had their airspace flushed with N_2 gas and sealed with a fermentation lock containing deionised water. Suspensions for each condition were prepared in triplicate. Flasks were then incubated in a

shaking incubator for 20 hours at 47 °C and 120 rpm. The cell suspensions were then centrifuged and the supernatants recovered for analysis by LSV.

5.2.7 Accumulation of uric acid and cell mortality for multiple strains under different temperature conditions

A. adeninivorans LS3, G1212 and G1221 cells were cultivated, harvested and washed as described above. Each cell pellet was then re-suspended in 15 mL PBS and the OD_{600} of each cell suspension determined as described above. 100 µL of each cell suspension was also serially diluted to 10^{-7} and 100 µL of this dilution was spread on YEPD agar plates in triplicate, incubated for 24 h at 30 °C for enumeration of cells. Samples were prepared for incubation by pipetting 1.2 mL volumes of cell suspension into micro-centrifuge tubes, and were then incubated horizontally in a shaking incubator (150 rpm) for 20 hours at either 37 °C or 45 °C. Suspensions for each combination of *A. adeninivorans* strain and temperature were prepared in sextuplicate. After incubation, 100 µL volumes of cell suspension were drawn from each of a random pair of samples of each strain, serially diluted to 10^{-6} for the 37 °C condition and 10^{-3} for the 45 °C condition and 100 µL of the dilution spread on YEPD agar plates in duplicate for enumeration after 72 h incubation at 30 °C. The samples were then centrifuged (10,000×g 8 minutes, 4 °C) and the supernatant recovered by pipette for LSV.

5.2.8 Accumulation of uric acid under different pH conditions

A. adeninivorans LS3 cells were cultivated, harvested and washed as described above. PBS solutions were prepared with adjusted pH values of 6, 8, 9 and 10 by adding 1M HCl or 1M NaOH to PBS until the desired initial value was obtained. pH was measured using a Thermo Scientific Orion 3 Star benchtop pH meter with a Eutech Instruments pH single-junction gel-filled probe ECFC7252101B (Thermo Fisher Scientific Australia Pty Ltd. Vic 3179, Australia). Each cell pellet was then re-suspended in 15 mL of one of the adjusted PBS solutions and the OD_{600} of each cell suspension determined as described above. Suspensions for each pH condition were prepared in triplicate. The airspace in each sample tube was flushed with N_2 gas and the lids screwed on tightly. The tubes were then incubated horizontally in a shaking incubator (80 rpm) for 20 hours at 45 °C. The cell suspensions were then centrifuged and the supernatants recovered for LSV and cyclic voltammetry (CV). The pH of the supernatant samples was also re-measured after the incubation.

5.3 Results

5.3.1 Aerated cell suspension

When the cell suspension was aerated by shaking during incubation, the accumulation of uric acid in the supernatant of the *A. adeninivorans* cell suspension was dramatically reduced compared with a cell suspension incubated in a sealed anaerobic container (Fig. 5.2). Given that uric acid has a much lower redox potential (E° = +0.59 V at pH 7 vs. a normal hydrogen electrode (NHE) (Simic and Jovanovic, 1989)) than that of oxygen (E°= +1.229 V at pH 7 vs. a standard hydrogen electrode (SHE) (Atkins, 1997)), we attributed this discrepancy to the uric acid secreted by *A. adeninivorans* being readily oxidised by dissolved oxygen. This is consistent with the observation in Chapter 3 that the electrochemically active molecule present in *A. adeninivorans* suspensions is readily degraded when left exposed to air rather than being analysed immediately or preserved by sparging with N_2 (Williams et al., 2014). As less than 30% of the uric acid observed when oxygen is excluded is accumulated in the presence of air, the utility of *A. adeninivorans* as a microbial catalyst will likely be dramatically impaired under aerobic conditions.

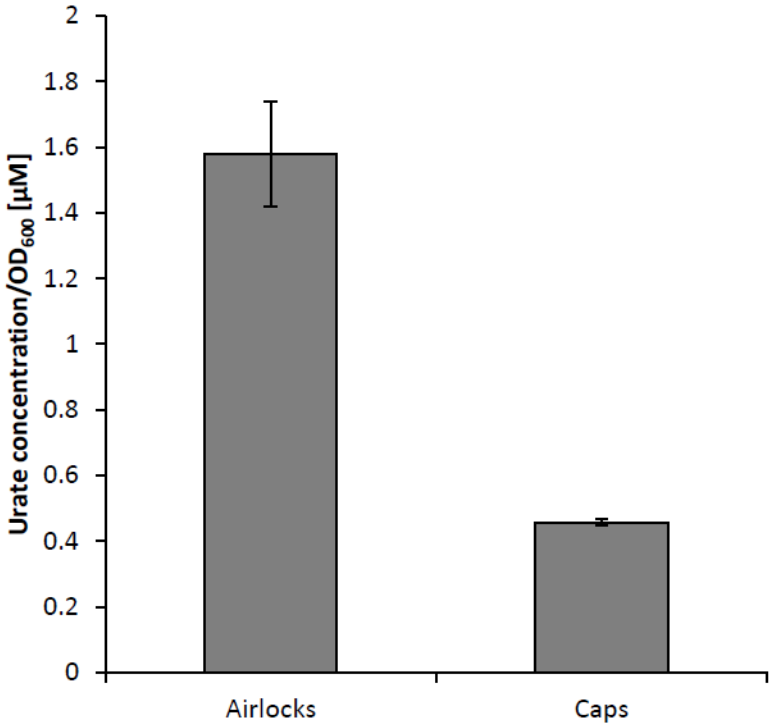

Figure 5.2: Comparison of the concentration of uric acid (per unit optical density of the cell suspension at 600 nm) in supernatants from cell suspensions of *A. adeninivorans* incubated for 20 h in flasks with loose caps permitting gas exchange and in sealed flasks with air purged from the flask head space with oxygen-free nitrogen. Where air was excluded from the flask, a substantially higher concentration of uric acid accumulated over the course of incubation. Error bars are one standard deviation.

5.3.2 High- vs low-aeration during cell growth

A. adeninivorans cultures incubated in the culture flask with deep indents in the sides were subjected to a great deal more turbulence, entraining more air in the medium and ensuring greater aeration of the culture medium. The cultures incubated in the non-indented smooth flasks, while shaken at the same speed and also under aerobic conditions, were subjected to visibly less turbulence, and as a result, less thorough aeration. Although the subsequent process of cell washing, resuspension and incubation was carried out identically for cells from both conditions, the cells which were incubated in more turbulent culture flasks subsequently displayed the accumulation of a markedly higher concentration of uric acid in the extracellular buffer than did the cells derived from the more quiescent environment of the non-indented flask (Fig 5.3). This suggests that although anaerobic conditions are superior for accumulating high concentrations of uric acid as shown in Fig. 5.2, cells grown in a more thoroughly aerated medium nevertheless are more vigorous producers of uric acid. This implies that the major contributor to the superiority of anaerobic conditions for accumulating uric acid may be the reduced oxidation of uric acid in the extracellular buffer by dissolved oxygen, and not necessarily some cell behavior characteristic of anaerobic environments which promotes higher uric acid production.

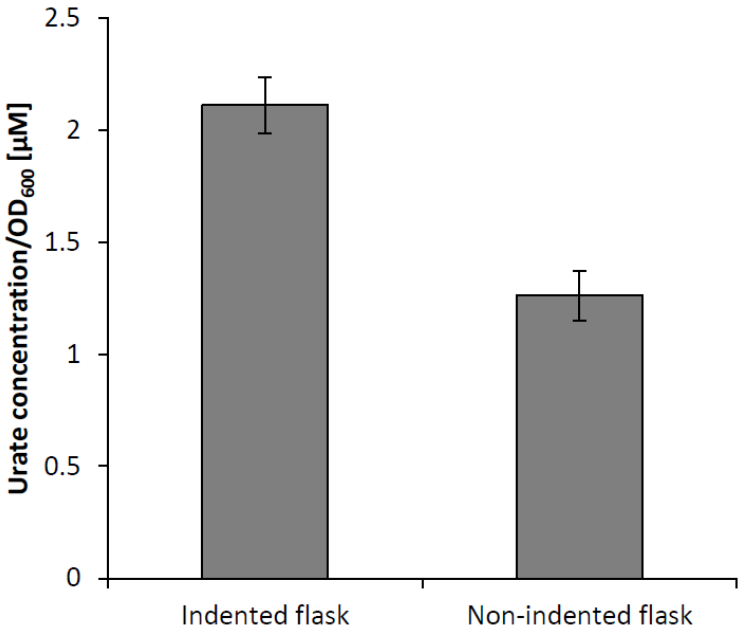

Figure 5.3: Comparison of the concentration of uric acid (per unit optical density of the cell suspension at 600 nm) in supernatants from cell suspensions of *A. adeninivorans*. Cell cultures were incubated for 20 h either in flasks with deep indentations allowing for high turbulence and greater aeration of the culture medium or flasks without indentations prior to washing and re-suspension and a second phase of incubation in PBS. A substantially higher concentration of uric acid accumulated in suspensions of cells cultured in an indented flask. Error bars are one standard deviation.

5.3.3 Starvation vs excess glucose in cell suspension

Introducing the presence of a high concentration of glucose in the suspension buffer reduced the concentration of uric acid that accumulated in the supernatant over the incubation period when compared with cells incubated in starvation conditions (Fig. 5.4). This suggests that the fermentative activity caused by the presence of glucose and absence of oxygen may suppress the overproduction and/or export of uric acid. A similar effect, though to a lesser extent was observed in the presence of the glycerol. This implies that the suppression of uric acid is not solely a glucose-dependent attribute. These cultures were originally grown in YEPG broth to ensure that any genes required for glycerol uptake and/or metabolism were expressed before the cells were harvested for the second incubation. Glycerol is known to be, in most cases, a non-fermentable carbon source, requiring the presence of oxygen to be metabolised. While the air was displaced from the air space in the flask by N_2, it is possible a small amount of oxygen remained dissolved in the buffer solution. Regardless, these results show that starvation conditions are more effective at enhancing the production of uric acid by *A. adeninivorans*, presumably so long as the cells have sufficient stores of nutrients to continue functioning.

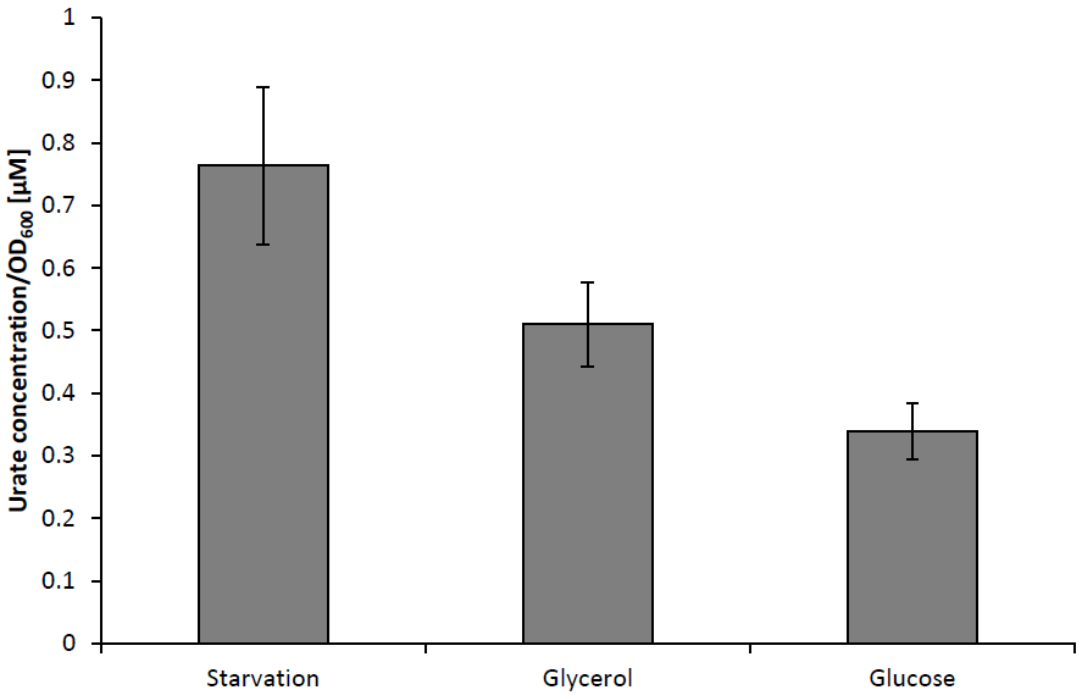

Figure 5.4: Comparison of the concentration of uric acid (per unit optical density of the cell suspension at 600 nm) in supernatants from cell suspensions of *A. adeninivorans* incubated for 20 h without a carbon source, with a high concentration of glucose or glycerol. The uric acid concentration observed diminishes sharply when glucose is present, and also to a lesser extent in the presence of glycerol. Error bars are one standard deviation.

5.3.4 Temperature adjustment

Fig. 5.5 shows that in the lower temperature condition (37 °C), the observed accumulation of uric acid was highest in suspensions of the urate oxidase knockout mutant, G1221. Given that the uric acid secreted by *A. adeninivorans* was been shown to be derived from purine catabolism in Chapter 4 (Williams et al., 2014), it is reasonable to attribute the increased concentration to the inability of G1221 to oxidise uric acid to allantoin. Fig. 3 also shows that the G1212 suspension accumulated significantly less uric acid than either of the other strains.

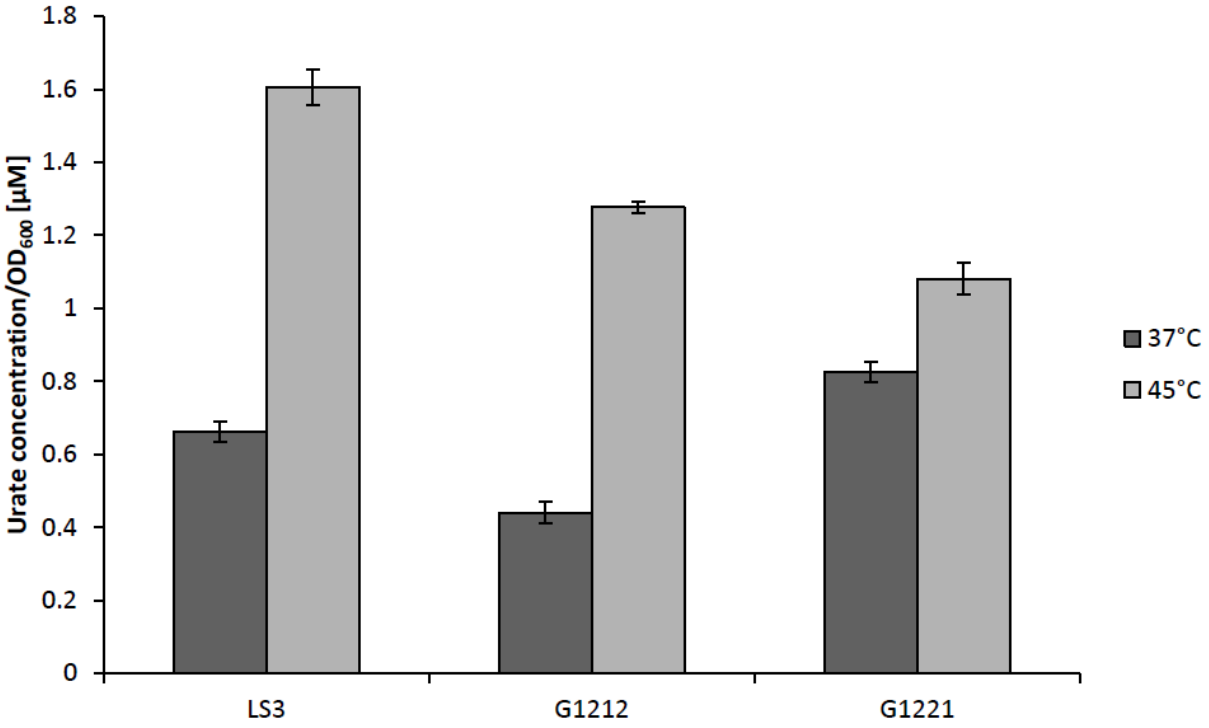

Figure 5.5: Comparison of the concentration of uric acid (per unit optical density of the cell suspension at 600 nm) in supernatants from cells suspensions of *A. adeninivorans* LS3, G1212 and G1221 incubated for 20 h at 37 °C or 45 °C. At 37 °C the *auox* mutant G1221 produces more uric acid than the other two strains, but its advantage disappears at high temperatures. Error bars are one standard deviation.

The effect of high and low temperature combined with starvation conditions was investigated to explore the potential of a secondary MFC stage with these conditions. Fig. 5.6 shows that the cell mortality rate for both G1212 and G1221 was significantly (p<0.05) higher after the 20 h incubation in PBS compared with the wild type LS3, both at 37 °C and 45 °C. At 45 °C, all strains accumulated a higher concentration of uric acid than in the lower temperature condition, and in the case of LS3 and G1212, in excess of a 2-fold increase. The cell mortality rate of LS3 was much closer to that of the mutant strains showing a 99.50% drop in viable cell population after the 20 h incubation (compared

with 99.99% in G1212 and G1221) at this temperature, however it also showed the highest observed concentration of uric acid. However, G1221 only exhibited a small increase in uric acid accumulation, resulting in the lowest concentration observed amongst the three strains. As a result, the selection of which strain would be optimal to use as a microbial catalyst may be dependent not only on the operating temperature selected for a theoretical MFC, but also on the expected operating duration. The precipitous falloff in viable cell count over 20 h is especially noticeable in G1221 even at the temperature where it is superior for uric acid accumulation, and this may make this strain unsuitable for long term use in an MFC.

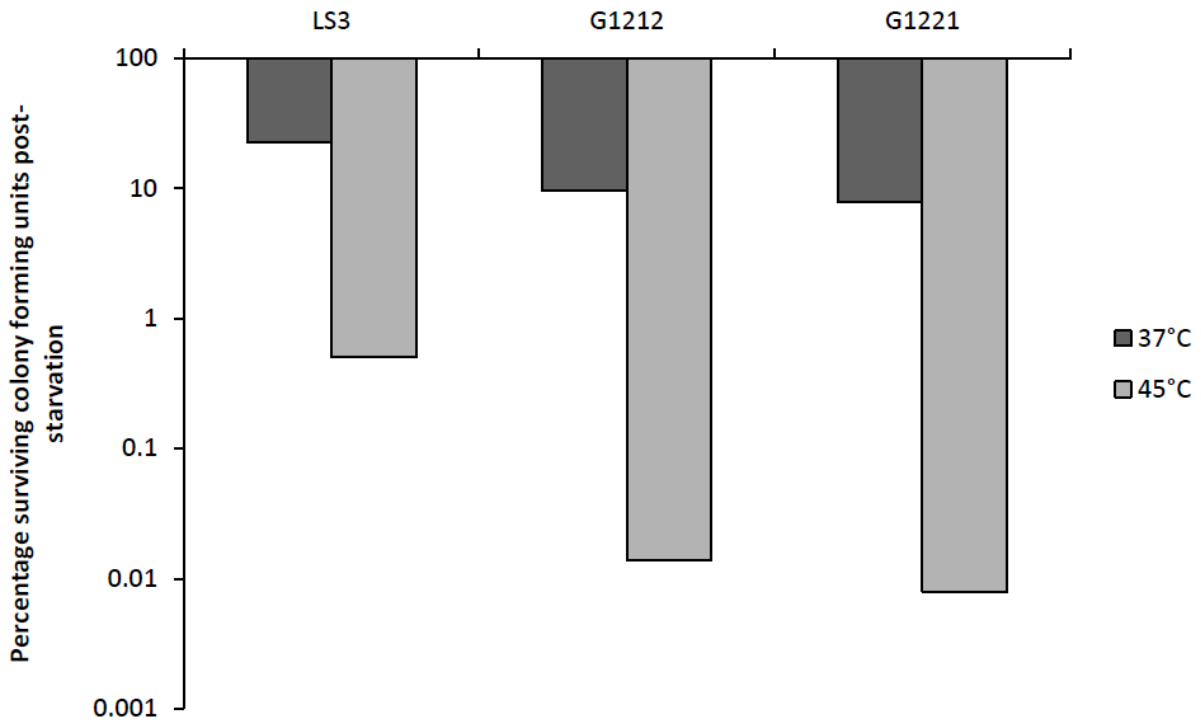

Figure 5.6: Comparison of the percentage of colony forming units of *A. adeninivorans* LS3, G1212 and G1221 observed by plate count after 20 h incubation in starvation conditions at 37 °C or 45 °C. While cell death increases in all strains at elevated incubation temperature, at both temperatures the mutant strains have a much higher death rate.

5.3.5 Buffer pH adjustment

Fig. 5.7 shows that the accumulation of uric acid observed in the supernatant samples increased almost 3-fold between the pH 6 and pH 8 conditions, after which it slowly declined (concentrations observed in pH 9 and pH 10 conditions are not significantly different, p=0.11). A similar pattern can be observed in the final pH values of each sample after the 20 hour incubation as shown in Fig. 5.8; the final supernatant pH was approximately 7 for the samples with initial pHs of 8 to 10, with the ΔpH increasing accordingly. G1224, the mutant strain shown not to produce any electrochemically detectable uric acid in Chapter 4, was used as a control to determine if the secreted uric acid itself had any effect on pH, but was observed to present the same changes in pH as LS3 (Fig. 5.9). The lack of increase in uric acid concentration above pH 8 may be due to the conflicting influence of the increasing stability of urate ions in more alkaline conditions with the deleterious effect alkaline conditions have on *A. adeninivorans* metabolism (Stöckmann et al., 2014).

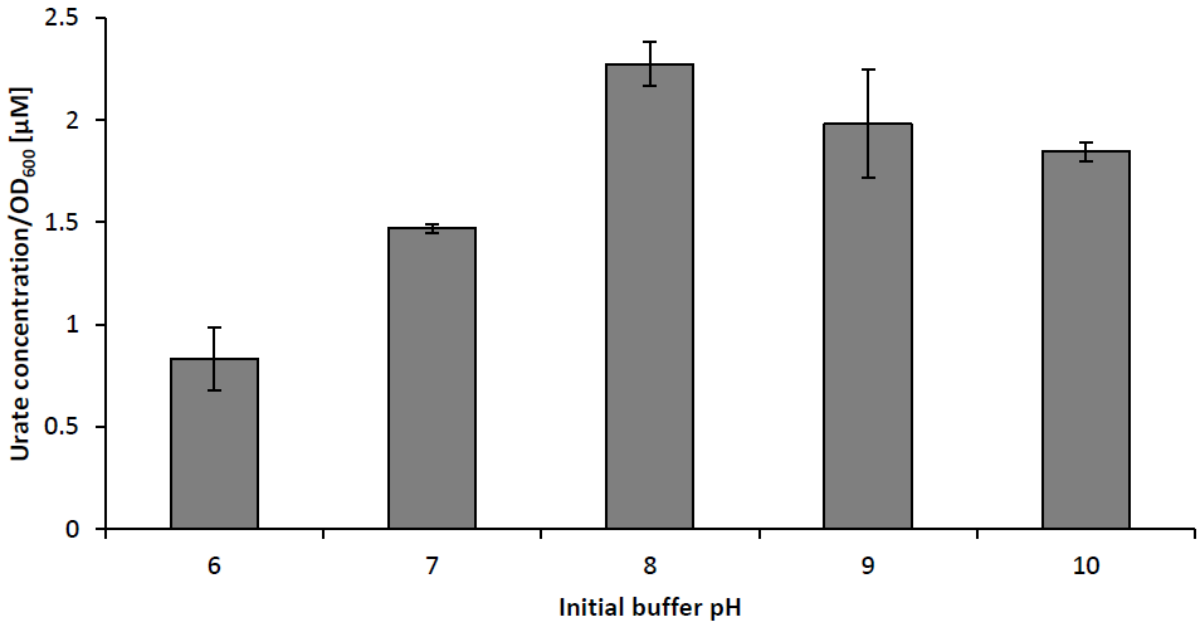

Figure 5.7: Comparison of the concentration of uric acid (per unit optical density of the cell suspension at 600 nm) in supernatants from cell suspensions of *A. adeninivorans* LS3 adjusted to a range of initial pH values. The highest observed concentration was in the pH 8 suspension, with the concentration of uric acid dropping sharply in more acidic suspensions. Error bars are one standard deviation.

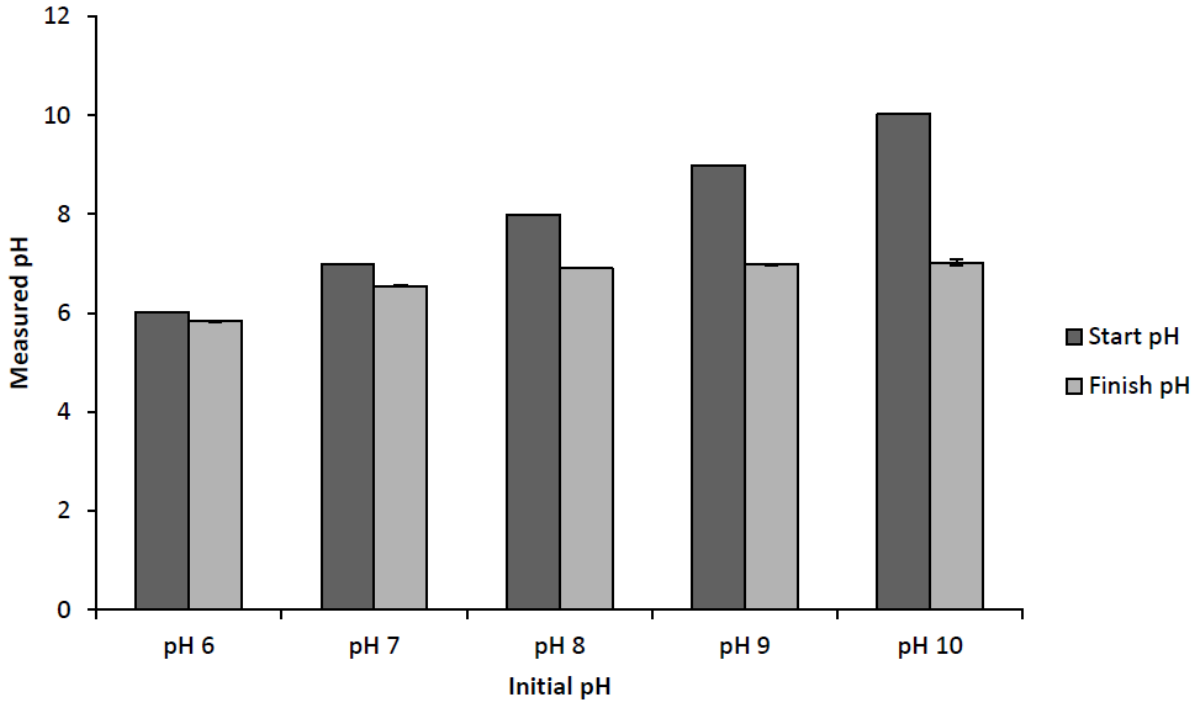

Figure 5.8: Comparison between the initial and final pH of cell suspensions of *A. adeninivorans* LS3. All suspensions became more acidic over 20 h incubation, but the change was more pronounced in samples with intial pH 8 to 10, which converged on a final pH of approximately 7. Error bars are one standard deviation.

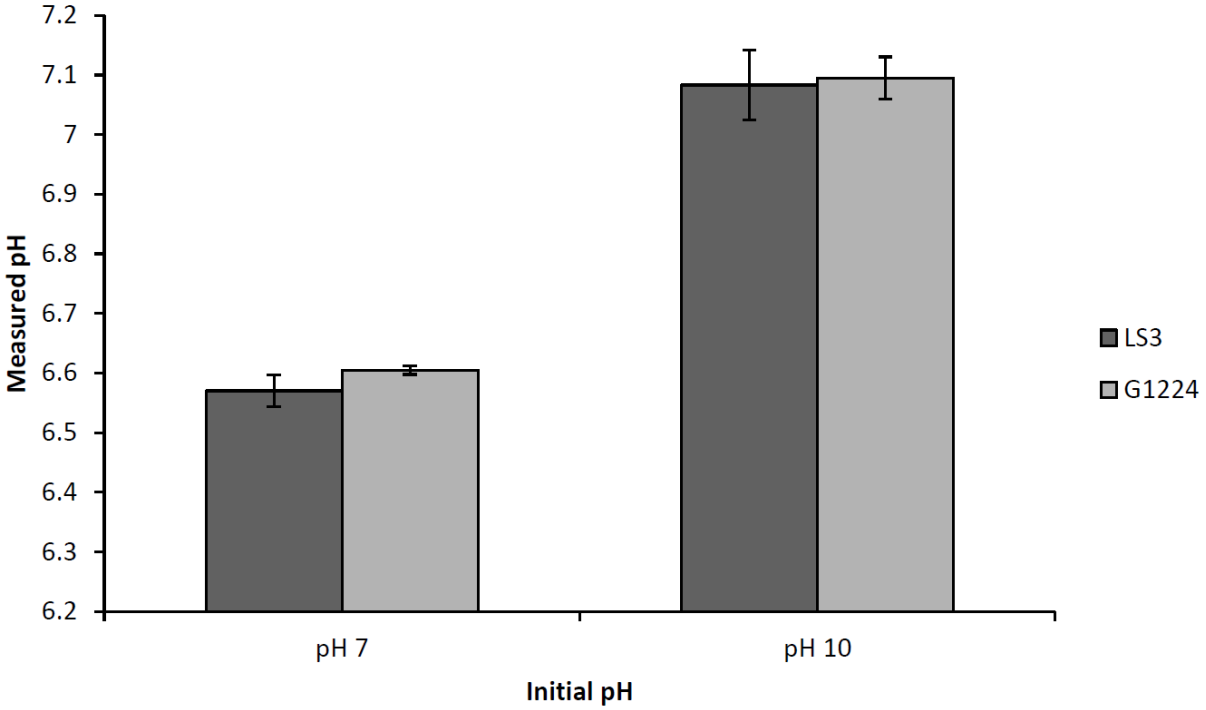

Figure 5.9: Comparison between the final pH observed in supernatants derived from suspensions of *A. adeninivorans* LS3 and G1224 suspended in pH 7 PBS and pH 10 PBS. This was done to control for any influence of uric acid produced by the cells. G1224 has a purine breakdown pathway which terminates with xanthine as the final waste product, rendering it incapable of producing uric acid. That the observed final pH values for G1224 are the same as for LS3 indicates that uric acid is not a driving force for the decreasing pH of *A. adeninivorans* suspensions shown in Fig. 5.8. Error bars are one standard deviation.

The peak anodic potential of the uric acid in the sample (the local maximum at +0.42 V for the pH 7 condition) was found to occur at more positive voltages in more acidic samples and more negative voltages in alkaline ones (Fig. 5.10). There was also a greater broadening of the uric acid oxidation peak the more alkaline the sample, possibly due to a combination of the increased uric acid production and the more complex equilibrium between the singly-charged acid urate ion which is dominant at pH values near neutral and the much less stable dually-charged urate ion which are able to form in strongly alkaline solutions.

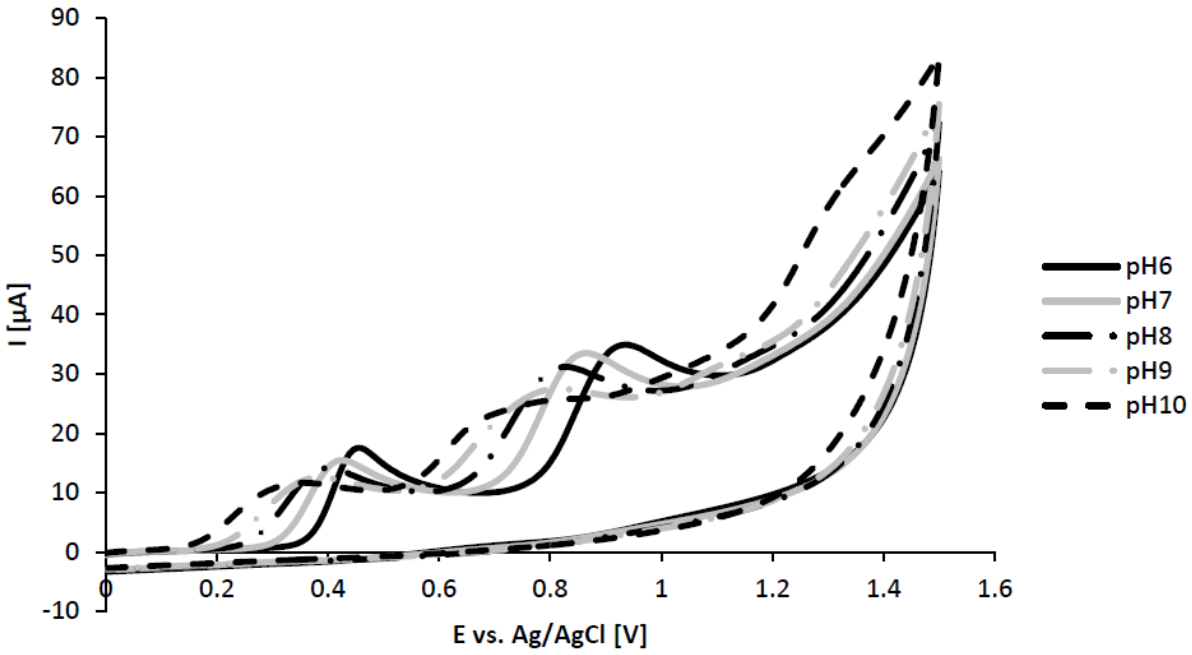

Figure 5.10: Cyclic voltammograms of supernatants from cell suspensions of *A. adeninivorans* LS3 with a range of initial pH values. In general, the oxidation peaks, including the one corresponding to uric acid, occurred at a lower potential the higher the initial pH of the cell suspension.

While these results broadly suggest an improved production of uric acid by *A. adeninivorans* at modestly higher pH, the organism appears to actively resist such a change to its environment by making it more acidic. Lowering the pH would also increase the theoretical redox potential of uric acid, rendering it a less favourable anolyte for an MFC.

5.4 Discussion

In order to exploit the uric acid secretory properties of *A. adeninivorans* so that it might be employed as a mediator-free microbial catalyst in an MFC, the conditions under which the cells might be encouraged to produce an abundance of uric acid need to be carefully appraised, along with the potential practical burdens that applying such conditions might place on this conceptual MFC from an design perspective.

The electrons transferred to an MFC anode by a secreted metabolite typically represent only a fraction of those that can be harvested by employing a mediator (Haslett et al., 2011; Hubenova and Mitov, 2010). While this is a trade-off for dispensing with the practical problems associated with the use and reclamation of chemical mediators, it is nonetheless appropriate to both maximise the production of the secreted reduced metabolite and conserve its stability in solution so that the greatest number of molecules possible are oxidised at the anode to produce current. The most immediate problem presented in this regard is oxidation by dissolved oxygen. As Fig 5.2 shows, in a situation where a suspension of *A. adeninivorans* was exposed to atmospheric oxygen, only a fraction of the uric acid secreted was observed in solution. This illustrates the sensitivity of uric acid to one of the key challenges in exploiting a reduced solution species as a way of harvesting electrons from cells in an MFC: oxygen has a very positive redox potential relative to uric acid, and therefore dissolved oxygen competes with the anode to oxidise the exoelectrogenic molecule. This problem is not limited only to self-mediated MFCs but can afflict any MFC employing a mediator which can be reduced by oxygen before transferring electrons to the anode. The most obvious solution to this problem is to simply exclude oxygen from the MFC, however, this bears the concomitant condition of restricting the cells to anaerobic metabolic processes. The drawbacks of this approach are vividly highlighted in Fig 5.3, wherein is it demonstrated that thorough aeration of the culture medium during the growth phase results in a cell suspension which, even when transferred to the anaerobic phase, demonstrates superior uric acid production compared with less well-aerated cells placed under the same conditions. This suggests that at least to some extent the metabolic vigour expressed by the cells where a large amount of dissolved oxygen is available continues to affect production of uric acid under anaerobic conditions, hinting at the possibility that uric acid production may in fact be superior in thoroughly oxygenated cultures, but that this is not readily measurable due to the rapidity of chemical oxidation of uric acid under these conditions. Inasmuch as it is not measurable, so also is it not available for utilisation by a theoretical MFC.

Restriction to anaerobic metabolism is also a very significant problem for the core concept of MFCs as a wastewater remediation measure, especially since the capacity to metabolise a broad range of substrates is one of the key arguments favouring the use of yeast cells as biocatalysts in MFCs. While there may be some carbon sources in a waste stream that can be fermented under anaerobic

conditions, generally speaking oxygen is often necessary for the more complex pathways involved in metabolising more unusual carbon and nitrogen sources. In order to retain aerobic metabolism, one needs to either enable the anode to outcompete the oxygen present, or to separate the growth process (utilising oxygen) from an oxygen-free anodic oxidation process.

In the first case, there are two main strategies: 1) to improve the affinity of the anode for electron harvesting/transport by electrode modification, and 2) to reduce the amount of time a given molecule of the reduced molecule (in this case, uric acid) is resident in solution before coming into contact with the anode where the electrons may be harvested. The simplest approach to addressing these is to select and/or modify electrodes for high conductivity and high surface area. Common large-surface-area electrodes include carbon cloths and meshes, which showed improved performance after being heat-treated (Wang et al., 2009), and carbon felts, which have been shown to achieve high power densities when modified with nickel-island nanostructures (Hubenova et al., 2011). In the latter case, the yeast *Candida melibiosica* was shown to form an immature biofilm on the anode surface after 30 hours of cultivation, which may have contributed to the improved electron transfer. In this case the modified electrode allowed higher power densities to be obtained in a semi-aerobic arrangement than had been previously obtained with unmodified carbon felt under anaerobic conditions. Forming an electrochemically active anodic biofilm is a property that has been exploited successfully in bacteria-based MFCs (e.g. *Geobacter sulfurreducens* (Bond and Lovley, 2003), *Rhodoferax ferrireducens* (Chaudhuri and Lovley, 2003), *Shewanella putrifaciens* (Kim et al., 2002), *Klebsiella* sp. IR21 (Lee et al., 2016)), and aids in allowing electrons to rapidly be harvested by the anode. While many yeasts demonstrate the ability to form biofilms on abiotic surfaces (Verstrepen and Klis, 2006), it is not known if *A. adeninivorans* exhibits such a trait or to what extent.

A common strategy, especially with some of the favoured bacterial genera used as MFC catalysts such as *Geobacter*, *Rhodoferax*, and *Shewanella* to develop microbial biofilms is to polarise the anode to encourage the microbial catalyst to adhere to its surface and use it as a terminal electron acceptor (Kannaiah Goud and Venkata Mohan, 2013). This approach is effective because metabolically these types of microorganisms can use an external solid electron acceptor (e.g. iron (II) oxide) as an endpoint to their metabolic processes in nature, and therefore they are readily conditioned to grow on an anode as a substitute for the electron acceptors in their natural habitat (Schröder, 2007). In the case of *C. melibiosica*, anodic biofilm formation is speculated to be a strategy associated with tolerance for metal toxicity rather than electrochemical effects (Hubenova et al., 2011). In the case of *A. adeninivorans*, it was shown that the uric acid generating the electrochemical signals observed originates from purine catabolism in Chapter 4 (Williams et al., 2014). Furthermore, the elevated uric acid production of the Δ*auox* strain G1221 shows that the steps of purine degradation that normally follow the production of uric acid are still present and functioning in wild-type *A. adeninivorans*, in spite of the secretion of an "overflow" of uric acid from this process, with no known survival benefit

to the organism. As such, it appears that the uric acid production observed is a superfluous waste-disposal process, which means that it is unlikely that there is any significant metabolic benefit associated with growth on an electrode surface to encourage the formation of a biofilm by *A. adeninivorans* to improve the electron transfer kinetics to the electrode via uric acid. Alternatively, the charged amino groups in the chitin component of the yeast cell wall could potentially be exploited to attempt to electrostatically encourage a yeast microbial catalyst such as *A. adeninivorans* to associate with the electrode, however the surface charge of the yeast cell changes with the pH and ion composition of the environment (Volkov, 2015), factors which are actively altered by the cell's own metabolism.

Whichever strategy is attempted, the difficulty in raising the anode's competitiveness with oxygen for uric acid oxidation will be a challenging but necessary hurdle to overcome. The cell suspensions examined accumulated very little uric acid despite an optical density far higher than a naturally cultivated cell culture will reach under normal conditions, meaning minimising the losses to non-anodic oxidation will be crucial in maximising power density in an *A. adeninivorans*-catalysed MFC.

In order to apply the approach of separating growth phase from the electricity-generating phase, waste remediation would need to take place in an independent, well-aerated culture vessel where the cells are cultured and then transferring the cells to an anaerobic anode chamber where the reduced molecules are secreted and harvested for a period before recycling the cells back to aerobic growth. As shown in Fig. 5.4, the accumulation of uric acid in the supernatant of an anaerobic suspension of *A. adeninivorans* was observed to be higher under conditions of complete starvation than when dextrose was added to the buffer. There are several possible causes for this, including a suppression of uric acid production/secretion when glucose metabolism is active, or the oxidation of secreted uric acid by metabolic waste products. As noted above, however, cell cultures in a well-aerated culture medium (containing abundant dextrose) appeared to exhibit higher uric acid production during subsequent incubation under anaerobic starvation conditions, suggesting the combination of glucose and anaerobic conditions may produce this suppression effect.

It is also possible that *A. adeninivorans* is susceptible to sugar-induced cell death, a phenomenon observed in some yeasts whereby the presence of an abundance of glucose in the absence of the full complement of growth nutrients initially promotes cell growth but also induces the production of reactive oxygen species (ROS), triggering apoptosis (Granot et al., 2003) and reducing the population of viable cells. Alternatively, uric acid, as a potent antioxidant could interact with the ROS produced, reducing the detectable concentration of uric acid. Curiously however, despite the fact that oxygen was excluded from the culture flask, a reduction in uric acid concentration was also observed where the non-fermentable carbon source glycerol was added to the suspension buffer, albeit a more modest one.

The suppression of uric acid secretion observed in the presence of glucose is corroborated by a previous investigation of *A. adeninivorans* being incorporated into an MFC utilising a $KMnO_4$ catholyte, wherein electron transfer measured as power density of a non-mediated MFC was observed to be lower when glucose was present in the anolyte, both in aerobic and anaerobic conditions (Haslett, 2011). While these observations support an anaerobic starvation phase for uric acid production separated from an aerobic culture phase, such an approach is practically challenging to implement; whether one chooses to keep the cell culture *in situ* exchanging the medium between nutrition and starvation cycles, or keep the media in situ and move the cells, the process adds an awkward additional complication to running the MFC, in addition to wasting whatever uric acid may be secreted during the aerobic phase.

The operating temperature of the MFC is important for both metabolic and practical reasons. It is immediately obvious that an MFC which runs effectively at ambient temperatures is more convenient from a design and implementation perspective compared with one which requires energy to be put into the system for heating or cooling. In conjunction with this, the behaviour and tolerances of the yeast component needs to be taken into account, such that its performance as a microbial catalyst is optimised to the greatest extent. It was observed in Chapter 3 that the estimated concentration of uric acid accumulating in the supernatant of *A. adeninivorans* LS3 cell suspensions was higher at higher incubation temperatures (Williams et al., 2014), and this has been confirmed in this study via LSV; this response to high temperature is also seen in the mutant strains G1212 and G1221. The attempt to further improve uric acid production of *A. adeninivorans* by truncating purine catabolism by deleting the gene encoding urate oxidase was met with mixed results however. At 37 °C, G1221 outperformed both the wild type and the auxotrophic gene expression platform strain, demonstrating that genetic modification to purine catabolism is a valid approach to increase uric acid production, and thereby improve the suitability of *A. adeninivorans* as a self-mediating microbial catalyst. At 45 °C however, the elevated production relative to the other strains is no longer evident. The small increase in uric acid production compared with the 37 °C condition results in G1221 producing the lowest yield of the strains studied. One possible implication of this observation is that one of the contributing factors to the elevation in uric acid production with increasing temperature is thermal inactivation of uricase. Liu et al. (1994) found a 50% loss in activity of urate oxidase purified from *Candida* sp. after 5 minutes incubation at 45 °C. This may mean that an extended incubation of *A. adeninivorans* at 45 °C may serve to some extent as a temperature-driven approximation of the phenotype of the gene knockout mutation in G1221.

This factor alone is, however, insufficient to explain the discrepancies between the observed concentrations of uric acid in LS3 and G1221, and the poor performance of G1212. Given the substantially higher cell death exhibited by the mutant strains after 20 hours of starvation at 37 °C (90.49% for G1212 and 92.07% for G1221) shown in Fig. 4, it is probable that cell death may

contribute to the reduced uric acid concentration observed for G1212, with such a reduction in G1221 masked by the effect of the gene knockout causing a net concentration increase.

The cause of this elevated mortality in the mutant strains is not known. The G1212 strain possesses a tryptophan auxotrophy used in its role as a selectable expression platform, and it is possible that under starvation conditions a shortage of this amino acid might play a role in triggering an apoptosis pathway (Eisler et al., 2004). This would not explain the similarly elevated mortality rate in G1221, a mutant selected based on complementation of the *atrp1* of G1212. In general, it appears that the mutant strains of *A. adeninivorans* have lost a measure of the resilience to cellular stresses that the wild type LS3 possesses. Loss of thermoresistance in mutant strains of *A. adeninivorans* derived from LS3 has been observed in previous studies of this organism (Wartmann et al., 2000).

Even if this problem were to be solved and a new mutant developed that did not respond so poorly to starvation conditions, the more resilient LS3 strain nonetheless suffers a 77.39% loss in viable population over 20 hours, suggesting that long starvation phases are impractical due to the high mortality rate. This is further exacerbated if the temperature is elevated to take advantage of the increased uric acid production, with population loss increasing to 99.50% in LS3 and 99.99% in the mutant strains, meaning near complete culture death in the 45 °C condition, in spite of a reputation in the literature for high temperature tolerance (Wartmann et al., 1995). This places severe limitations on the organism's ability to exploit high-temperature starvation conditions for high uric acid production. Coupled with the energy demand of keeping an MFC heated above ambient temperature, this makes improving the performance of the G1221 mutant at temperatures closer to ambient seem a more favourable option for optimising uric acid production as an electron export method.

The pH conditions of the cell suspension in an MFC influence many important factors affecting performance. We have observed that increasing the pH up to 8 results in an improved yield of uric acid (as shown in Fig. 5.7), and this is accompanied by the peak anodic potential moving in the negative direction (Fig. 5.9). In an MFC this confers the dual advantages of making more electrons available to the anode and increasing the difference in redox potential between the anode and cathode reactions, resulting in a higher voltage. It is, however, not without drawbacks. The precipitous drop in growth rate in conditions in excess of pH 6.5 (Stöckmann et al., 2014) exhibited by *A. adeninivorans*, to the point of a near complete lack of growth near pH 8, shows that these conditions are biologically suboptimal for the yeast cells. Over the course of the incubation, the pH of the suspension fluid drops, with the increase in acidity becoming more pronounced the higher the initial pH of the suspension (Fig. 5.8). Even in the pH 6 condition, which already results in a higher oxidation potential (reducing the theoretical potential of an MFC), the cells continue to lower the pH of their environment, albeit at a reduced rate, and Stöckmann et al. (2014) reported that *A. adeninivorans* cultures could drop the pH to 2.1. This means that in an arrangement where the feedstock is introduced directly into the anode

chamber as the growth substrate, optimising pH for uric acid production will severely impair growth, and failing to control the pH of the anode chamber will cause the MFC performance to degrade as both electron availability and voltage drop with pH. Even in the starvation situation, where growth is not a concern, feedback control on pH will be required to maintain alkaline conditions in the MFC, adding additional complexity to the system and potentially increasing cell mortality by adding an extra physiological stress to the already starving cells. Presuming all these factors could be overcome, increasing the pH of the anode chamber could potentially risk reducing the availability of the protons needed to pass from the anode compartment to the cathode compartment to balance the electrochemical reaction, creating additional resistance to the flow of electrons from anode to cathode.

These observations suggest that in a situation where an *A. adeninivorans* biofilm is able to be formed on the anode, MFC performance may degrade even more rapidly over time. With the cells acidifying their environment along with the hydrogen ions liberated in oxidation half reactions at the anode, the poor mass transfer kinetics of hydrogen ions diffusing from the biofilm to the bulk fluid of the anode chamber may result in the biofilm rapidly becoming acidic (Torres et al., 2008) and reducing the potential difference between the anode and cathode reactions, as well as reducing the concentration of uric acid produced.

Many of the examined modifications to *A. adeninivorans* culture conditions do show some capacity to increase the uric acid production compared with the very small amount produced under ambient conditions. However the fact that the conditions for higher production also have deleterious effects on cell survival and metabolism hamper their suitability as strategies for enhancing the performance of *A. adeninivorans* as a self-mediating microbial catalyst in a yeast-based MFC. Coupled with the fact that power densities in mediatorless *A. adeninivorans* MFCs have been observed to be very low without using an artificial soluble mediator, there is currently no clear path for developing the use of *A. adeninivorans* as a practical MFC. Many of these issues will also exist for any self-mediating yeast-catalysed microbial fuel cells because the necessity for aerobic growth to maximise metabolic rate and substrate diversity of the yeast catalyst is opposed to the tendency for free oxygen to competitively oxidise secreted reduced molecules. As a result, development of an effective method for simultaneously permitting aerobic metabolism in the biocatalyst while ensuring oxidation of soluble reduced molecules takes place only at the anode is a critical hurdle to overcome for the development of yeast-based, self-mediating MFCs.

5.5 References

Atkins, P.W. (1997). Physical Chemistry, 6th edn (New York: W.H. Freeman and Company).

Bond, D.R., and Lovley, D.R. (2003). Electricity production by *Geobacter sulfurreducens* attached to electrodes. Applied and Environmental Microbiology *69*, 1548-1555.

Chaudhuri, S.K., and Lovley, D.R. (2003). Electricity generation by direct oxidation of glucose in mediatorless microbial fuel cells. Nature Biotechnology *21*, 1229-1232.

Eisler, H., Fröhlich, K.U., and Heidenreich, E. (2004). Starvation for an essential amino acid induces apoptosis and oxidative stress in yeast. Experimental Cell Research *300*, 345-353.

Granot, D., Levine, A., and Dor-Hefetz, E. (2003). Sugar-induced apoptosis in yeast cells. FEMS Yeast Research *4*, 7-13.

Haslett, N.D. (2011). Development of a microbial fuel cell for organic waste bioremediation and simultaneous electricity generation. In Faculty of Agriculture and Life Sciences (Christchurch, New Zealand: Lincoln University).

Haslett, N.D., Rawson, F.J., Barrière, F., Kunze, G., Pasco, N., Gooneratne, R., and Baronian, K.H.R. (2011). Characterisation of yeast microbial fuel cell with the yeast *Arxula adeninivorans* as the biocatalyst. Biosensors and Bioelectronics *26*, 3742-3747.

Hubenova, Y., and Mitov, M. (2010). Potential application of *Candida melibiosica* in biofuel cells. Bioelectrochemistry *78*, 57-61.

Hubenova, Y.V., Rashkov, R.S., Buchvarov, V.D., Arnaudova, M.H., Babanova, S.M., and Mitov, M.Y. (2011). Improvement of yeast-biofuel cell output by electrode modifications. Industrial and Engineering Chemistry Research *50*, 557-564.

Kannaiah Goud, R., and Venkata Mohan, S. (2013). Prolonged applied potential to anode facilitate selective enrichment of bio-electrochemically active Proteobacteria for mediating electron transfer: Microbial dynamics and bio-catalytic analysis. Bioresource Technology *137*, 160-170.

Kim, H.J., Park, H.S., Hyun, M.S., Chang, I.S., Kim, M., and Kim, B.H. (2002). A mediator-less microbial fuel cell using a metal reducing bacterium, *Shewanella putrefaciens*. Enzyme and Microbial Technology *30*, 145-152.

Klabunde, J., Kunze, G., Gellissen, G., and Hollenberg, C.P. (2003). Integration of heterologous genes in several yeast species using vectors containing a *Hansenula polymorpha*-derived rDNA-targeting element. FEMS Yeast Research *4*, 185-193.

Lee, Y.Y., Kim, T.G., and Cho, K.S. (2016). Enhancement of electricity production in a mediatorless air–cathode microbial fuel cell using *Klebsiella* sp. IR21. Bioprocess and Biosystems Engineering, 1-10.

Liu, J., Li, G., Liu, H., and Zhou, X. (1994). Purification and properties of uricase from *Candida* sp. and its application in uric acid analysis in serum. Applied Biochemistry and Biotechnology - Part A Enzyme Engineering and Biotechnology *47*, 57-63.

Rösel, H., and Kunze, G. (1998). Integrative transformation of the dimorphic yeast *Arxula adeninivorans* LS3 based on hygromycin B resistance. Current Genetics *33*, 157-163.

Schröder, U. (2007). Anodic electron transfer mechanisms in microbial fuel cells and their energy efficiency. Physical Chemistry Chemical Physics *9*, 2619-2629.

Simic, M.G., and Jovanovic, S.V. (1989). Antioxidation mechanisms of uric acid. Journal of the American Chemical Society *111*, 5778-5782.

Steinborn, G., Wartmann, T., Gellissen, G., and Kunze, G. (2007). Construction of an *Arxula adeninivorans* host-vector system based on trp1 complementation. Journal of Biotechnology *127*, 392-401.

Stöckmann, C., Palmen, T.G., Schroer, K., Kunze, G., Gellissen, G., and Büchs, J. (2014). Definition of culture conditions for *Arxula adeninivorans*, a rational basis for studying heterologous gene expression in this dimorphic yeast. Journal of Industrial Microbiology and Biotechnology *41*, 965-976.

Tanaka, A., Ohnishi, N., Fukui, S. (1967). Studies on the formation of vitamins and their function in hydrocarbon fermentation. Production of vitamin B6 by *Candida albicans* in hydrocarbon medium. Journal of Fermentation Technology *45*, 617-632.

Torres, C.I., Marcus, A.K., and Rittmann, B.E. (2008). Proton transport inside the biofilm limits electrical current generation by anode-respiring bacteria. Biotechnology and Bioengineering *100*, 872-881.

Verstrepen, K.J., and Klis, F.M. (2006). Flocculation, adhesion and biofilm formation in yeasts. Molecular Microbiology *60*, 5-15.

Volkov, V. (2015). Quantitative description of ion transport via plasma membrane of yeast and small cells. Frontiers in Plant Science *6*, 5-22.

Wang, X., Cheng, S., Feng, Y., Merrill, M.D., Saito, T., and Logan, B.E. (2009). Use of carbon mesh anodes and the effect of different pretreatment methods on power production in microbial fuel cells. Environmental Science and Technology *43*, 6870-6874.

Wartmann, T., Erdmann, J., Kunze, I., and Kunze, G. (2000). Morphology-related effects on gene expression and protein accumulation of the yeast *Arxula adeninivorans* LS3. Archives of Microbiology *173*, 253-261.

Wartmann, T., Krüger, A., Adler, K., Duc, B.M., Kunze, I., and Kunze, G. (1995). Temperature-dependent dimorphism of the yeast *Arxula adeninivorans* Ls3. Antonie van Leeuwenhoek *68*, 215-223.

Williams, J., Trautwein-Schult, A., Jankowska, D., Kunze, G., Squire, M.A., and Baronian, K. (2014). Identification of uric acid as the redox molecule secreted by the yeast *Arxula adeninivorans*. Applied Microbiology and Biotechnology *98*, 2223-2229.

Chapter 6

Power production in a non-mediated MFC catalysed by *Arxula adeninivorans*

6.1 Introduction

A. adeninivorans has been previously studied as a microbial catalyst for use in a yeast-based MFC (Haslett et al., 2011). The format of this cell was a double-chambered MFC incorporating carbon fibre mesh electrodes and a Nafion 115 proton-exchange membrane (PEM). The *A. adeninivorans* LS3 cells were suspended in the anode chamber, with $KMnO_4$ in the cathode chamber to serve as the electron acceptor. It was in this study that it was first noted that a surge of electron transfer from *A. adeninivorans* was observed even under conditions where the mediator used in the study (tetramethyl-1,4-phenylenediamine) was absent, and that this was due to an electrochemically active solution species produced by the cells. It was on this basis that it was concluded that *A. adeninivorans* had potential as a self-mediating microbial catalyst for a mediator-free MFC.

The practicality of an MFC is not simply a question of the power density that can be obtained from a given arrangement of components in a laboratory setting at a single point in time. Ultimately, a successful economic argument must be made for long-term usage and upscale potential of a particular MFC design to justify continued investigation. This is a particularly demanding requirement especially in the case of yeast-based, non-mediated MFCs, which very often have substantially lower power densities than their artificially-mediated counterparts (Hubenova and Mitov, 2015). In the case of the MFC examined by Haslett et al. (2011), the use of $KMnO_4$ as a catholyte has a crippling drawback, in that the cathode reaction causes a dark brown MnO_2 precipitate to adhere to the cathode, PEM, and other surfaces inside the cathode compartment of the MFC. This caused severe fouling and significantly obstructed both the cathode surface and the cathode-facing side of the PEM (based on personal inspection of the apparatus used). This precipitate is very difficult to remove using common solvents, and renders cathodes non-functional and virtually unsalvageable within <40 h total usage time (Haslett, 2011). Because of this, use of $KMnO_4$ as a catholyte in this MFC arrangement must be ruled out as impractical, regardless of the power density it might generate, as it is destructive to the MFC components.

The alternative chemical catholyte proposed in this thesis is Dynawhite bleach (Jasol, Christchurch, New Zealand). Dynawhite is a common, inexpensive, mass produced household laundry bleach with 3

to 5% NaOCl as the active ingredient, and represents in this context an archetypal "lowest common denominator" for chemical catholytes, lacking the economic cost of the quality control imposed on analytical-grade laboratory reagents, while still functioning as a powerful oxidant. NaOCl undergoes two different oxidation half-cell reactions. The first of these (here, half-cell potentials are stated vs. SHE):

$$\mathrm{H^+ + HOCl} + e^- \rightarrow \frac{1}{2}\mathrm{Cl_{2(g)}} + \mathrm{H_2O} \qquad E° = +1.63\ \mathrm{V}$$

is dominant in acidic conditions, while the second:

$$\mathrm{ClO^- + H_2O} + 2\mathrm{e^-} \rightarrow \mathrm{Cl^-} + 2\mathrm{OH^-} \qquad E° = +0.89\ \mathrm{V}$$

predominates under neutral and basic conditions (Cotton and Wilkinson, 1972). It is probable that the second reaction will be the one manifest in a Dynawhite-based catholyte, as household bleach typically has a pH of 12-13.

As a catholyte, NaOCl also has the advantages of being biodegradable (hence environmentally friendly, naturally decomposing into sodium chloride and sodium chlorate over time) and inimical to the growth of microbial contaminants which may invade the cathode compartment of the MFC. NaOCl has been examined previously as a chemical catholyte (Medeiros and Zoski, 1998), and has further been incorporated in an MFC previously and used as a chemical catholyte to drive sludge digestion (Ghadge et al., 2015).

The most commonly used PEM material in most MFCs throughout the literature is Nafion, a highly thermally and mechanically stable polymer with good corrosion resistance, which only conducts cations through its pores. The major drawback of Nafion is that it is very expensive (>US$1200/m^2; www.fuelcellstore.com, College Station, Texas, USA), making scale-up of MFCs incorporating Nafion relatively costly. An alternative membrane which has been examined as a lower-cost alternative to Nafion is Ultrex CMI-7000 cation exchange membrane, which, while sometimes exhibiting poorer performance than Nafion in power production (Sotres et al., 2015), is an order of magnitude less expensive, and therefore much more economical in scaling up (US$111/m^2; www.membranesinternational.com, Ringwood, NJ 07456, USA).

In this study, the attempt will be made to determine if the stable, linear increase in power density over time in a non-mediated *A. adeninivorans* catalysed MFC described by Haslett et al. (2011) (Fig. 6.1) can be reproduced in an MFC substituting a NaOCl catholyte in place of MNO_4 and an Ultrex membrane in place of Nafion.

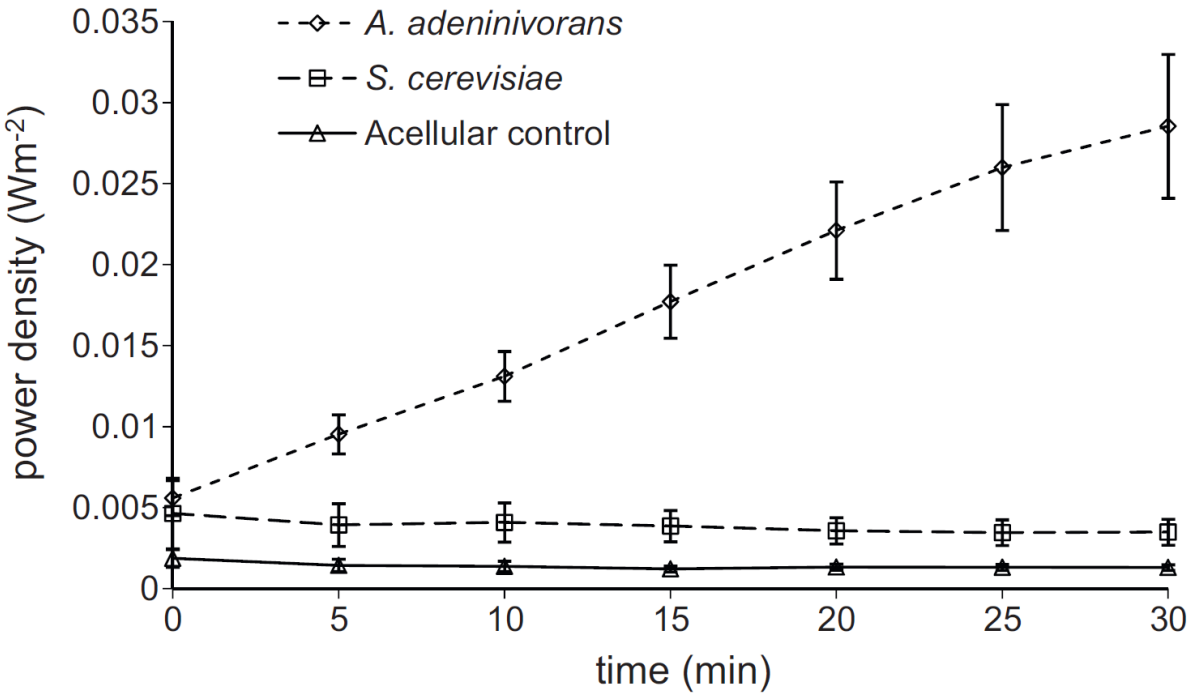

Figure 6.1: Power output in mediatorless *A. adeninivorans* and *S. cerevisiae* MFCs, reproduced from Haslett et al. (2011) with permission. Cell OD_{600}=2.5, temperature 37°C, rotated at 80rpm, external resistance 100 Ω, electrode surface area 0.001018 m^2.

6.2 Materials and methods

6.2.1 Yeast strains, media and growth conditions

Two different strains of *A. adeniniovrans* were used in these experiments: *A. adeninivorans* LS3, the wild-type strain, and *A. adeninivorans* G1221, the urate oxidase gene knockout strain. Both of these strains have been described in the preceding chapters. These strains were obtained from the Leibniz Institute of Plant Genetics and Crop Plant Research (IPK).

A. adeninivorans LS3 and G1221 were grown under non-selective conditions for 20 hours at 37 °C in a YEPD broth medium [yeast extract 10 g L^{-1} (Oxoid, LP0021, Oxoid Limited, Basingstoke, Hampshire RG24 8PW, UK), peptone 20 g L^{-1} (Oxoid, LP0044, Oxoid Limited, Basingstoke, Hampshire RG24 8PW, UK), dextrose 20 g L^{-1} (LabServ, AR, Thermo Fisher Scientific Australia Pty Ltd., Scoresby, Vic 3179, Australia) sterilised at 121 °C], aerated by agitation in a shaking incubator.

6.2.2 Buffers and reagents

Cells were suspended in phosphate buffered saline (PBS, 0.05 M K_2HPO_4/KH_2PO_4, 0.1 M KCl), pH 7. Suspension PBS was sparged with N_2 gas before use.

Catholyte solution was prepared as a 1:1 mixture of PBS and Dynawhite. Catholyte was freshly prepared before each experiment.

6.2.3 Preparation of cell suspension anolyte

A. adeninivorans cells were cultivated aerobically in indented culture flasks containing 100 mL YEPD broth. The cells in each flask were centrifuged (10,000 g, 8 min, 4 °C), discarding the supernatant, and washed twice with sterile deionised water. Each cell pellet was then re-suspended in 15 mL PBS. OD_{600} for the suspension was determined by measuring absorbance at 600 nm on an Amersham Biosciences Novaspec III visible spectrophotometer. Additional buffer was added to the suspension until an OD_{600} of 2.5 was obtained. Cell suspensions were freshly prepared each day; suspensions older than 12 h were discarded.

6.2.4 Fuel cell apparatus

A two-chambered MFC was used in these experiments. The main body of the MFC was fabricated from polycarbonate, forming two 15 mL chambers, separated by an Ultrex CMI-7000 membrane. Rubber gaskets were placed between adjacent components to form a seal and prevent leakage. The assembly was fastened tightly together with bolts and thumbscrews (Fig. 6.2).

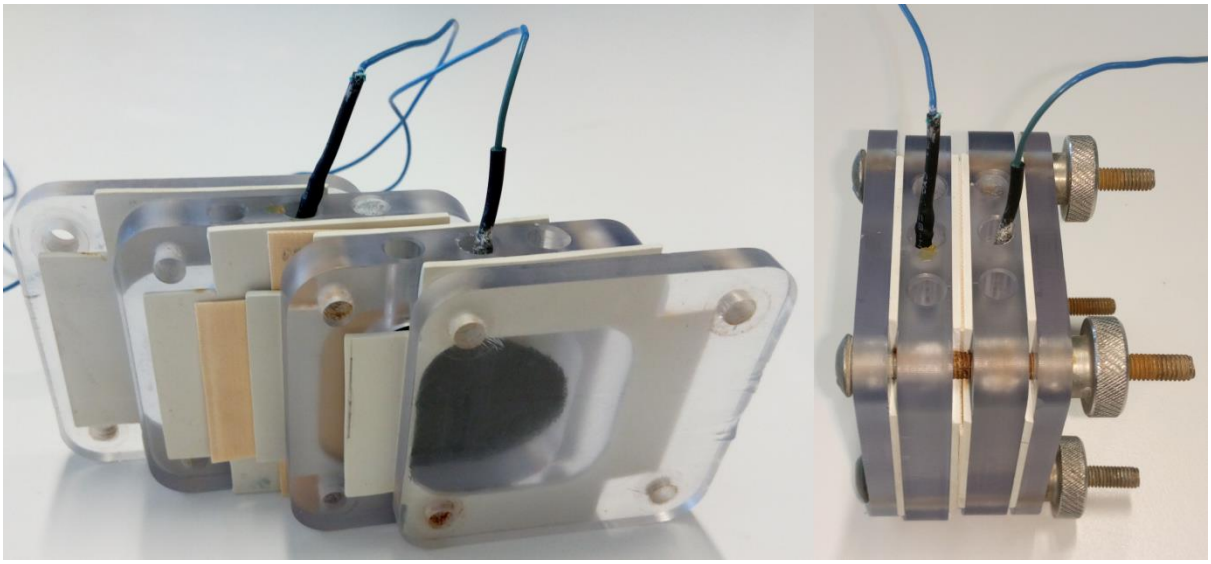

Figure 6.2: *Left*: MFC components spread to show different layers of apparatus. From the left: polycarbonate wall, rubber gasket, polycarbonate anode chamber, rubber gasket, ion exchange membrane, rubber gasket, polycarbonate cathode chamber, rubber gasket, polycarbonate wall. *Right*: MFC components assembled and secured with thumbscrews.

Electrodes were fabricated from punched circles of carbon cloth (CCWP4005, www.fuelcellearth.com, Woburn, Massachusetts, USA) with a diameter of 0.038 m (cross sectional area of 0.00134 m^2). Electrode leads were mode from braided copper wire. Electrodes were soaked overnight in acetone to de-grease and rinsed thoroughly with distilled water before use. Electrodes are shown in Fig. 6.3.

Figure 6.3: Carbon cloth electrodes. While the electrode on the left is a cathode and the right an anode the design and fabrication is the same.

External load/resistance was applied by a 0-10,000 Ω ten-turn linear potentiometer connected to the electrode leads. Resistance settings on the potentiometer were checked with a digital multimeter (Hung Chang Model 4510). Voltage across the load was also measured using this multimeter.

Experiments were conducted inside a shaking incubator (INFORS HT Ecotron Incubation Shaker), used as a temperature-controlled chamber and set to oscillate at 80 rpm to keep the cells in suspension. Temperature of the anolyte cell suspension was monitored using a digital thermometer (Omega HH801B digital thermometer).

6.2.5 Power-time analysis

In order to examine the changes in power density over time with a fixed external load applied to the MFC, 15 mL of OD_{600} 2.5 *A. adeninivorans* cell suspension was pipetted into the anode chamber and 15 mL of 1:1 Dynawhite:PBS catholyte was pipetted into the cathode chamber. The cell was then allowed to equilibrate until the digital thermometer indicated that the anolyte temperature was at the desired set-point for the experiment (typically 37 °C) and the multimeter indicated that the open-circuit voltage of the MFC had stabilised. The potentiometer was then set to 100 Ω and connected to the MFC. The voltage across the load was measured every 60 seconds for 30 minutes. The voltage was converted into power density by combining Ohm's law (Eqn. 1.1):

$$V = I \cdot R \qquad \text{(Equation 1.1)}$$

where V is voltage in volts (V), I is current in amperes (A) and R is resistance in ohms (Ω), with the equation for power density (Eqn. 1.2):

$$PD = \frac{V \cdot I}{SA} \qquad \text{(Equation 1.2)}$$

where PD is power density in watts per square metre (W m^{-2}), and SA is surface area in square metres (m^2), giving Eqn 1.3:

$$PD = \frac{\frac{V^2}{R}}{SA} \qquad \text{(Equation 1.3)}$$

6.2.6 Power-load analysis

In order to examine the behaviour of power density relative to external load applied to the MFC, 15 mL of OD_{600} 2.5 *A. adeninivorans* cell suspension was pipetted into the anode chamber and 15 mL of 1:1 Dynawhite:PBS catholyte was pipetted into the cathode chamber. The cell was then allowed to equilibrate until the thermometer indicated that the anolyte temperature was at the desired set-point for the experiment (typically 37 °C) and the multimeter indicated that the open-circuit voltage of the MFC had stabilised. The potentiometer was then connected and the voltage across it measured for the following loads: 100 Ω, 200 Ω, 300 Ω, 400 Ω, 500 Ω, 600 Ω, 700 Ω, 800 Ω, 900 Ω, 1000 Ω, 2000 Ω, 3000 Ω, 4000 Ω, 5000 Ω, 6000 Ω, 7000 Ω, 8000 Ω, 9000 Ω and 10000 Ω. Voltages were then converted into power densities using the equations described above.

6.3 Results

6.3.1 Power-time analysis

The power-time curve is a visualisation of the power density as it changes over time. It is useful for determining the amount of power transfer an MFC is capable of at steady state when run for an extended period with a fixed external load. The power density of an acellular control MFC containing only PBS in the anode chamber is shown in Fig. 6.4.

The first measurement was taken at the first clearly displayed voltage at the moment the circuit was closed with the external load applied. This value was rather erratic, hence the extremely large error bar at time = 0. It is difficult to know to what extent the high power density of the first point is due to the response of the MFC to suddenly becoming polarised when the circuit is closed, as opposed to being an artefact of the speed at which the multimeter used to perform the measurements is able to register and display a rapidly changing voltage, not to mention the response time of the analyst recording it. As such, no conclusions should necessarily be drawn from the first point, save that in the short span of time immediately following the closing of the circuit, the voltage dropped precipitously from the open circuit voltage to approach an operating steady state, and by extension the power density dropped sharply also. It could be argued that the open circuit potential should be recorded as the true voltage at t=0, however no external load is present when the circuit is open, so no power density can be calculated.

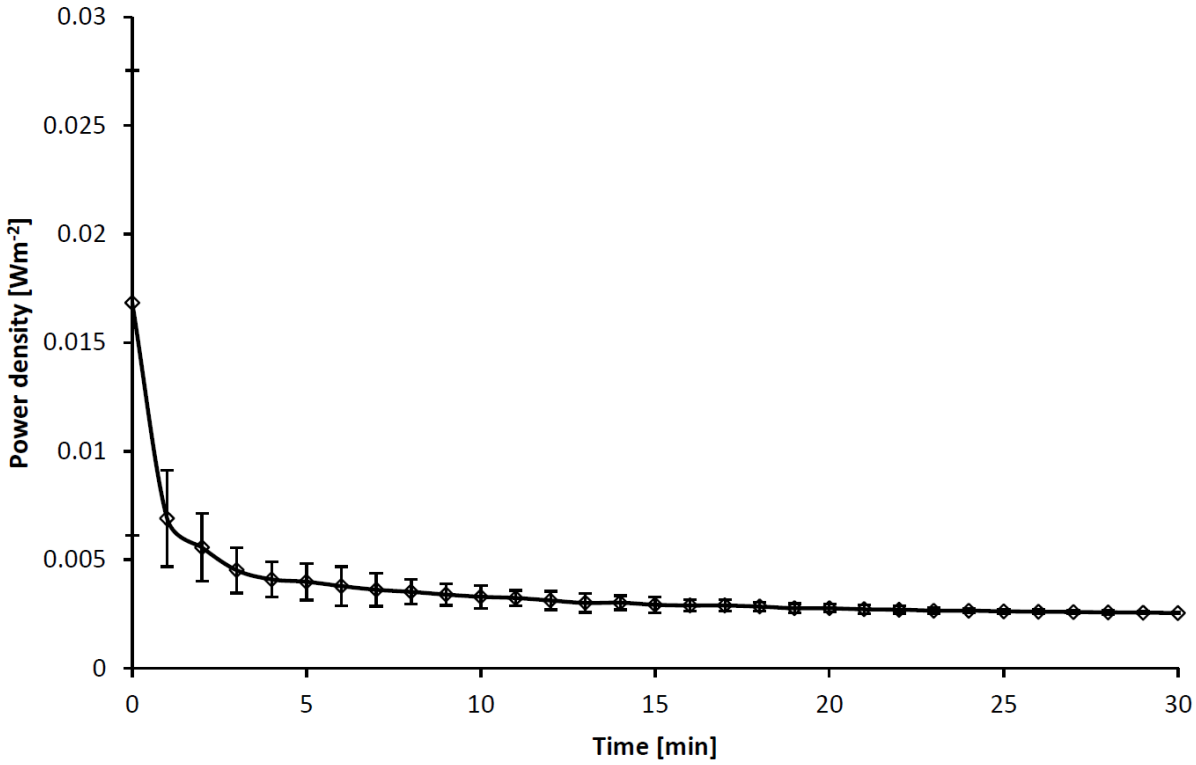

Figure 6.4: The change in power density over time in an acellular control MFC containing PBS in the anode chamber rather than a cell suspension, and a 1:1 solution of Dynawhite and PBS in the cathode chamber. The MFC was connected to a 100 Ω external load. The internal temperature of the cell was maintained at 37 °C. The solutions were kept mixed by the oscillating table in the incubator (80 rpm). Error bars are one standard deviation.

In this case, the acellular control MFC, it can be seen that the power density dropped very sharply over the first few minutes, with the power density at 5 minutes being only about 58% of the power density at 1 minute. The power density continued to drop slowly with the rate of decline slowing over time also, eventually reaching 0.0025 W m^{-2} at the end of the 30 minute experiment. This curve represents the background electron transfer from the buffer to the anode, against which the *A. adeninivorans*-containing MFCs are to be compared. The same experiment was performed with an OD_{600} 2.5 *A. adeninivorans* LS3 suspension in the anode chamber, resulting in the curve shown in Fig. 6.5.

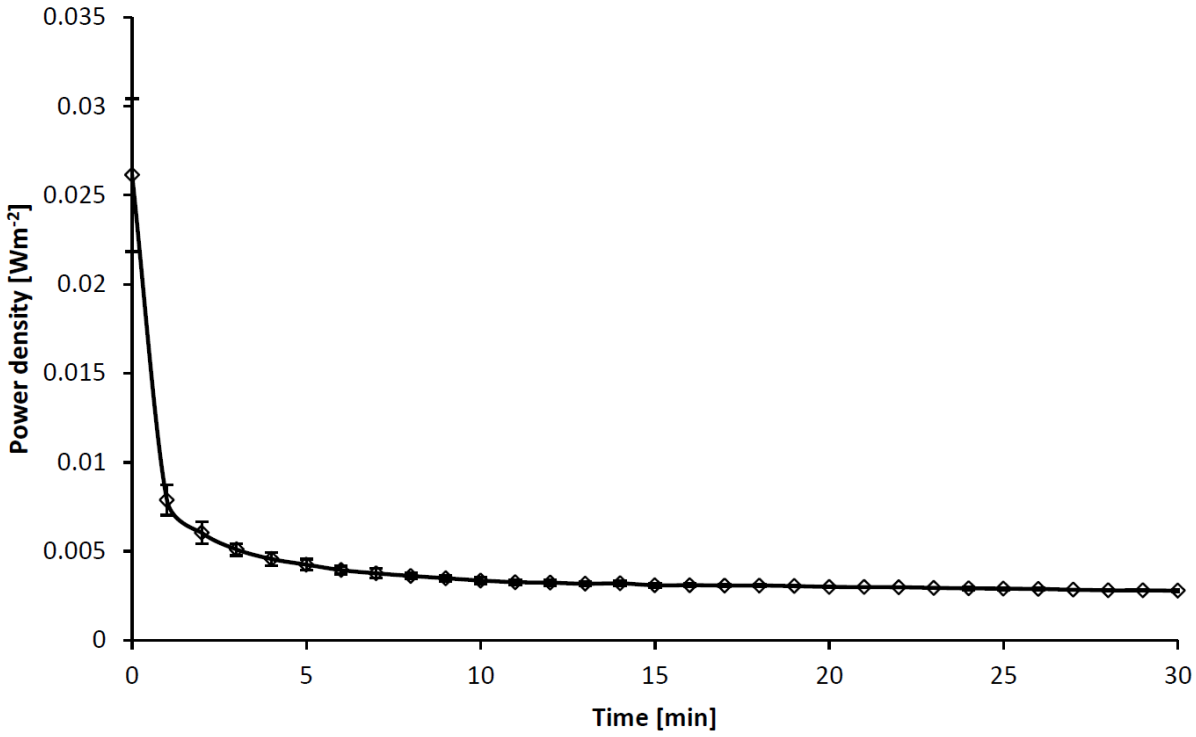

Figure 6.5: The change in power density over time in an MFC containing an OD_{600} 2.5 *A. adeninivorans* LS3 suspension in the anode chamber, and a 1:1 solution of Dynawhite and PBS in the cathode chamber. The MFC was connected to a 100 Ω external load. The internal temperature of the cell was maintained at 37 °C. The solutions were kept mixed by the oscillating table in the incubator (80 rpm). Error bars are one standard deviation.

This graph shows that for the MFC containing an OD_{600} 2.5 *A. adeninivorans* LS3 solution in the anode chamber, the change in power density over time conformed to a trend approximately the same as that observed for the acellular control, with a rapid initial drop followed by a slowing rate of decay. In general, the power densities throughout the experiment were slightly higher for this MFC at a given time than for the same time in the acellular control, decaying to 0.0028 W m^{-2} over 30 minutes. This implies that there was a greater concentration of available electrons present in the anolyte compared with the acellular control, presumably as a result of the excretion of uric acid by LS3, but the rate at which they were produced was insufficient to produce an accumulation of voltage at this external load. A similar pattern is seen once more for the case of the MFC containing an OD_{600} 2.5 *A. adeninivorans* G1221 suspension, as shown in Fig. 6.6.

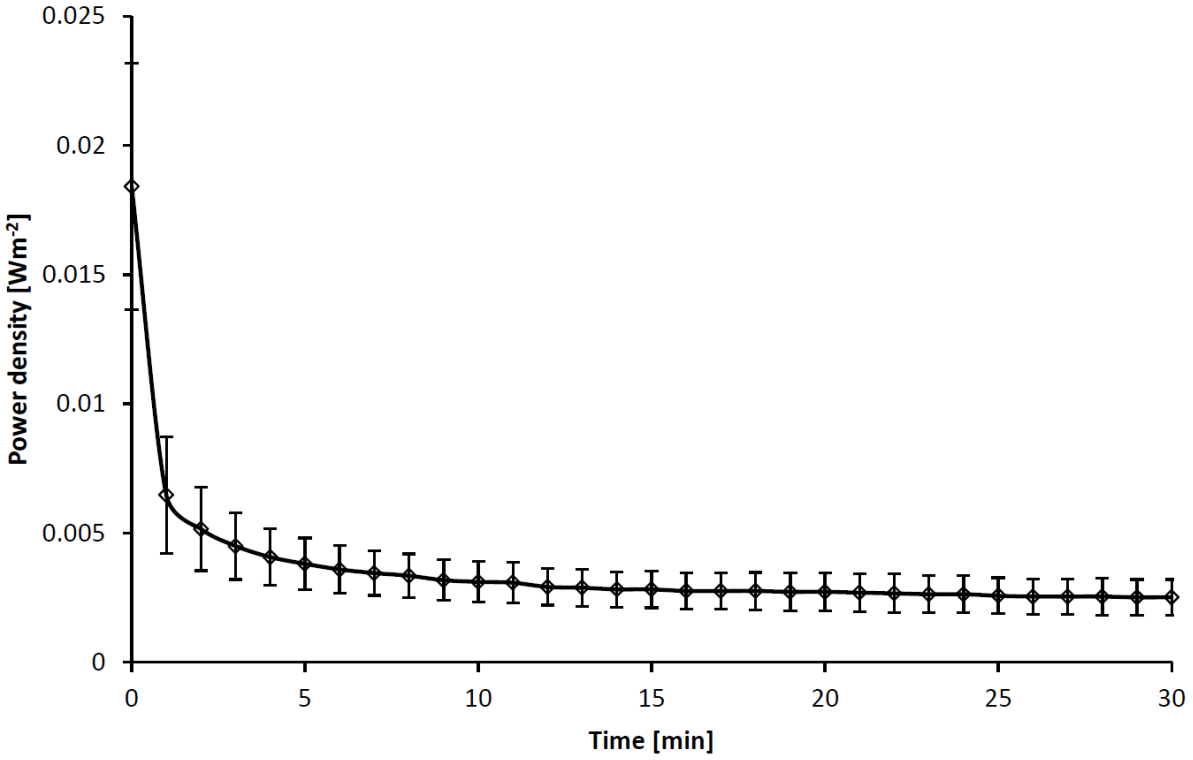

Figure 6.6: The change in power density over time in an acellular control MFC containing an OD_{600} 2.5 *A. adeninivorans* LS3 suspension in the anode chamber, and a 1:1 solution of Dynawhite and PBS in the cathode chamber. The MFC was connected to a 100 Ω external load. The internal temperature of the cell was maintained at 37°C. The solutions were kept mixed by the oscillating table in the incubator (80 rpm). Due to a lack of concordance amongst the data, the curve corresponding to the most reasonable range of values was selected, and error estimated at ± 1 standard deviation of the set of values recorded at that time across all sets of data for these experimental conditions, including the data not depicted here.

In this case, the shape of the curve is once more the same as for the two experiments already described, albeit the power densities for G1221 are closer to those of the acellular control than those of the LS3 experiment, with a final power density of 0.0025 W m^{-2}. Few conclusions can be drawn from this experiment, as the error is quite large (due to the lack of successfully collected concordant sets of data), save that since in no case was there an accumulation of voltage observed, G1221 is probably also incapable of excreting sufficient uric acid to increase the concentration of available electrons faster that they can be transferred to the anode.

6.3.2 Power-load analysis

The power-load analysis is useful for characterising the behaviour of the MFC with regard to the power density at a given external load. It can also reveal the optimal external load for producing the

maximum power density. The power-load curve for an MFC containing only PBS in the anode compartment is show in Fig. 6.7.

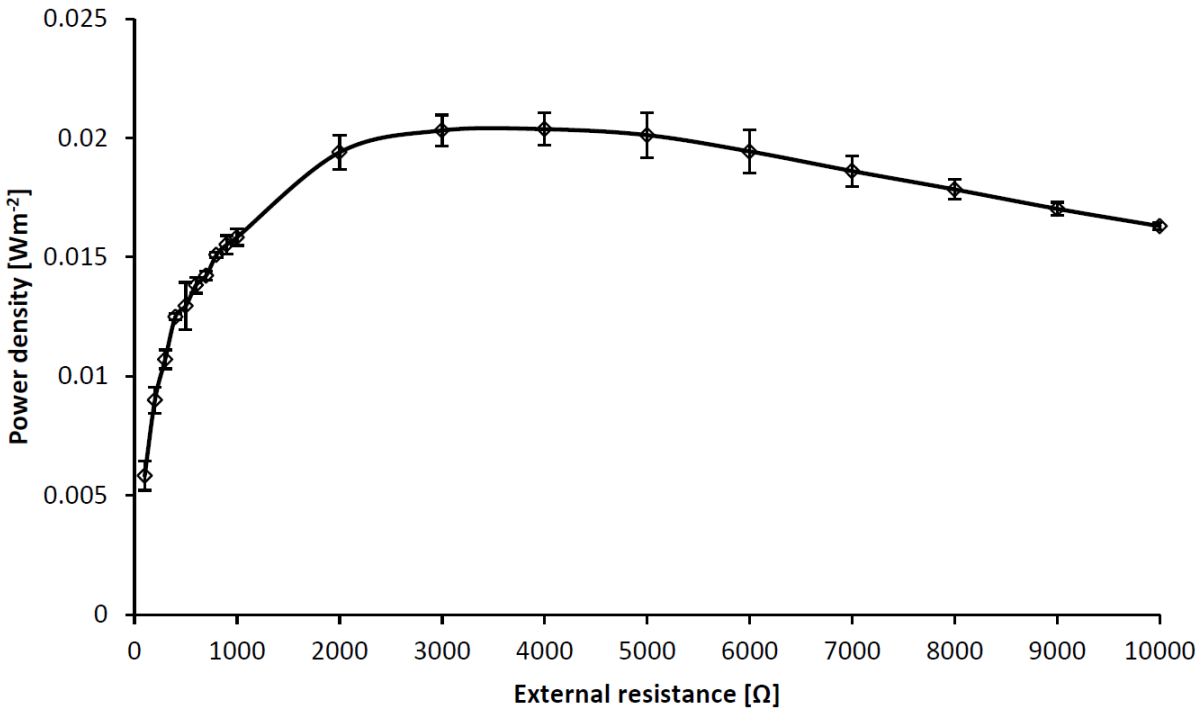

Figure 6.7: The effect of varying external loads on the power density of an acellular control, that is, the MFC run with PBS in the anode chamber rather than a cell suspension, and a 1:1 solution of Dynawhite and PBS in the cathode chamber. The internal temperature of the cell was maintained at 37 °C. The solutions were kept mixed by the oscillating table in the incubator (80 rpm). Error bars are one standard deviation.

From the graph we can determine that maximum of 0.02 W m^{-2} of power was produced by an acellular MFC with just PBS in the anode. The peak power density was observed at an external load of approximately 3000 to 4000 Ω. As the external load increases, the voltage (joules per coulomb, or the work done by 6.242×10^{18} electrons) across the load increases while the current (the rate at which electrons pass a given point) through the load decreases, meaning fewer electrons are required to perform the maximum amount of work theoretically possible at that load. As a result, there is a point, at the apex of the power-load curve, where the amount of electrons available is equal to the amount required to do the maximum amount of work possible for that load, and maximum transfer of power is achieved. This principle is known as Jacobi's Law, or the maximum power transfer theorem. If this principle holds for the MFC, then it can be inferred that the internal resistance of the MFC is equal to the external resistance where the highest power density is observed, that is to say, the internal resistance is approximately 3000 to 4000 Ω. The high external load required to achieve maximum power density implies that the kinetics of transfer of electrons to the electrode is quite slow, which is

not surprising given that the PBS in the anode compartment was not expected to supply a substantial number of electrons to the anode.

In the case of the acellular control MFC, this curve represents the background transfer of electrons from the buffer to the anode. Fig. 6.8 shows a similar experiment done with an OD_{600} 2.5 *A. adeninivorans* LS3 suspension in the anode chamber.

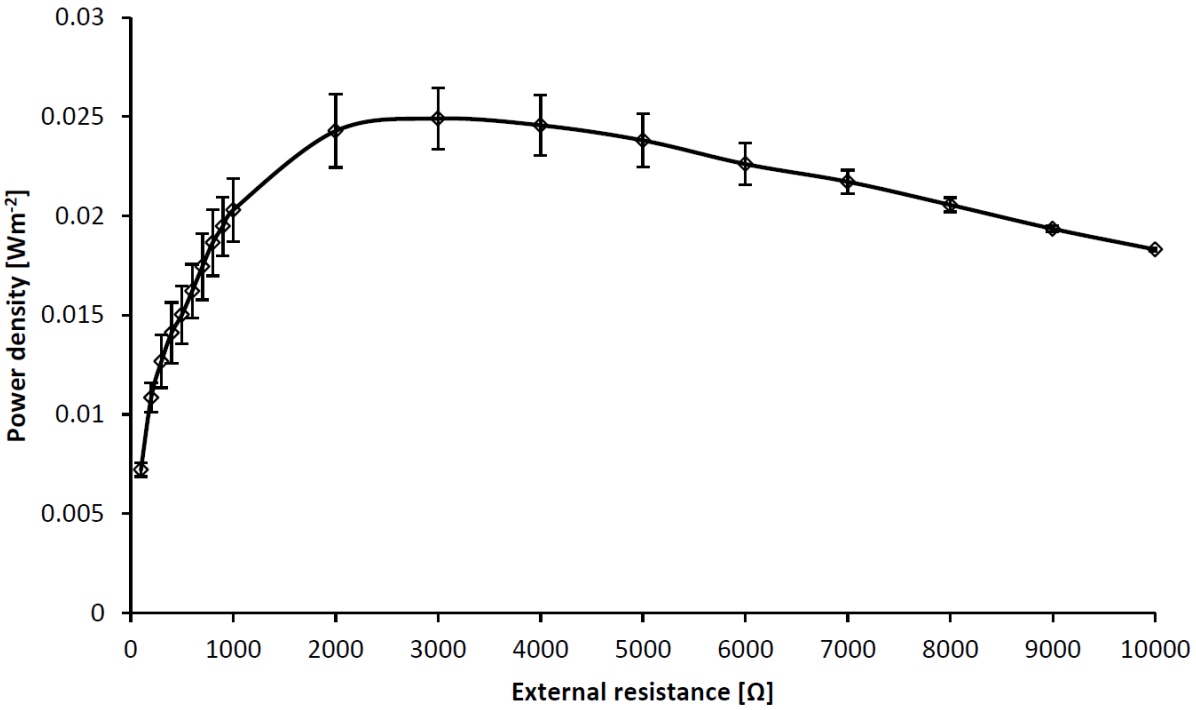

Figure 6.8: The effect of varying external loads on the power density of an MFC run with an OD_{600} 2.5 *A. adeninivorans* LS3 suspension in the anode chamber, and a 1:1 solution of Dynawhite and PBS in the cathode chamber. The internal temperature of the cell was maintained at 37 °C. The solutions were kept mixed by the oscillating table in the incubator (80 rpm). Error bars are one standard deviation.

From this power-load curve we can determine that for the MFC with OD_{600} 2.5 *A. adeninivorans* solution in the anode, 0.025 W m^{-2} of power was produced. The higher maximum power density implies that more electrons are available to the anode to do the work of charge transfer than in the acellular case. This is presumably due to the presence of additional electrons in the anolyte by means of the oxidation of uric acid present in the anolyte.

Peak power density appears to have been obtained around 3000 Ω. Due to the magnitude of the error it is difficult to draw any definitive conclusions about whether peak power density is obtained at a lower external load than for the acellular case in Fig. 6.7, though the shape of the graph does

potentially suggest this. Peak power density at a lower external load suggests a greater abundance of electrons is available to the anode, such that maximum power is transferred at a higher current.

The shape of this power-load curve is broadly similar to that of the acellular control, suggesting that the contribution of electrons supplied by LS3 was relatively small, even compared to the background electron transfer from the buffer, or that the kinetics of electron transfer from LS3 to the anode were similarly slow when compared with the background electron transfer. Possibly both factors contributed to the MFC behaviour observed. The same general pattern can be seen in Fig. 6.9, where an OD_{600} 2.5 *A. adeninivorans* G1221 suspension was substituted in place of LS3.

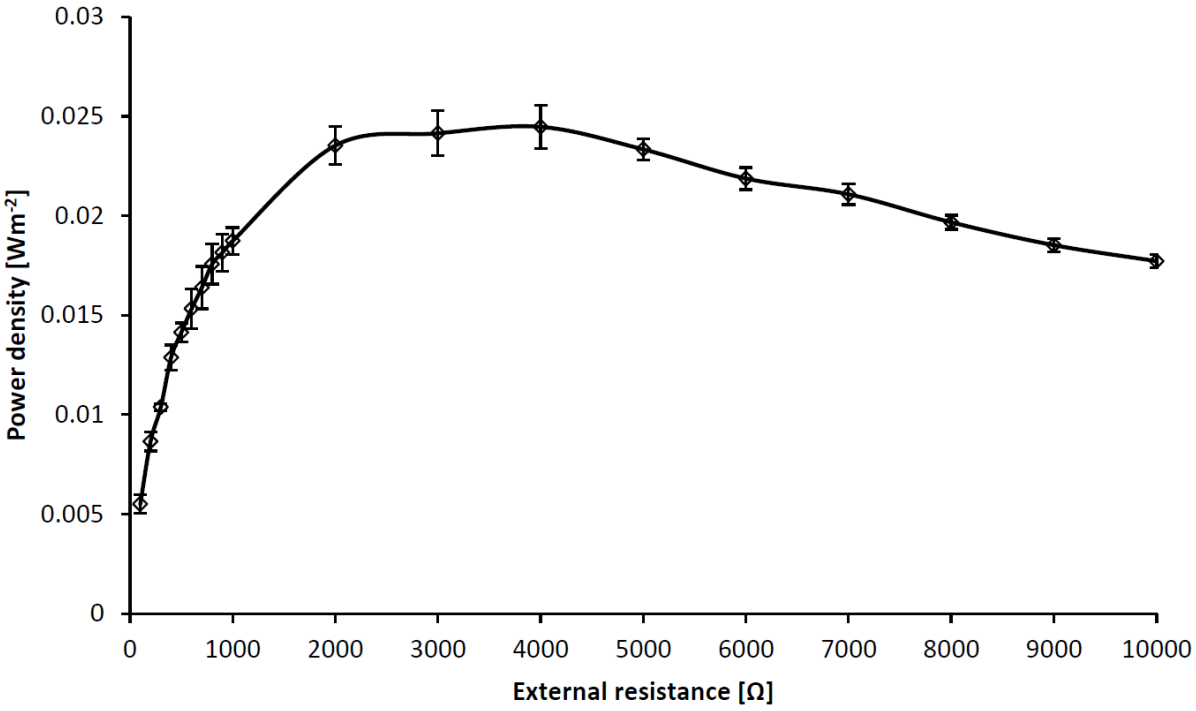

Figure 6.9: The effect of varying external loads on the power density of an MFC run with an OD_{600} 2.5 *A. adeninivorans* G1221 suspension in the anode chamber, and a 1:1 solution of Dynawhite and PBS in the cathode chamber. The internal temperature of the cell was maintained at 37 °C. The solutions were kept mixed by the oscillating table in the incubator (80 rpm). Error bars are one standard deviation.

This power load curve is fairly similar to the one for LS3, with a maximum power density of 0.024 W m^{-2}, obtained at an external resistance of 4000 Ω. While the error bars are somewhat smaller in in this case than for LS3, the canonical form of the power-load curve was reproduced unsteadily for G1221; in particular the power density at 3000 Ω was somewhat lower than the arc of the curve immediately beforehand suggests it might have been, "flattening" the area around the peak power density. One interpretation might be that the G1221 suspension simply supplied fewer electrons to the anode than

LS3, although their similar maximum power densities make it more tempting to theorise that the collection of additional sets of concordant data would reveal a smoother curve more closely resembling that of LS3.

6.3.3 MFC and electrode potentials

As part of the examination of the use of Dynawhite as a chemical catholyte, steady-state open circuit potentials were recorded for many of the experiments for each of the anolyte types employed. These potentials are displayed in Fig. 6.10.

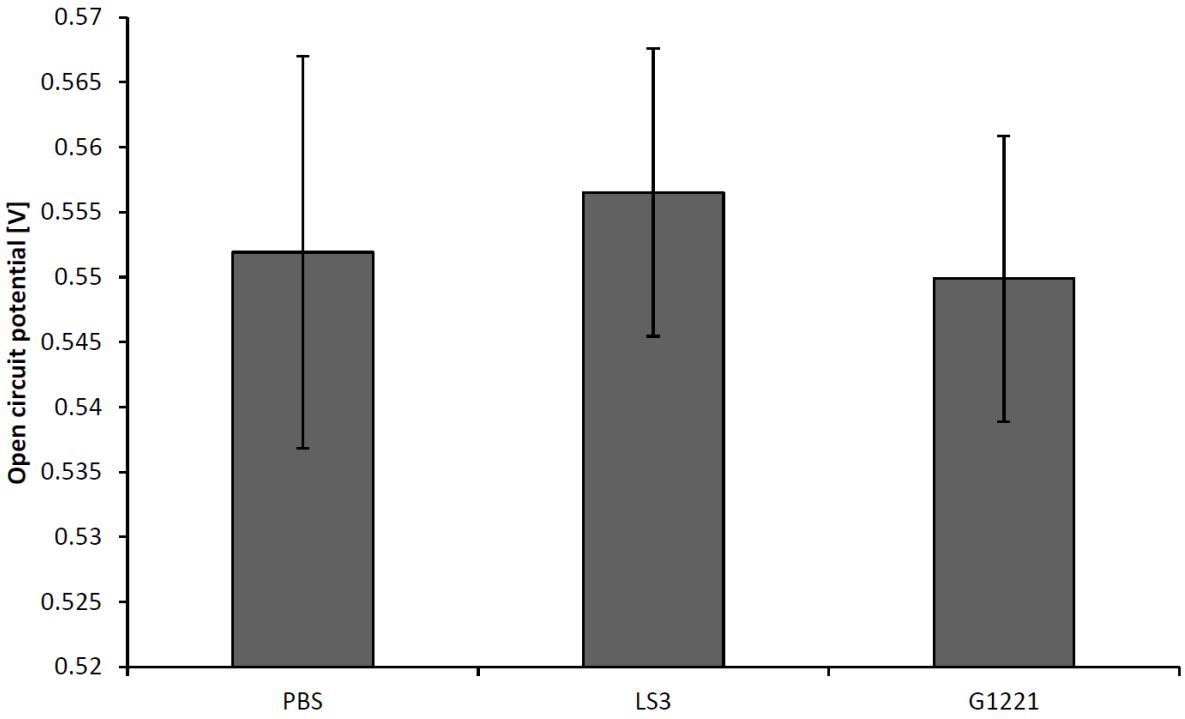

Figure 6.10: A comparison of the open circuit potentials observed in MFCs with anode chambers containing PBS, a suspension of *A. adeninivorans* LS3, or a suspension of *A. adeninivorans* G1221. Error bars are one standard deviation.

The MFCs containing an OD_{600} 2.5 *A. adeninivorans* LS3 suspension had a slightly higher average open circuit potential than the control or G1221 MFCs, however the variation in all three cases was sufficiently great that no real conclusion can be drawn; within error, the open circuit potentials can be considered similar. This implies that the addition of *A. adeninivorans* and the uric acid it excretes to the anode chamber has little or no effect on the open circuit potential of the MFC. Presumably, based on the results of the experiments detailed in chapter 5, if an anolyte containing *A. adeninivorans* was permitted sufficient time to accumulate a substantial concentration of uric acid, some perturbation in

the MFC potential might be observed, however in the case of an operating MFC this is unlikely to occur unless the external load was very much larger than the internal resistance of the MFC.

The theoretical open circuit potential of the cell is the difference between the anode potential and the cathode potential. A breakdown of these component potentials is shown in Fig 6.11. The average potential measured for the carbon cloth electrode immersed in the 1:1 Dynawhite/PBS solution, serving as the cathode for the MFC was +0.64 V vs. the Ag/AgCl reference electrode. Correcting for the potential of the reference electrode (+0.210 V vs. SHE) gives a half-cell potential of +0.85 V, relatively close to the +0.89 V standard half-cell potential for the reduction of hypochlorite under alkaline conditions. The remaining discrepancy is most likely a loss in efficiency due to the combination of various overpotentials associated with electrochemical cells.

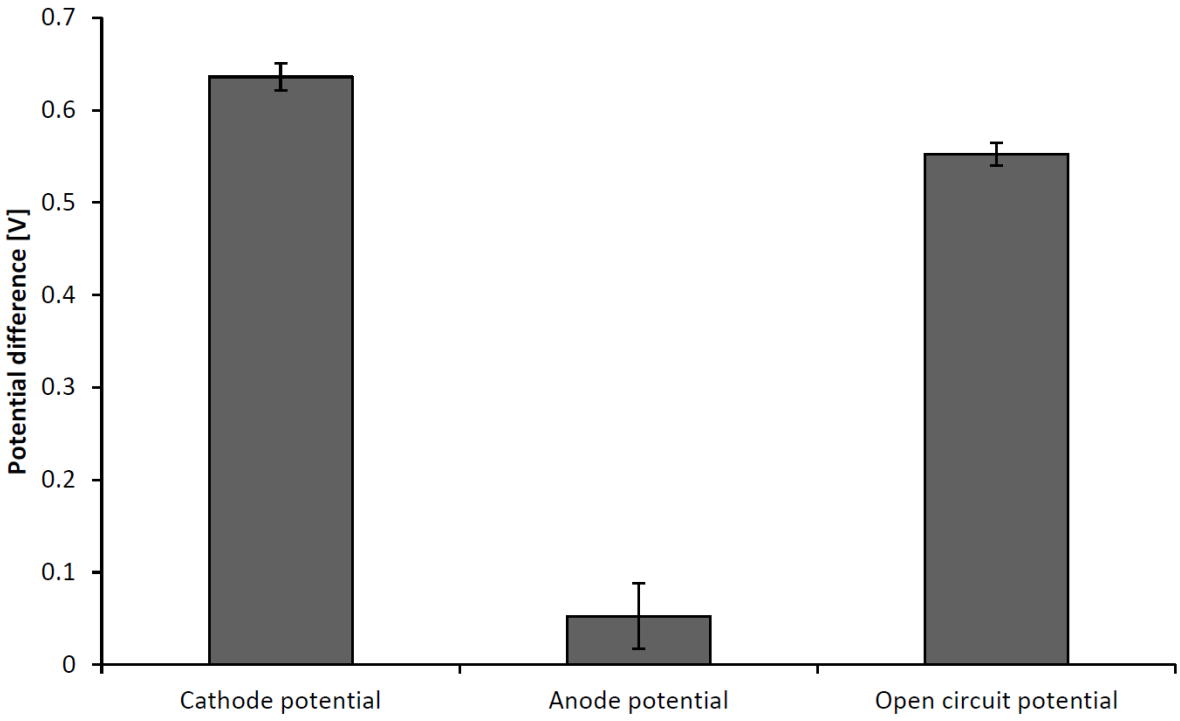

Figure 6.11: A comparison of the potentials of the cathode and the anode measured against a Ag/AgCl electrode (+0.210 V vs. SHE), along with the open circuit potential of the MFC. Error bars are one standard deviation.

The average potential measured for the anode was +0.05 V vs. Ag/AgCl. Given the average open circuit potential for the MFCs examined was +0.55 V, this anode potential is lower than the +0.09 V required to balance the cell. Direct measurements of anode potential tended to be unstable however, and varied widely compared to measurements of cathode or open cell potential, as depicted by the significantly larger error bars for anode potential in Fig. 6.11, so it is possible some or all of the

discrepancy may be attributed to the difficulties in measuring the anode potential. These difficulties may be related to the fact that the anolyte is only weakly electrochemically active, and the simple act of introducing the current of the multimeter and chemistry of the reference electrode to the anolyte may have disturbed the chemistry of the anode chamber.

6.4 Discussion

The intent with this project as a whole was to move forward with the mediator-free *A. adeninivorans* MFC concept first proposed as a possibility by Haslett et al. (2011). As discussed in the previous chapters, one avenue of enquiry toward this end was to improve the understanding of the source of the electrochemical activity exhibited by *A. adeninivorans* in the absence of a mediator molecule, and seek to emphasise or improve it. As shown in chapter 5, exploring various culture parameters with the aim of increasing the amount of uric acid produced did not reveal any methods of improving yield without significant mitigating drawbacks. Since the implementation of such methods was problematic, attention was turned to various other problems with the Haslett et al. (2011) concept MFC, namely the economic problems of the destruction of the membrane and cathode by MnO_2 fouling, and the substantial cost of Nafion membranes in any theoretical up-scaling of the MFC.

Having substituted Dynawhite in place of $KMnO_4$ and Ultrex in place of Nafion, the immediate objective was to determine if this revamped MFC could reproduce the rapidly accumulating power density depicted in the graph reproduced from Haslett et al. (2011) shown in Fig. 6.1. Aside from the fact that Fig. 6.4 depicts the approach toward steady state where Fig. 6.1 omits it, the trends and magnitudes of power density over time in the acellular control MFC used in this work appears to be similar the acellular control for the Haslett et al. (2011) MFC, suggesting that the two MFCs are approximately equivalent in the absence of cells. A stark difference emerges however once the OD_{600} 2.5 cell suspension of LS3 is introduced. Fig. 6.1 depicts an apparently linear increase in power density over the time period studied in the $KMnO_4$ MFC, compared to the rapid drop-off in power density observed for the NaOCl MFC which exhibits a trend more or less parallel to the acellular control (Fig 6.5).

In order to obtain a power-time relationship of a linear increase in power density over time, it would be necessary for the voltage across the load to be continuously increasing over time. This could be accomplished by a change in the reaction chemistry in the cathode chamber as the MFC is operating, or by the availability of electrons to the anode increasing over time due to secretion of uric acid. The former explanation is difficult to support for the $KMnO_4$ MFC, albeit not impossible. MnO_4^- has several possible redox half-reactions which can take place in the cathode. Under acidic conditions, the following reaction occurs:

$$MnO_4^- + 8H^+ + 5e^- \rightarrow Mn^{2+} + 4H_2O \qquad E° = +1.51\ V$$

For this reaction to continue as the MFC runs, H^+ would need to be supplied continuously to the catholyte through the PEM to keep the pH low. If the catholyte is not kept acidified, at neutral pH the following reaction will predominate:

$$MnO_4^- + 2H_2O + 3e^- \rightarrow MnO_{2(s)} + 4OH^- \qquad E° = +0.6\ V$$

This reaction is the one responsible for producing the dark brown MnO_2 fouling observed on the electrodes, PEM and cathode chamber walls. Therefore it can be supposed that if anything, the H^+ in solution is being gradually exhausted and the cathode half-reaction is converging on the more negative half-cell potential, so cathode chemistry is unlikely to favour a gradually increasing observed voltage.

The other possibility, that an increasing amount of uric acid in the anolyte is increasing electron availability to the circuit and driving the current, and therefore the voltage and power density, up, is the explanation which correlates with the motivation behind the optimisation experiments described in chapter 5. In order to manifest the upward trend in power density shown in Fig.6.1, the *A. adeninivorans* cells in the MFC would need to be excreting uric acid faster than it can be oxidised, such that it is accumulating in the extracellular buffer, causing the concentration of electron-bearing reduced molecules to increase as time passes. Given that this over-supply was reported to be occurring with an external load of 100 Ω, this means that the peak power transfer, where electron availability at the anode is exactly the same as the rate at which they can be utilised by the circuit, would occur at an external load lower than 100 Ω, further implying that the internal resistance of the MFC is lower than 100 Ω. This is a far cry from the vastly higher internal resistance of around 3000 Ω inferred from the power-load curve for the MFC developed in this chapter operating with the OD_{600} 2.5 suspension of LS3 in the anode chamber (Fig. 6.8). This would imply that the MFC described by Haslett et al. (2011) has vastly superior electron transfer kinetics to the MFC described here, however the organism, suspension buffer and operating temperature are the same, so this seems unlikely. The significant point of difference between the anodes of the two MFCs is that the electrodes used in this study were fabricated from carbon cloth, as opposed to the loose-woven carbon fibre mesh used by Haslett et al. (2011). However, there is no reason to believe that the electrode material used in this study should be significantly inferior, given both materials are established as usable and comparable in their suitability as anodes in the literature (Cheng and Logan, 2007; Wang et al., 2009).

Given that the anode chemistry and organism are functionally the same for the Haslett et al. (2011) MFC and the MFC examined in this study, the other major changes implemented in the design of the

MFC presented here are next to be considered. While Nafion appears to receive the most attention and widespread use as a PEM for two-chambered MFCs in the literature, studies have shown that alternative ion exchange membranes such as the one used in this study are capable of being used successfully in place of Nafion, and with no significant increase in internal resistance of the MFC (Dhar and Lee, 2013; Jung et al., 2007). In fact, in these studies, internal resistances of well in excess of 1000 Ω were routinely reported for MFCs with aqueous cathodes running on anaerobic sludge regardless of whether Nafion or an ion-exchange membrane was used. Similarly, the use of NaOCl as a chemical catholyte is receiving increasing interest, particularly for roles in sludge digestion (Ghadge et al., 2015), and does not appear to exhibit any properties that could cause such a discrepancy. Notably, an MFC with a NaOCl catholyte has been shown to operate at a relatively high power density (148.4 mW m^{-2}) with an internal resistane of only 15 Ω (Jadhav et al., 2014).

What has not been thoroughly examined however, is the potential effect of a combination of an Ultrex ion exchange membrane and hypochlorite on MFC power density. It was observed that as a membrane was exposed to NaOCl, it would gradually become bleached and pale over time (Fig. 6.12). One membrane which had been exposed to NaOCl for in excess of 72 h is believed to have failed, as the MFC in which it was fitted experienced a significant drop on open circuit potential. Whenever this membrane was re-used, this loss in potential would be observed, and the problem was rectified simply by replacing the membrane. It was concluded that the membrane had begun leaking. The deleterious effects that hypochlorite can have on ion exchange membranes has been studied (Garcia-Vasquez et al., 2014) and it has been found that after extended exposure to strong oxidisers, cracks can be opened in the membrane causing leakage. This suggests that it may be inadvisable to use NaOCl and Ultrex membranes in the same MFC, as the lifespan of the membrane may be poor. Nevertheless, the mode of membrane failure observed in this study, where the open circuit potential drops in an obvious fashion, does not correlate to a several thousand ohm discrepancy in the internal resistance of the NaOCl MFC compared to the $KMnO_4$ one.

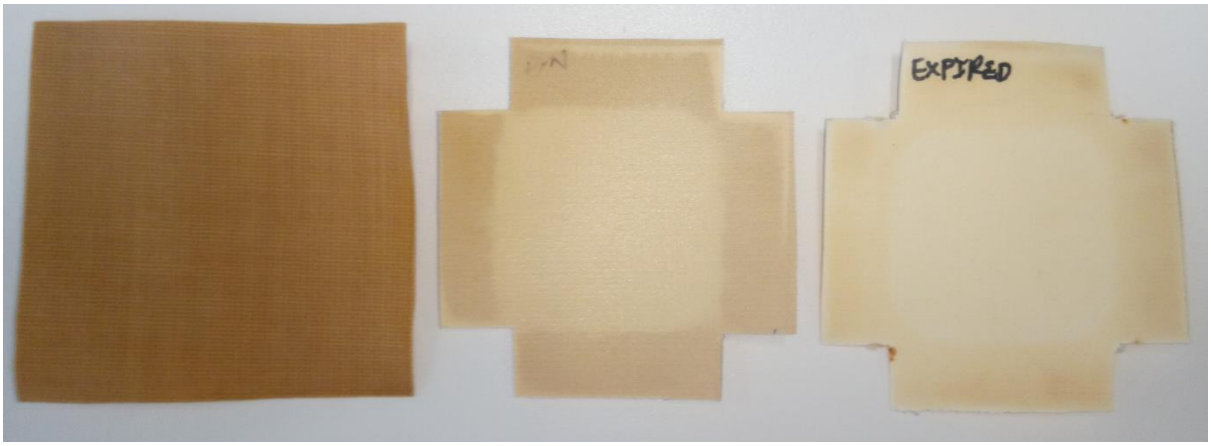

Figure 6.12: *Left*: unused ion-exchange membrane. *Centre:* Ion-exchange membrane after approx. 12 hours exposure to NaOCl. *Right*: Ion-exchange membrane after approx. 72 hours exposure to NaOCl.

There is no obvious way to reconcile the apparent discrepancy between the sluggish power production of the *A. adeninivorans* MFCs examined in this study (Fig 6.5, Fig 6.6) and the much more vigorous MFC described by Haslett et al. (2011) (Fig. 6.1), despite the fundamental similarity of the two systems. Given the studies conducted on *A. adeninivorans* uric acid production in the previous chapters, and especially the observations about how readily it is oxidised by dissolved O_2, the claim that an OD_{600} 2.5 suspension can produce enough uric acid to accumulate in solution faster than it can be oxidised with a small external load like 100 Ω seems highly unlikely, especially given the same study also describes observing a peak in power density of 70 mW m^{-2} follow by a rapid decline over the next 15 min to <10 mW m^{-2}, an observation that seems mutually exclusive with the data depicted in Fig. 6.1, but much more in line with the expectations set by the changes in power density over time shown in Fig. 6.5.

The most reasonable way to move forward with the investigation of the *A. adeninivorans* MFC presented in this thesis would be to repeat the studies of power density over time with an external load matched to the internal resistance of the MFC, inferred from Fig. 6.8 to be approximately 3000 Ω. This data is more characteristic of the long term behaviour of an MFC, representing the peak power transfer and should be mathematically equivalent the performance at 50% efficiency. In general the G1221 strain has not shown any obvious advantages over LS3 in these studies (Fig 6.6, Fig. 6.9), however as the power densities observed are so low, it is possible that any superior power density falls within the bounds of error. Further studies of power density over time with an external load matched to the internal resistance of the MFC may provide a clearer distinction between the two strains.

The selection of OD_{600} 2.5 as the cell suspension density for this study was made on the basis of attempting to replicate the power densities described by Haslett et al. (2011) with a modified MFC. However, in order to accumulate sufficient quantities of uric acid for electrochemical study, the

experiments in previous chapters needed to use very dense cell suspensions of up to OD_{600} 100-200. It may be beneficial to examine the performance of an MFC with a dense cell suspension in the anode chamber; however it is also possible that employing extremely dense suspensions may cause the cells themselves to obstruct the electrode surface, resulting in a decrease in power density at some point. Additional studies of the power-load curve would need to be conducted to determine what, if any, the effects of high density cell suspensions on the anode kinetics are, and what the optimal cell density might be.

Initially, before the studies described in this chapter were undertaken, pilot tests were attempted on a single-chamber MFC with an air cathode. This is a widely used MFC format, due to the unlimited availability of atmospheric oxygen, and its relatively high standard redox potential ($E°$ = +1.23 V vs. SHE). The cathode for this MFC was comprised of a paste of 10% platinum on carbon applied directly to the membrane with a piece of carbon cloth clamped overtop to function as a current collector and retain moisture. While this MFC did function, the open circuit potential appeared quite low (rarely more than 0.30V with LS3 in the anode chamber) and unstable, and tended to vary as the cathode dried out or was moistened. The issues with the cathode drying out were naturally exacerbated at warmer operating temperatures, and the re-moistening required introduced an additional problem of the carbon particles migrating through the cloth with the moisture and being washed away. In addition, it was difficult to avoid wasting the cathode paste when disassembling and cleaning the cell. Given that the carbon contained a platinum catalyst to help reduce the overpotential at the cathode (substantially increasing the economic cost of the cathode), coupled with the other difficulties, this cell design was deemed not worth pursuing, and the decision was made to select a chemical catholyte.

Hypochlorite, in the form of Dynawhite, proved to be a relatively effective oxidising agent, as well as an economically favourable one, with the cathode potential achieving close to the theoretical maximum for the half-cell reaction under neutral pH conditions (Fig 6.11). Despite this, this potential is substantially lower than the popular oxygen cathode, and NaOCl would be a significantly more effective catholyte if the higher redox half-cell potential of $E°$ = +1.63 V was able to be harnessed. As a reaction which predominates in acidic conditions, however, it encounters the same problem of depleting H^+ and switching to a lower potential half-reaction as described for $KMnO_4$. Harnessing this acidic reaction could have the potential added benefit of producing Cl_2 as a product, which, if re-dissolved in water, would dissociate thus:

$$Cl_2 + H_2O \rightleftharpoons HClO + Cl^- + H^+$$

This would result in a (at least partially) self-regenerating catholyte.

In addition to the damage done to the membrane mentioned above, hypochlorite did exhibit some other drawbacks as a chemical catholyte. The most obvious of these was that if catholyte solution worked its way into the joint where the wire and carbon cloth met, it would corrode the wire and cause the electrical connection to deteriorate. Because of this, the multimeter was used to check the resistance of the electrodes from the end of the carbon cloth to the exposed wire at the far end of the lead. Any electrodes with electrical discontinuity or resistance above 15 Ω were retired and replaced. In addition to this, it was discovered that when the lead of a heavily used electrode was stripped of its insulation, dark streaks were visible on some of the strands of copper, implying that the corrosion was able to spread down some length of the lead. This implies that in terms of improving electrode design, it is important to ensure that hypochlorite solution is not capable of coming into contact with the copper wire. This was highlighted in one particular case where a cathode was consistently causing the MFC to produce dramatically lower voltages than expected based on the behaviour of the others. It was found that unique among the electrodes, the lead of this electrode contained silver-plated copper wire. It was concluded that some secondary reaction may have been occurring between the hypochlorite and the silver in the wire which was interfering with the MFC.

In addition to the damage that can potentially be done to the copper wire by hypochlorite solution, metals such as copper, nickel, iron and cobalt catalyse the natural decomposition of NaOCl into NaCl and O_2. This increases the importance of avoiding contact between the wire and the catholyte solution. Another factor affecting NaOCl decomposition is light; ideally an MFC designed for use with NaOCl should have a completely opaque cathode chamber in order to avoid unnecessary exposure of the catholyte to light, which also catalyses natural degradation.

The MFC examined in this chapter was operated in an approximately semi-anaerobic manner. The PBS used for suspending *A. adeninivorans* cells was sparged with N_2 to reduce the amount of dissolved oxygen in solution in order to delay the oxidation of any uric acid produced by the cells. While the ports in the top of the MFC for the electrode leads, the thermocouple and injecting anolyte solution were not sealed, the oscillation used for mixing was not sufficiently turbulent to entrain significant atmospheric oxygen into the solution. This in and of itself was a problem; the low turbulence mixing possible in the small chamber volume was only capable of delaying the settling of the yeast cells, not keeping them suspended indefinitely. It was deemed necessary to periodically use a pipette to apply more thorough mixing to the cell suspension to ensure that it would not settle.

Overall, it is difficult to infer any new information as such about the value of *A. adeninivorans* as a microbial catalyst for a non-mediated MFC from these experiments, as they do not corroborate previously published reports of the power density that can be obtained from such an MFC. They do, instead, cast a pall of doubt over those reports, due to the unlikelihood of such a vast discrepancy in anode kinetics between the MFC described here and in previous reports despite the similarity of the

MFC designs concerned. Before pursuing any further investigations, it may be apropos to re-investigate the MFC detailed by Haslett et al. (2011) to determine the reproducibility of the results. It is worth noting, however, that a peak power density of 25 mW m^{-2}, while not impressive, is at least in the same general range of power outputs for non-mediated yeast-based MFCs (see Table 2.4).

6.5 References

Cheng, S., and Logan, B.E. (2007). Ammonia treatment of carbon cloth anodes to enhance power generation of microbial fuel cells. Electrochemistry Communications *9*, 492-496.

Cotton, F.A., and Wilkinson, G. (1972). Advanced Inorganic Chemistry: A Comprehensive Text, 3rd edn (New York, USA: Interscience Publishers).

Dhar, B.R., and Lee, H.S. (2013). Membranes for bioelectrochemical systems: challenges and research advances. Environmental Technology (United Kingdom) *34*, 1751-1764.

Garcia-Vasquez, W., Ghalloussi, R., Dammak, L., Larchet, C., Nikonenko, V., and Grande, D. (2014). Structure and properties of heterogeneous and homogeneous ion-exchange membranes subjected to ageing in sodium hypochlorite. Journal of Membrane Science *452*, 104-116.

Ghadge, A.N., Jadhav, D.A., Pradhan, H., and Ghangrekar, M.M. (2015). Enhancing waste activated sludge digestion and power production using hypochlorite as catholyte in clayware microbial fuel cell. Bioresource Technology *182*, 225-231.

Haslett, N.D. (2011). Development of a microbial fuel cell for organic waste bioremediation and simultaneous electricity generation. In Faculty of Agriculture and Life Sciences (Christchurch, New Zealand: Lincoln University).

Haslett, N.D., Rawson, F.J., Barrière, F., Kunze, G., Pasco, N., Gooneratne, R., and Baronian, K.H.R. (2011). Characterisation of yeast microbial fuel cell with the yeast *Arxula adeninivorans* as the biocatalyst. Biosensors and Bioelectronics *26*, 3742-3747.

Hubenova, Y., and Mitov, M. (2015). Extracellular electron transfer in yeast-based biofuel cells: A review. Bioelectrochemistry *106*, 177-185.

Jadhav, D.A., Ghadge, A.N., Mondal, D., and Ghangrekar, M.M. (2014). Comparison of oxygen and hypochlorite as cathodic electron acceptor in microbial fuel cells. Bioresource Technology *154*, 330-335.

Jung, R.K., Cheng, S., Oh, S.E., and Logan, B.E. (2007). Power generation using different cation, anion, and ultrafiltration membranes in microbial fuel cells. Environmental Science and Technology *41*, 1004-1009.

Medeiros, M.G., and Zoski, C.G. (1998). Investigation of a sodium hypochlorite catholyte for an aluminum aqueous battery system. Journal of Physical Chemistry B *102*, 9908-9914.

Sotres, A., Díaz-Marcos, J., Guivernau, M., Illa, J., Magrí, A., Prenafeta-Boldú, F.X., Bonmatí, A., and Viñas, M. (2015). Microbial community dynamics in two-chambered microbial fuel cells: Effect of different ion exchange membranes. Journal of Chemical Technology and Biotechnology *90*, 1497-1506.

Wang, X., Cheng, S., Feng, Y., Merrill, M.D., Saito, T., and Logan, B.E. (2009). Use of carbon mesh anodes and the effect of different pretreatment methods on power production in microbial fuel cells. Environmental Science and Technology *43*, 6870-6874.

Chapter 7

Conclusions

7.1 Identification of the unknown redox molecule secreted by *Arxula adeninivorans*

Dense cell suspensions of *A. adeninivorans* were incubated for 20 h at 47 °C to cause them to secrete elevated quantities of an unknown, electrochemically active reduced molecule into the extracellular buffer. The supernatant was then separated by isocratic elution on an HPLC column, and the fractions containing the previously observed electrochemical activity identified using CV. These fractions were analysed using mass spectrometry to identify the unknown as uric acid. This identity was supported by electrochemical analysis and UV-VIS spectroscopy. The identity of the molecule was further confirmed by proving to be a substrate for urate oxidase.

Uric acid is a diprotic acid, but typically only forms the singly charged hydrogen urate ion at biological pH. With E° = +0.59 V vs. NHE, it has the capacity to potentially serve as the electron donor at the anode of an MFC with a sufficiently more positive electron acceptor at the cathode. Unfortunately, the oxidation of uric acid is functionally irreversible, and it is readily oxidised by dissolved oxygen in solution. These are substantial drawbacks in a molecule intended for use as an electron shuttle in an MFC, and significantly mar the theoretical suitability of *A. adeninivorans* as a microbial catalyst for a non-mediated MFC.

7.2 Exploration of the source and purpose of uric acid secretion by *Arxula adeninivorans*

CV was used to investigate the electrochemical activity of supernatant samples drawn from dense cell suspensions of *Saccharomyces cerevisiae*, *Candida albicans*, *Candida lambica* and *Candida parapsilosis*, finding that none of these yeast species display any observable oxidation peaks which would correspond to the presence of uric acid. CV was also used to investigate a mutant strain of *A. adeninivorans* (G1224) with the gene for xanthine dehydrogenase disrupted, causing purine catabolism to terminate with xanthine/hypoxanthine production. This strain displayed no observable oxidation peaks which would correspond to the presence of uric acid, implying that purine catabolism is the most likely pathway responsible for the production of the uric acid observed.

The precise nature of the metabolic novelty which causes the production of such conspicuous levels of uric acid is unclear, though possible explanations could include disruptions in regulation of purine production or salvage. Likewise, the selective advantage that preserves this trait remains unknown, though some signalling or quorum sensing function is possible.

As uric acid production via purine catabolism is essentially a waste disposal process, disproportionate upregulation of such an attribute will inherently have an element of increased metabolic wastefulness. That *A. adeninivorans* is able to transfer electrons from the cell to an anode by means of uric acid is fortuitous for a non-mediated MFC, but largely coincidental; there is no clear reason why such a capability should convey any benefit to the organism.

7.3 Environmental and metabolic parameters affecting the uric acid production of *Arxula adeninivorans*

LSV was used to quantify the concentration of uric acid in supernatant samples drawn from dense cell suspensions of *A. adeninivorans* subjected to a variety of culture conditions. Cell suspensions that were incubated in aerobic conditions accumulated very little uric acid in the extracellular buffer over 20 h compared to those incubated in anaerobic conditions, confirming the earlier observation about uric acid's instability in the presence of oxygen. Cultures that were thoroughly aerated during the growth phase accumulated more uric acid in the subsequent suspension incubation phase than cultures which were poorly aerated during growth. This implies that abundant oxygen is necessary for high uric acid production but detrimental to its persistence in solution. Introducing carbon sources to the suspension incubation phase reduced the concentration of uric acid accumulated in the extracellular buffer relative to starvation conditions. Coupled with the findings regarding the role of oxygen and aeration, this means that growth conditions and uric acid production conditions for *A. adeninivorans* are directly opposed.

A mutant strain of *A. adeninivorans* (G1221) with the gene for urate oxidase disrupted (preventing any steps of purine catabolism following uric acid production from occurring) was found to accumulate a modestly higher concentration of uric acid at 37 °C than the wild type (LS3). At 45 °C, both LS3 and G1221 accumulated elevated concentrations of uric acid, however under these conditions LS3 exhibited higher production. Plate count enumeration showed a substantially higher rate of mortality for G1221 compared to LS3 at both temperatures, a trait it shared with the auxotrophic strain on which it was based (G1212). For all strains, however, mortality rate exceeded 99% at 45 °C, meaning that while elevating the temperature could improve uric acid production in an *A. adeninivorans* MFC, it would significantly shorten the lifespan of the cell culture.

Adjusting the initial pH of the extracellular buffer showed that the highest amount of uric acid was accumulated in a buffer with an initial pH of 8. Elevated pH was also found to decrease the redox potential of uric acid. While this suggests that increasing the pH of the anode chamber of an *A. adeninivorans* MFC would both improve uric acid production and potential difference between the cathode and anode, *A. adeninivorans* was found to actively reduce the pH of its environment to pH 7 over 20 h in buffers with initial pH of 8 or higher. Elevating the pH of the anode chamber also risks starving the cathode of the H^+ normally supplied through the membrane from the anode chamber.

In sum, no parameters were found which increased uric acid production by *A. adeninivorans* without some severe drawback to offset the improvement in either the short or long term.

7.4 Power production in a non-mediated MFC catalysed by *A. adeninivorans*

An *A. adeninivorans*-catalyzed MFC was constructed incorporating a CMI-7000 cation-exchange membrane in place of a Nafion PEM, and using Dynawhite (3-5% NaOCl) as a chemical catholyte with a view toward supplanting the destructive $KMnO_4$ catholyte described by Haslett et al. (2011) and dramatically decreasing the potential upscaling cost of the design. No artificial mediators were used in this design.

The average open circuit potential for this MFC design was 0.55 V. The maximum power density observed was 25 mWm^{-2} with an external load of approximately 3 kΩ, operating at 37 °C. Haslett et al. (2011) reports a maximum power density of 70 mWm^{-2} but describes it as a momentary surge in power which rapidly declined to <10 mWm^{-2} over 15 min. Similar behaviour was observed in this study, where a surge of power occurred as the circuit was closed, followed by a rapid decline to 2.8 mWm^{-2} over 30 min.

The behaviour described by Haslett et al. (2011) claiming a gradual accumulation of power density increasing from 5 to 27 mWm^{-2} over 30 min with an external load of 100 Ω was unable to be replicated in this study. Further, this claim is mutually contradictory with the rapid decline in current described above. This thesis concludes therefore that these claims are dubious and would need to be replicated to establish credibility.

The substitutions of Dynawhite in place of $KMnO_4$ and a cation-exchange membrane in place of a PEM both appeared to function satisfactorily, however the two substitutions are not compatible long-term. Exposure of the cation-exchange membrane to NaOCl for extended periods (72 h) caused the membrane to perish and allow leakage between the anode and cathode chambers.

7.5 Summary and future outlook

The unknown reduced molecule secreted by the yeast *A. adeninivorans* was identified as uric acid, and determined to originate from the purine catabolism pathway. There is no clear reason for the selection or maintenance of this trait, which appears to simply be an anomalous overproduction of a waste product. Out of all the parameters examined as avenues to increase uric acid production by *A. adeninivorans* for use in a non-mediated MFC, none accomplished this end without significant disadvantages. As such, there is no known method of substantially improving the output of uric acid by *A. adeninivorans* to the point where it can form the basis of a high-power density, non-mediated MFC. In fact, observations of the MFC developed in this study coupled with a close reading of the literature suggest that the potential of *A. adeninivorans* in this role has been historically overstated. In addition, it is also worth noting that the genetically modified strains of *A. adeninivorans* appear to potentially have a compromised thermotolerance compared to the wild type. Since thermotolerance is a major basis for selecting *A. adeninivorans* as a platform for genetic manipulation, this attribute should be further investigated.

Fundamentally, uric acid is an unsuitable molecule for use as an electron delivery vector, because it is especially vulnerable to the longstanding problem of electron shuttles being oxidised by oxygen in the medium, and worse still, irreversibly oxidised. It is, however, an ideal example of the fundamental flaw in the reasoning behind the concept of a secreted molecule being used as an electron shuttle in an MFC, that is:

1. One selects a yeast as a catalyst because it has a broad substrate range.
2. In order to metabolise many of those substrates and generate electrons, it needs oxygen.
3. A secreted electron shuttle can transfer those electrons to the anode.
4. However, the oxygen will consume many of those electrons before they get to the anode.

In this way, it is self-defeating, or at least highly inefficient.

In order for yeasts to have a future in the role of microbial catalysts for MFCs in the absence of artificial mediators, a better strategy would be to focus on systems where electrons can be transferred to the anode directly. However, as far as direct electron transfer goes, bacteria have demonstrated far superior capabilities. As such, the best way to create a future for *A. adeninivorans* as a microbial catalyst may be to develop it into a platform capable of displaying novel proteins on the cell surface, isolating the bacterial surface proteins involved in direct electron transfer and “transplanting” them into *A. adeninivorans*. This is, however, a complex solution to a problem which is likely more easily solved by careful selection and enrichment of an appropriate microbial consortium with the right metabolic capabilities to begin with.

Appendix 1

Linear sweep voltammetry: Calibration for uric acid

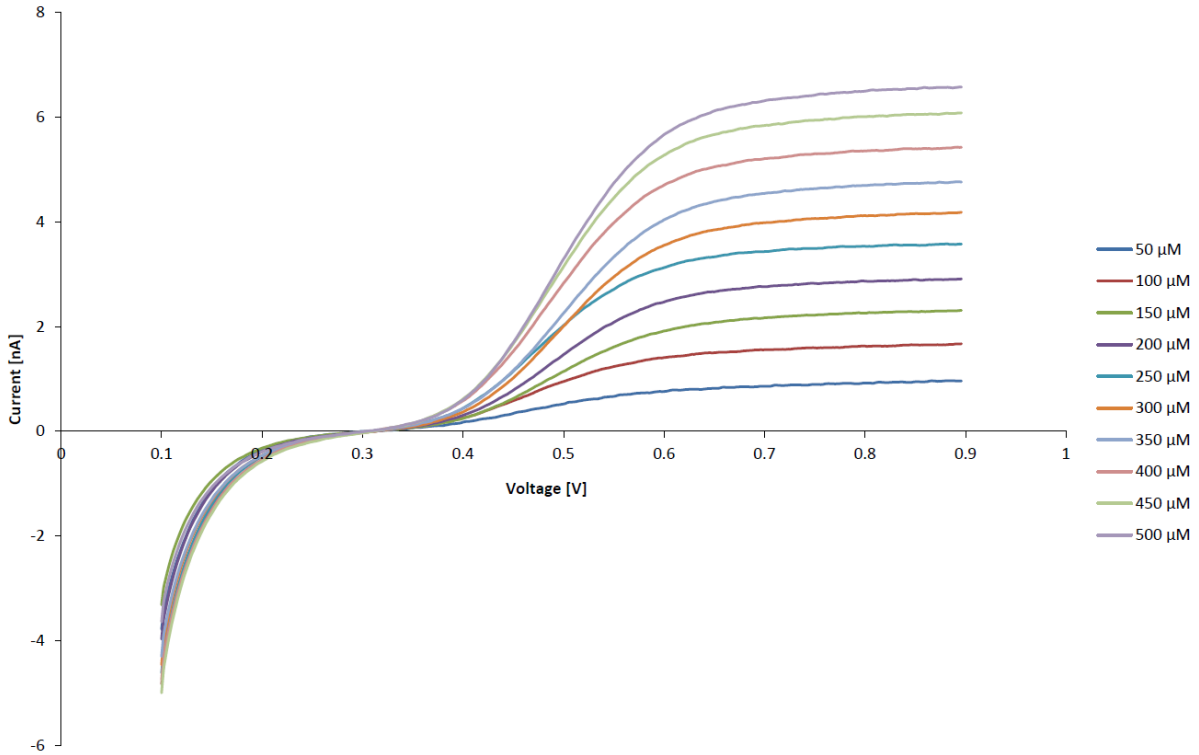

Figure A.1: Linear sweep voltammetry plots for a range of different prepared concentrations of sodium urate solution. The curves depicted are composites of triplicate measurements at each point. Current was measured at 2 mV increments throughout the sweep. The method used for performing these analyses is described in section 6.3.3.

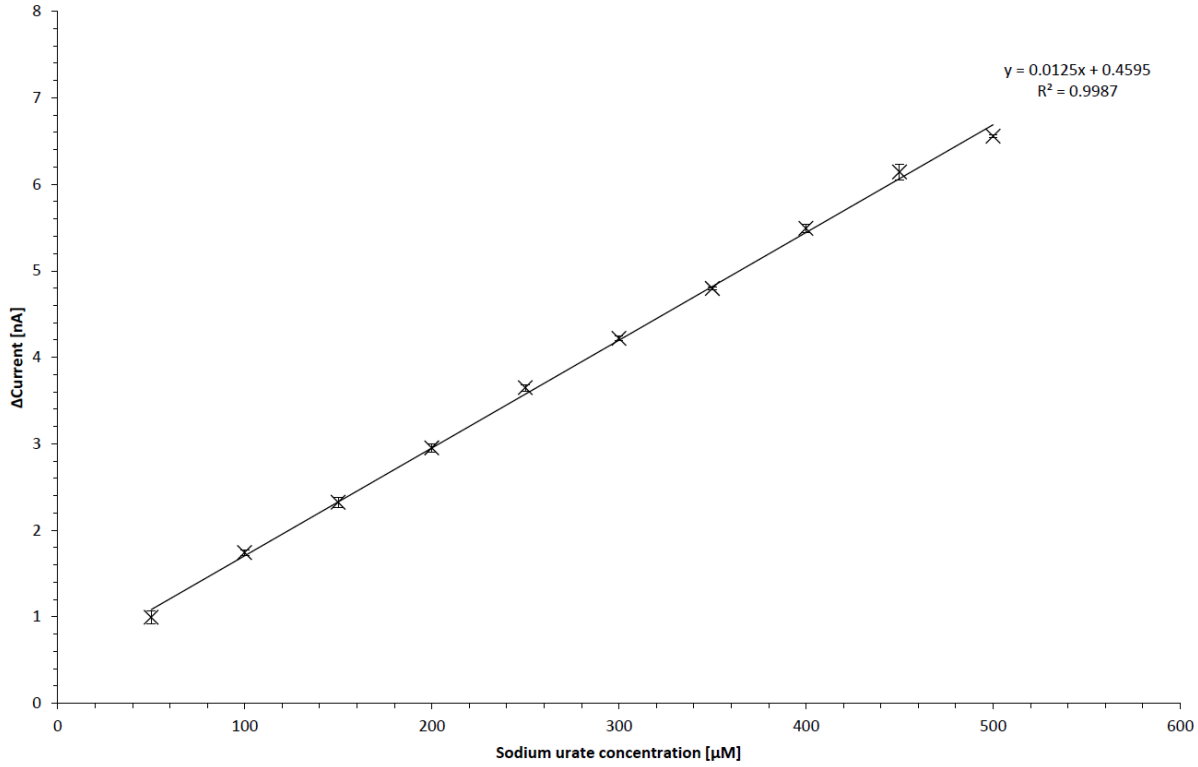

Figure A.2: Calibration curve used to infer urate concentration from changes in current between +0.25 V and +0.75 V on a LSV curve. Data points are derived from the change in current between these two potentials for each of the urate concentrations presented in Fig. A.1. Error bars are one standard deviation.

Appendix 2

Publication: “Identification of uric acid as the redox molecule secreted by the yeast *Arxula adeninivorans*”

Identification of uric acid as the redox molecule secreted by the yeast *Arxula adeninivorans*
Williams, J., Trautwein-Schult, A., Jankowska, D. et al.
Applied Microbiology and Biotechnology (2014) 98, issue 5: 2223-2229.
doi:10.1007/s00253-013-5487-4

Appendix 3

Proofs for publication: “Environmental and metabolic parameters affecting uric acid production of *Arxula adeninivorans*”

Environmental and metabolic parameters affecting the uric acid production of *Arxula adeninivorans*

Williams, J., Trautwein-Schult, A., Kunze, G. et al.

Applied Microbiology and Biotechnology (June 2017) 101, issue 11: 4725-4736.
doi:10.1007/s00253-017-8199-3